MATERIALS, METHODS, AND INSTRUMENTATION FOR PREPARATIVE-SCALE ISOELECTRIC TRAPPING SEPARATIONS

A Dissertation

by

ROBERT YATES NORTH

Submitted to the Office of Graduate Studies of
Texas A&M University
in partial fulfillment of the requirements for the degree of

DOCTOR OF PHILOSOPHY

May 2009

Major Subject: Chemistry

MATERIALS, METHODS, AND INSTRUMENTATION FOR PREPARATIVE-SCALE ISOELECTRIC TRAPPING SEPARATIONS

A Dissertation

by

ROBERT YATES NORTH

Submitted to the Office of Graduate Studies of
Texas A&M University
in partial fulfillment of the requirements for the degree of

DOCTOR OF PHILOSOPHY

Approved by:

Chair of Committee,	Gyula Vigh
Committee Members,	David H. Russell
	Manuel P. Soriaga
	Victor M. Ugaz
Head of Department,	David H. Russell

May 2009

Major Subject: Chemistry

ABSTRACT

Materials, Methods, and Instrumentation for Preparative-Scale Isoelectric Trapping Separations. (May 2009)

Robert Yates North, B.S., Hillsdale College

Chair of Advisory Committee: Dr. Gyula Vigh

Isoelectric trapping (IET) has become an accepted preparative-scale electrophoretic separation technique. However, there are still a number of shortcomings that limit its utility. The performance of the current preparative-scale IET systems is limited by the serial arrangement of the separation compartments, the difficulties in the selection of the appropriate buffering membranes, the effect of Joule heating that may alter separation selectivity and a lack of methods for the determination of the true, operational pH value inside the buffering membranes. In order to bolster the current membrane pH determination methods which rely on the separation of complex ampholytic mixtures, a fluorescent carrier ampholyte mixture was synthesized. The use of a fluorescent mixture allows for a reduced load of carrier ampholytes, thereby reducing a possible source of error in the pH determinations. A mixture of carrier ampholytes tagged with an alkoxypyrenetrisulfonate fluorophore was shown to have suitable fluorescence and ampholytic properties and used to accurately determine the pH of high pH buffering membranes under actual IET conditions. In a more elegant solution to the difficulties associated with pH determinations, a method utilizing commercial UV-transparent

carrier ampholytes as the ampholyte mixture to be separated was developed. By using commercial carrier ampholytes and eliminating the need to synthesize, purify, and blend fluorescently tagged ampholytes, the new method greatly simplified the determination of the operational pH value of the buffering membranes. In order to address the remaining limitations, a new system has been developed that relies on (i) parallel arrangement of the electrodes and the collection compartments, (ii) a directionally-controlled convection system for the delivery of analytes, (iii) short anode-to-cathode distances, (iv) short intermembrane distances, and (v) an external cooling system. This system has been tested in four operational modes and used for the separation of small molecule ampholytic mixtures, for the separation of protein isoforms, and direct purification of a target pI marker from a crude reaction mixture.

ACKNOWLEDGEMENTS

My friends and family, there is no doubt that without them this work would have been an impossible task. They have been an invaluable source of encouragement and support throughout the process.

My advisor, Professor Gyula Vigh, whose zeal for educating his students is unmatched by anyone who I have ever met. His inspiring lectures, thorough analysis of any experimental results he was brought, and thoughtful advice were all instrumental in the completion of this work. I am thankful to have been one of his graduate students.

The members of the separations science group both past and present for their advice, fellowship, and knowledge: Ann, Brian, Brent, Edward, Evan, Joshua, Kingsley, Nellie, Omar, Roy, and Sanjiv. Particularly, I would like to acknowledge Sanjiv for being a sounding board for any ideas I brought him and his advice both personally and professionally.

The staff of the Texas A&M and machine and glass shops, particularly Tony Montalbano for all the advice and help during the manufacture of my device.

TABLE OF CONTENTS

Page

Page

Page

LIST OF FIGURES

FIGURE Page

FIGURE Page

FIGURE Page

FIGURE Page

FIGURE Page

FIGURE Page

FIGURE Page

FIGURE Page

NOMENCLATURE

IEF	Isoelectric focusing
TRIS	Tris(hydroxymethyl)aminomethane
CA	Carrier ampholyte
IPG	Immobilized pH gradient
MCE	Multi-compartment electrolyzer
MSA	Methanesulfonic acid
CE	Capillary electrophoresis
cIEF	Capillary isoelectric focusing
DMSO	Dimethylsulfoxide
cIEF-LIF	Capillary isoelectric focusing with laser induced fluorescence detection
IDA	Iminodiacetic acid
ARG	Arginine
PVC	Poly(vinyl chloride)
PVAC	Poly(vinyl acetate)
$BzSO_3H$	Benzenesulfonic acid
$PTSA^-$	*p*-Toluenesulfonate
$BzTMA^+$	Benzyltrimethylammonium
BzTEAOH	Benzyltriethylammonium hydroxide
HEPES	4-(2-Hydroxyethyl)-1-piperazineethanesulfonic acid
ANDS	7-Amino-1,3-napthalenedisulfonic acid

ESI-MS	Electrospray ionization mass spectrometry

1. INTRODUCTION

1.1 Isoelectric focusing

1.1.1 Principles of isoelectric focusing

Isoelectric focusing (IEF) is a separation method based on the electrophoretic migration of ampholytes in pH gradients (with pH increasing from anode to cathode). The electrophoretic migration of any analyte depends on the net charge of the analyte; the migration direction is dictated by the sign of the net charge of the analyte, the migration velocity is determined by the charge to size ratio of the analyte and the magnitude of the electric field strength (V/cm). Since the sign and magnitude of the net charge of ampholytes depends on the pH in their environment, ampholytes migrating across a pH gradient accumulate at a point where their net charge and electrophoretic velocity become zero. The pH at that point is taken as the isoelectric point or pI value of the ampholyte. The pI value can also be calculated (estimated) by Equation 1 from the pK_a values closest to the isoionic point [1,2].

$$pI = \frac{1}{2}\left(pK_1 - pK_2\right)$$

If the pH gradient and a sufficiently high electrical potential are maintained, each ampholyte in the system will remain "focused" as a band where diffusional mass transport in both directions is balanced by electrophoretic migration in the reverse direction [1].

This dissertation follows the style and format of *Electrophoresis*.

Ampholytes that possess different pI values stop migrating at different locations in the pH gradient, thus separation based on pI differences can be achieved. Equation 2 relates the pI value difference (ΔpI) between the nearest resolved ampholytic neighbors to the experimental parameters as:

$$\Delta pI = 3.17\sqrt{D\left[d(pH)/dx\right]/E\left[d\mu/d(pH)\right]}$$

where D is the diffusion coefficient of the analyte, E is the field strength, d(pH)/dx is the slope of the pH gradient at the pI, and dμ/d(pH) is the slope of the analyte mobility vs. pH curve at the pI. Ampholytes whose pI values differ by as little as 0.002 have been separated by IEF [3].

1.1.2 Generation of pH gradients

Though modern power supplies make it experimentally trivial to maintain a constant electrical potential, generation of suitable, stable pH gradients proves to be a more difficult task. A simple pH gradient covering approximately 3 pH units can be created by electrophoresis in a solution of a salt formed from a weak acid and weak base provided that the pK_a values of the constituents differ by less than 1 [4,5]. However, these pH gradients are inherently unstable as diffusion and electrophoretic migration of the buffering ions constantly change the buffer ion concentrations and, consequently, the pH within the gradient. This temporal instability can be mitigated if the anolyte and catholyte solutions are constantly remixed at a flow rate that counters their electrophoretic depletion [6].

pH gradients can also be generated by utilizing the unequal temperature dependence of the pK_a values of weak electrolytes [7]. For example, tris(hydroxymethyl)aminomethane (TRIS) has a high dpK_a/dT value. When a TRIS solution is placed into a spatial temperature gradient, the degree of protonation of TRIS changes with the temperature, consequently a spatial pH gradient is formed in the solution. Such a system has two advantages: *(i)* it is the simplest chemical system in which a pH gradient can be formed and *(ii)* the pH gradient formed is independent of the electric field. Unfortunately, the pH gradients generated can only span a few tenths of a unit. Additionally, if the dpI/dT values of the ampholytic analytes and the dpH/dT of the buffer system are equal, no separation will occur.

Another method to generate pH gradients utilizes the change in the pK_a value of the buffer as the dielectric constant of the solution is changed by altering the spatial concentration of an organic solvent [8]. Its advantages and shortcomings are similar to those of the thermally generated pH gradients.

A stable pH gradient can be generated more efficiently by placing a mixture of ampholytic buffers into an electric field. Ampholytic buffers in sufficient concentration will establish a solution pH equal to their pI value. In an electric field, ampholytic buffers (carrier ampholytes, CA) arrange themselves according to their pI values increasing from anode to cathode. Each ampholyte in the system will remain "focused" as a band and establish a local pH equal to its pI, thus forming a pH gradient [2]. In its

simplest manifestation, a two-carrier ampholyte system, a step-wise pH gradient will be generated (Figure 1). However, if one uses a sufficient number of carrier ampholytes (at least 30 per pH unit), a smooth, "stepless" pH gradient can be generated (Figure 2) [9]. Various synthetic schemes have been utilized to generate carrier ampholyte mixtures with pI values ranging from 2.5-11 [10-15]. Though using carrier ampholyte mixtures provides an adequate solution to the problem of establishing a wide, smooth pH gradient, it is not without problems: analytes separated by IEF will be contaminated with carrier ampholytes hindering downstream analysis, such as mass spectrometry, and limiting the utility of preparative-scale IEF. Also, carrier ampholyte-based pH gradients change over time due to anodic and cathodic drift (isotachophoresis) [16]. Finally, peak resolution and reproducibility of the separation both depend on the quality of the carrier ampholyte mixture.

pH gradients can also be generated using a mixture of non-ampholytic weak electrolytes and ampholytes [17,18]. The main utility of such a system is in decreasing the slope of ampholytic pH gradients to maximize resolution. Unfortunately, inclusion of non-ampholytic molecules diminishes the stability of the pH gradient.

An elegant alternative solved many of the problems associated with the dynamically generated pH gradients: by immobilizing weak electrolytes into a gel, a temporally stable pH gradient based on Hendersson-Hasselbach's formula can be created (immobilized pH gradient, IPG) [3]. Eleven acrylamido weak electrolytes with pK_a

values ranging from 1.2 through ~14 can be combined in various proportions (adjusting both the slope and the range of the desired pH gradient) and can be copolymerized with acrylamide and bisacrylamide to generate the IPGs [19]. In IPG, there are no carrier ampholytes, thus there is no anodic or cathodic drift and the separated analytes can be recovered in pure form.

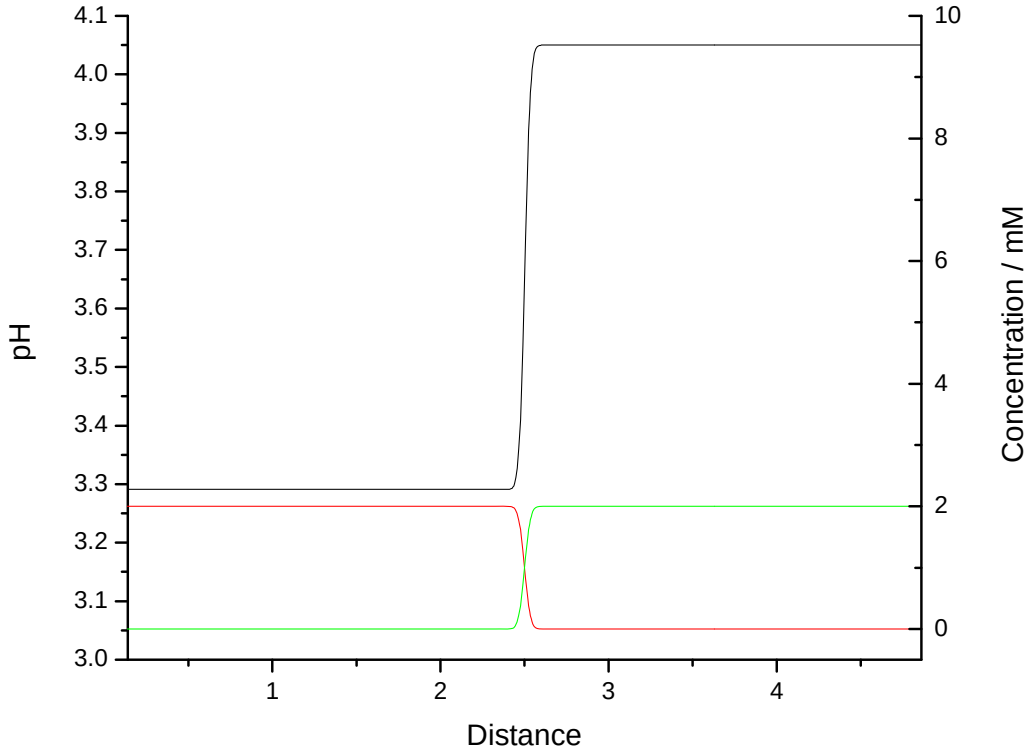

Figure 1. pH and concentration profile for a two-carrier ampholyte system. Black represents the theoretical pH, red the low pI ampholyte concentration, green the high pI ampholyte concentration. The carrier ampholytes have pI 3 and 4, both have a $\Delta pK_a = 1$. Profiles were generated by the Simul5 software [20].

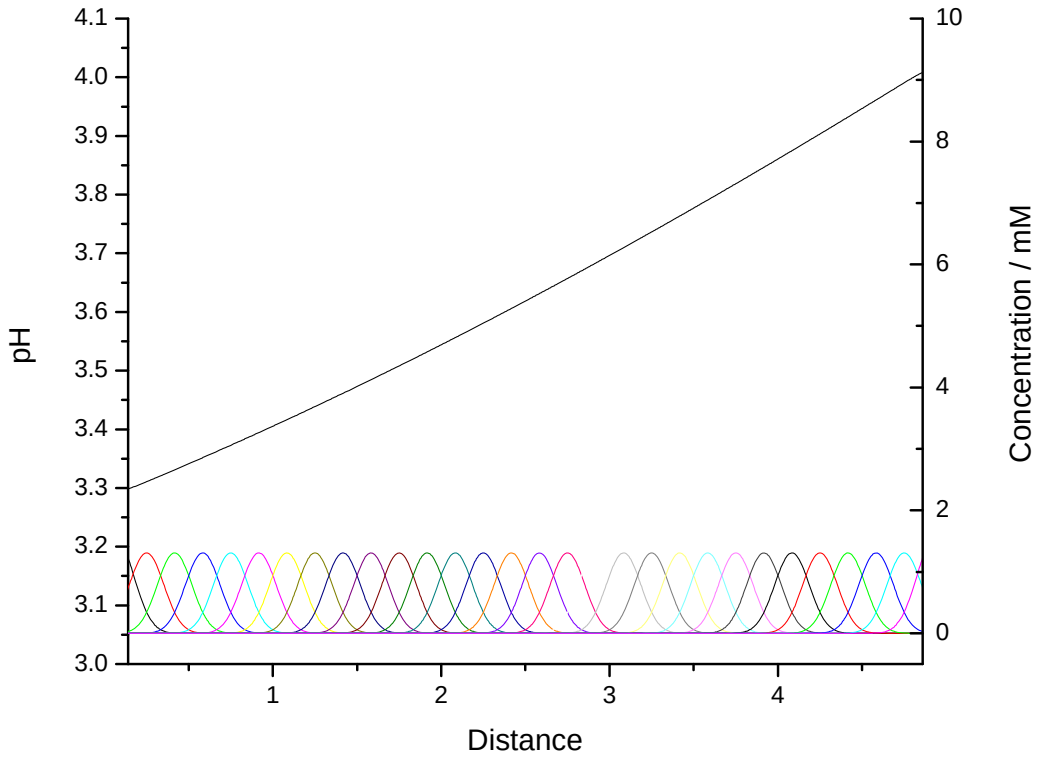

Figure 2. pH and concentration profile for a thirty-carrier ampholyte system. Black represents the theoretical pH, colored lines represent the ampholyte concentrations. The carrier ampholytes have pIs between 3 and 4, the ΔpI between adjacent ampholytes is 0.0333, all have a $\Delta pK_a = 1$. Profiles were generated by the Simul5 software [20].

1.2 Isoelectric trapping

Isoelectric trapping (IET) is an alternative to IEF separations that are achieved in continuous pH gradients as described in section 1.1. In IET, zones of immobilized buffers are arranged with increasing pH from anode to cathode. Ampholytes are separated by trapping them between regions of immobilized buffers whose pH values bracket the pI values of the ampholytes. Trapping occurs because *(i)* ampholytes with pI

values lower than the pH of an immobilized buffer zone become anionic in that zone (thus cannot pass through the zone toward the cathode) and *(ii)* ampholytes with pI values higher than the pH of an immobilized buffer zone become cationic in that zone (thus cannot pass through the zone toward the anode). The immobilized buffer zones can be implemented as gels, membranes or beads, they can be generated with functionalized agarose, acrylamide-based Immobline™ reagents, and hydrolytically stable functionalized poly(vinyl alcohol) (PVA) [6, 21-25]. Selection of the immobilized buffers dictates the shape and range of the pH gradient, as well as the achievable resolution.

1.2.1 Serially arranged IET devices

Most IET devices follow the basic design of a multi-compartment electrolyzer (MCE). MCEs are electrophoretic devices that contain individualized compartments, separated by selective or non-selective ion-permeable barriers to prevent convective mixing of the separated sample zones. Initially, these devices were used for electrodialysis and IEF in conventionally generated pH gradients with neutral or ion-exchange barriers. It wasn't until Martin and Hampson used "ampholytic" immobilized buffer barriers in a MCE that IET was finally realized [6]. In this pioneering work, two MCE devices were designed, both of which follow the basic design shown in Figure 3.

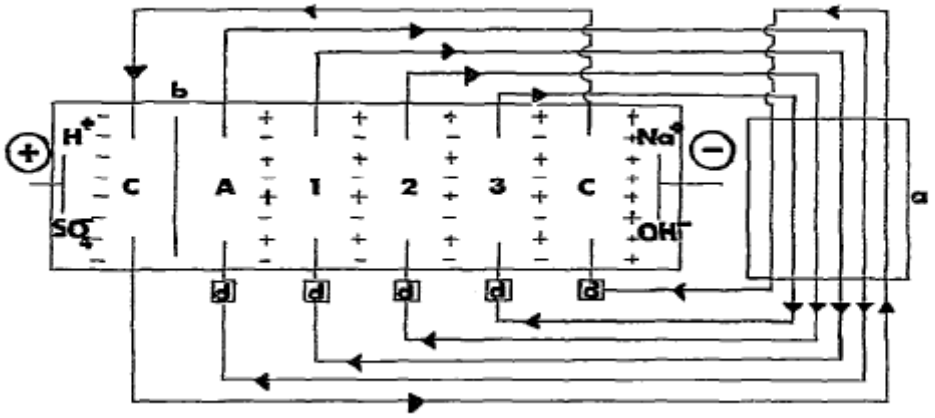

Figure 3. Amphoteric membranes created by combination of cationic and anionic ion exchange membranes (represented by + or – signs, respectively), **d**, external reservoir, **a**, cooler and pumps [6].

These systems were the first to utilize "ampholytic" barriers to achieve separation based on isoelectric point differences. In this format, compartments are arranged serially with the most acidic immobilized buffer enclosing the anode chamber and the most basic immobilized pH buffer enclosing the cathode chamber. The devices even included a recirculating, active cooling system in order to process large sample volumes. The system used cross-linked agarose membranes that were derivatized with varying amounts of chloroacetic acid and diethanolamine and buffered the pH between 4 and 6. However, in addition to the ampholytic barriers, a conventional monovalent buffer was used to supplement the pH gradient, similar to those described in section 1.1.2. The difficulties associated with maintaining a pH gradient with a monovalent buffer paired with the limited range and reproducibility of the agarose-based buffering barriers limited the utility of the system.

Nearly a decade later, with the advent of Immobiline-based IPGs it became possible to create precise, broad-range, immobilized pH gradients for use in a MCE. Initially, Immobiline-based IET devices utilized a single flow-cell bracketed by two IPG strips, one with a pH value below the pI of the target protein and one with a pH value above the pI of the target protein [26-31]. These devices were limited to trapping one component and were soon followed by multi-compartment devices, comparable to the one described by Martin et al., utilizing Immobiline-based buffers cast as thin, glass fiber filter-supported, membranes [32]. The first of the commercial multi-compartment devices, the Isoprime (Figure 4), was a modular system that could accommodate up to 8 collection chambers. Each collection chamber of the Isoprime could be attached to an external reservoir for processing of large volume samples and provide active cooling. The device was successful in the purification of a number of proteins, up to the preparative-scale (~100 mg) [33].

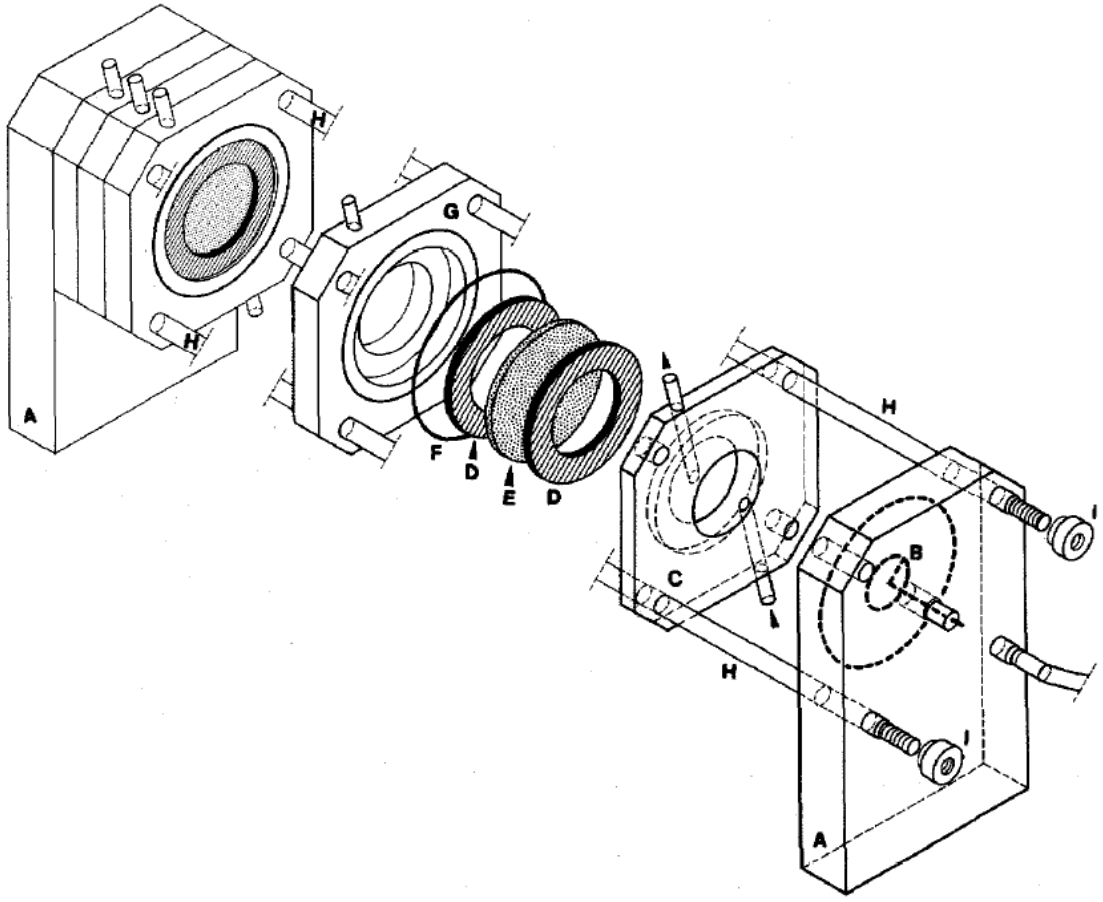

Figure 4. Exploded view of the Isoprime MCE. A = Rectangular supporting legs; B = Pt electrode; C = thin terminal flow chamber; D = rubber rings for supporting the membrane; E = isoelectric Immobiline membrane cast onto the glass-fibre filter; F = O-ring; G = one of the sample flow chambers; H = four threaded metal rods for assembling the apparatus; I = nuts to fasten the metal bolts [33].

In addition to the Isoprime, a number of other serially-arranged multi-compartment electrolyzers have been developed in recent years. The simplest of these utilized wells that contained stagnant liquid for semi-preparative scale separations. The Zoom IEF Fractionator, Figure 5, utilizes five 640 μL Teflon wells to process up to 50 mg of protein for downstream analysis [34]. A more advanced semi-preparative instrument, the

MSWIFT, uses 100-200 µL, thermally conductive ceramic wells that permit an increase in the operational power and is able to generate up to 20 fractions. The MSWIFT has also been championed for use in sample prefractionation [35].

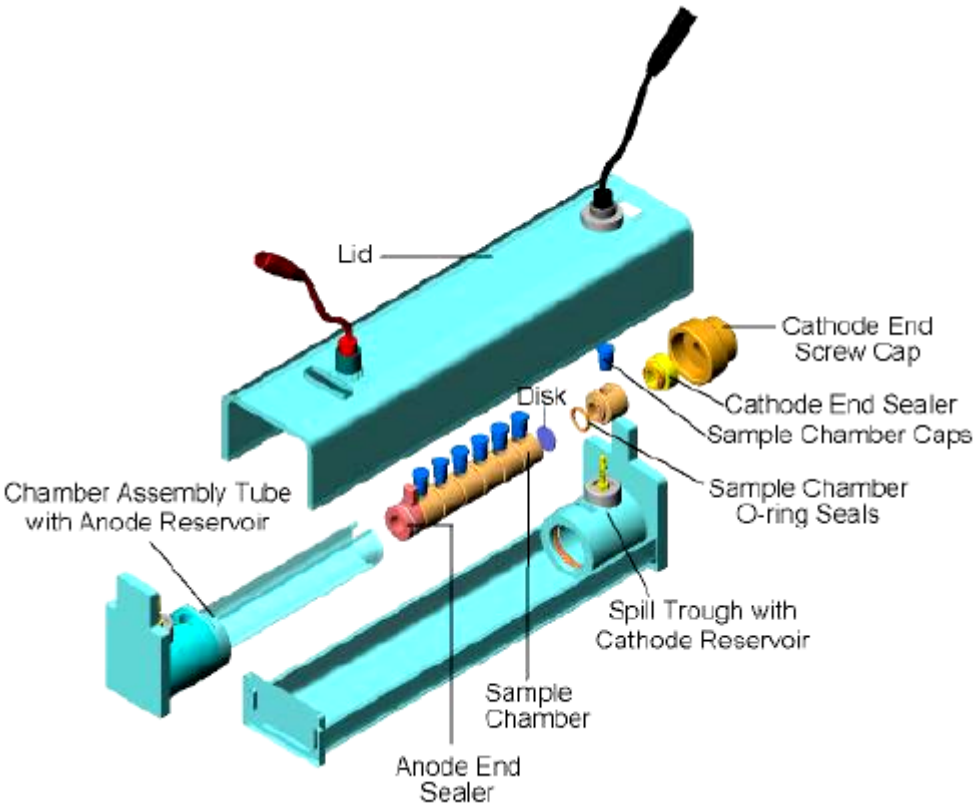

Figure 5. Exploded view of the Zoom IEF Fractionator [36].

A third serially-arranged system, designed to operate in the scale between the semi-preparative Zoom / MSWIFT and the Isoprime, is the IsoelectriQ. The IsoelectriQ utilizes up to seven 5mL compartments that are magnetically stirred and cooled by a Peltier device to process between 50-500 mg of protein [37]. In a deviation from the

well-type MCE, the Rotofor, a preparative IEF device was modified to utilize immobilized buffering membranes. The Rotofor uses a series of annular collection chambers that surround a cold-finger and was used to carry out IET separation of myoglobin and a yeast extract [38].

Though simple, in order for any of these serially arranged MCEs to handle larger samples, increasingly larger separation compartments must be used. In doing so, one increases the anode-to-cathode distance as well as the distance between the buffering membranes. This generates a two-fold problem as (*i*) increases in the anode-to-cathode distance lead to decreased electrical field strength that results in slower electrophoretic velocities and (*ii*) increased distance between the buffering membranes leads to longer migration time between events with separative value (when an ampholyte encounters an immobilized buffering membrane). Additionally, in a serial MCE, if the number of collection chambers is to be increased, the anode-to-cathode distance must also be increased that causes the aforementioned decrease in electrical field strength. All of these problems lead to longer separation times. In order to solve some of these issues, another generation of MCEs, the BF200IET or Twinflow, was designed [39]. A schematic of the Twinflow system is shown in Figure 6.

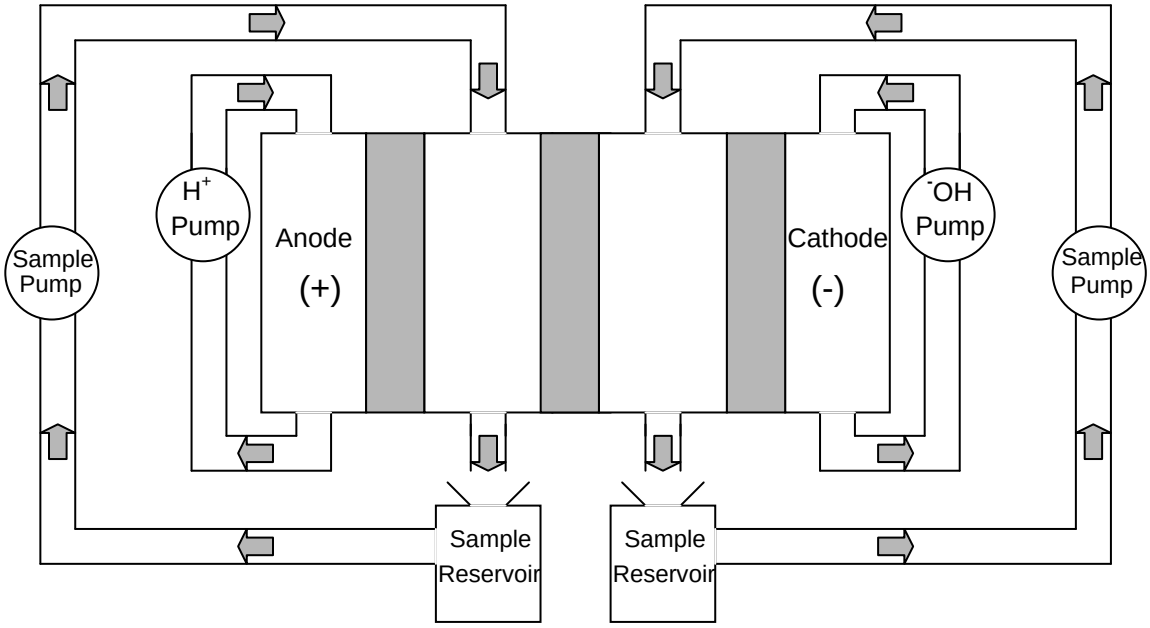

Figure 6. Schematic of the Twinflow MCE.

The Twinflow system consists of an anolyte chamber, a catholyte chamber, and two sample compartments. Each compartment is delimited by at least one buffering membrane. All solutions are recirculated through the chambers and an external cooling system. The Twinflow system has both a very short anode-to-cathode distance (8 mm) and a very short distance between the buffering membranes (1 mm). These two design parameters allow the system to operate at very high field strengths (greater than 1000 V/cm) with minimal migration distance between events with separative value. Obviously, this leads to relatively fast separation times. Though the volume of each separation compartment is relatively small (1.5 mL), large sample volumes can be processed as any size external reservoir can be connected to the separation unit. Additionally, because the Twinflow operates as a recirculating system, an active external

cooling system can be used to control the temperature in the compartments. The Twinflow does have one disadvantage compared to a traditional MCE: it is limited to two separation compartments and thus is only capable of binary IET separations. This means that the Twinflow cannot simultaneously produce multiple sample fractions nor can it isolate a target from a mixture that has components with pI values higher and lower than the target. In a natural progression, a system that applies the design principles of short anode-to-cathode distance, recirculated external cooling, compatibility with large external sample feeds, and short inter-membrane distances was designed [40]. This system, known as the Medusa multi-channel recirculating system (Figure 7), retains the essential design features of the Twinflow while adding the ability to simultaneously generate multiple sample fractions. Unfortunately, the Medusa system is still a serially arranged MCE. Thus, the anode-to-cathode distance, though shortened by a short inter-membrane distance, will always be dependant on the number of chambers used. This means that high field strength can only be maintained for a limited number of compartments. A second problem with serially arranged MCEs is the high voltage drop across the chambers that contain solutions with low conductivity. This problem becomes especially serious when operating at a system's maximal safe voltage. In such a case, all chambers, except those filled with a low conductivity liquid, will experience relatively low electric field strengths. Thus, analytes present in these chambers will have a very slow electrophoretic velocity and migrate very slowly into the chamber where they should remain trapped.

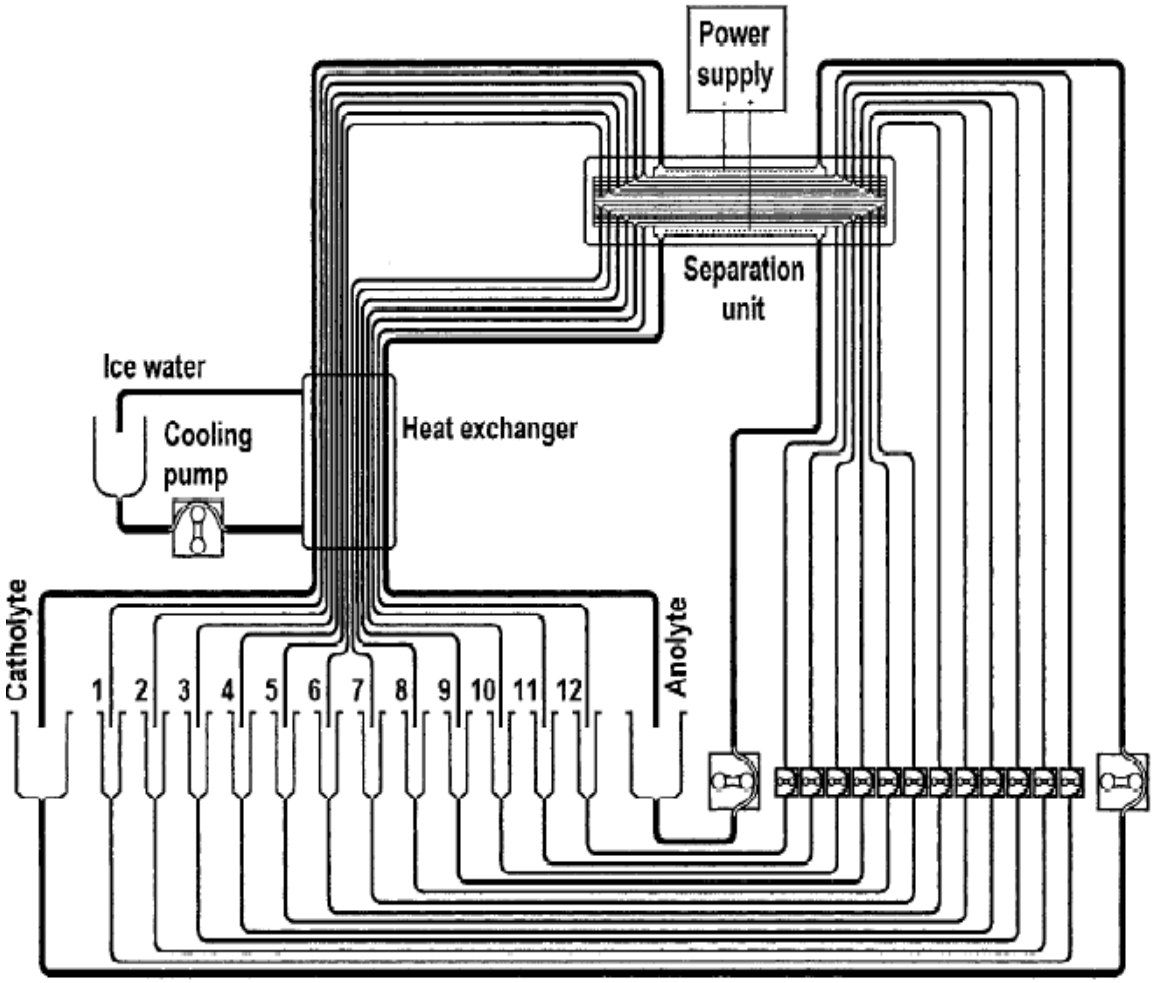

Figure 7. Schematic of the MEDUSA MCE [40].

1.2.2 IET devices with a parallel arrangement of the separation compartments

Recently, three devices appeared that rely on a parallel arrangement of the compartments to carry out IET. Unlike a serially arranged MCE, a parallel MCE's separation compartments are physically isolated from each other. Thus, the electrical potential is applied individually across each separation chamber. Therefore, unlike a serially

arranged MCE, the field strength is independent of the number of compartments and the majority of the available separation potential does not drop over the compartments where the conductivity is low. Two small-scale devices have been designed that utilize such an arrangement [41-43]. The first, now commercially available as the dPC™ Fractionator [41,42], utilizes an array of immobilized buffer plugs that is placed between two buffered sample solutions arranged so that the "isoelectric chip" is orthogonal to the electric field (Figure 8). Separation occurs as the analytes migrate into the gel plugs; when the pH in the gel plug is different from the pI of the analyte, the analyte migrates out of the channel, while analytes with pI = pH will remain trapped in the immobilized gel buffer. Though this system has been applied to a number of protein samples, it is limited to processing μg quantities of proteins [41]. Additionally, the system depends on a random delivery, by mixing, of the sample to the collection "plugs" and each sample is collected inside a gel matrix.

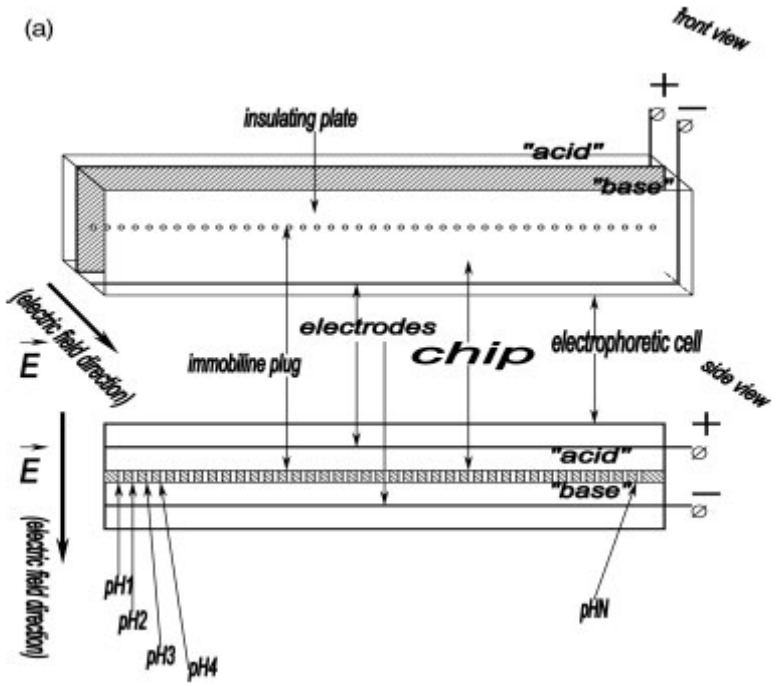

Figure 8. Schematic of the "isoelectric chip"-based dPC™ Fractionator [42].

Alternatively, another parallel-arranged system that allows the processing of increased sample quantities has also been developed: it has a flow-directed sample delivery, and collects samples in solution. Known as the ConFrac, the system operates by simultaneously flowing sample through two channels. Both channels pass buffering membrane-bracketed sample compartments that are placed side-by-side and are orthogonal to the sample channels. One sample channel allows the flow past a series of individualized anode chambers delimited by low pH buffering membranes. The second channel allows flow past a single cathode chamber delimited by a high pH buffering membrane. A schematic diagram of the system can be seen in Figure 9. The ConFrac has

been used to process mg quantities of protein samples and the isolation of small molecule isoelectric markers [43].

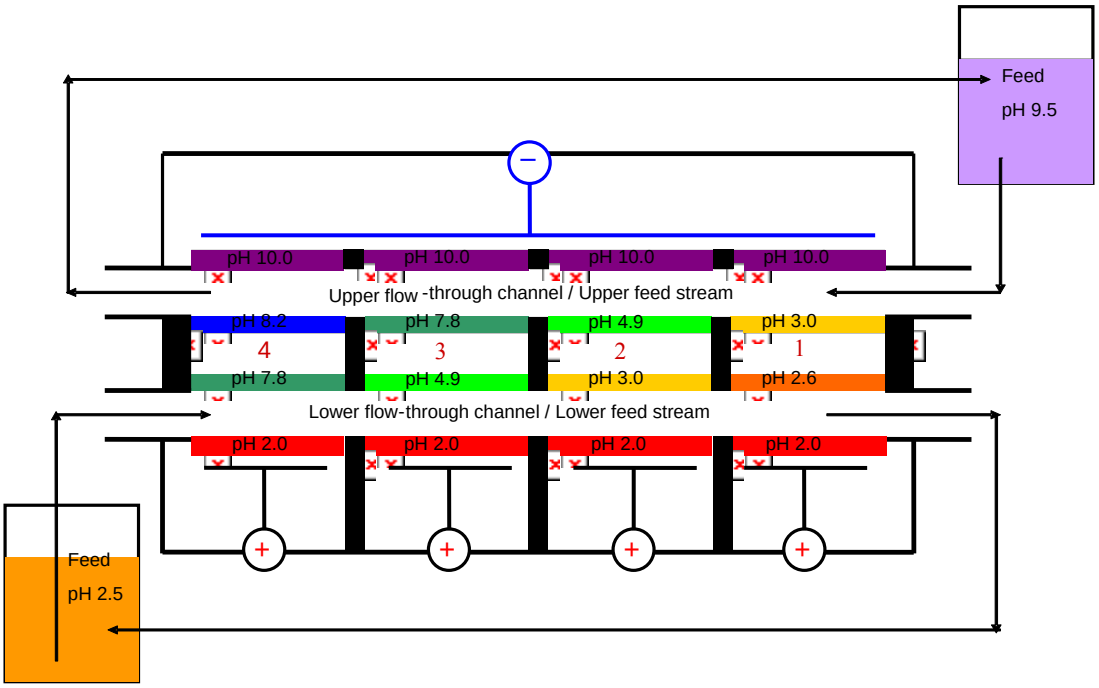

Figure 9. Schematic of the ConFrac system.

The only preparative scale IET device to apply a parallel arrangement is a system that utilizes two Twinflow systems connected through a sample transfer loop, known as the Biflow [44]. A schematic diagram of the system can be seen in Figure 10. The system was originally designed to isolate a single target from a sample which had additional isoelectric components with pI values both above and below the pI of the target. The system was used to successfully isolate mg quantities of both protein and small molecule targets from complex mixtures, but the implications of its properties as a parallel-arranged MCE were not explored.

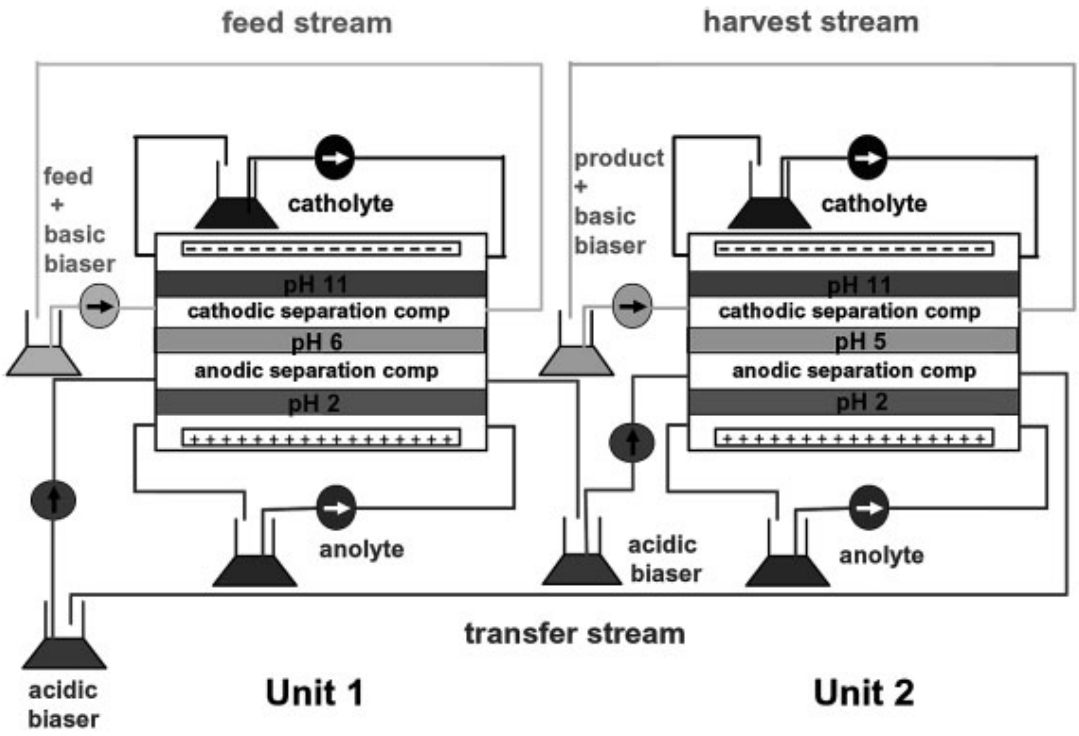

Figure 10. Schematic of the Biflow system [44].

2. LIMITATIONS PREVENTING OPTIMIZED ISOELECTRIC TRAPPING SEPARATIONS

2.1 Difficulties in determination of the pH inside buffering membranes

Rational separation design requires the knowledge of both the pI values of the analytes to be purified and the pH values of the available buffering membranes. The pI values of the analytes can be readily determined using a number of analytical techniques, [8, 45-49]. However, it is more difficult to accurately measure the pH value in the buffering membrane.

The simplest experimental solution would be to directly measure the pH using an electrochemical pH probe. However, since the buffering groups are covalently bonded to the membrane matrix, measurement of the surface pH of the membrane does not accurately reflect what is happening in the pores of the membrane. Due to the critical importance of knowing the pH values of the available buffering membranes, a number of indirect methods have been devised. The pioneers of IET, Martin et al. and Faupel et al. both recognized that by varying the pH of a homogeneous buffer solution that surrounds a buffering membrane, the direction and magnitude of the electroosmotic flow across the membrane can be altered [6,26]. The buffer pH at which the magnitude of the electroosmotic flow across the membrane becomes zero indicates the actual pH in the membrane. Though quite clever, this method is very labor intensive and yields a nominal pH value that can significantly differ from the effective pH value that exists under the

actual operating conditions of the membrane (the effective temperature inside the membrane strongly depends on the amount of Joule heat generated under typical preparative IET conditions).

In light of these difficulties, Righetti's group offered a convenient alternative: they developed a program (commercialized under the trade name “Doctor pH”) that calculates the pH in the Immobiline-based buffering membranes from the pKa values of the Immobilines involved and their amounts added to the polymerization batch [50-52]. Though elegant and convenient, this approach assumes identical incorporation rates for all of the Immobilines, is applicable only for Immobiline-based membranes, and does not permit post-synthesis determination of the membrane pH under actual operating IET conditions.

Alternatively, the operational pH of the buffering membrane can be determined, post synthesis, under typical IET separation conditions, by using the membrane to be characterized as the separation membrane in a binary IET separation of a mixture of pI markers [21-23]. After separation, the pI markers whose pI values are higher than the pH of the separation membrane are collected in the compartment at the cathodic side of the membrane, those with pI values lower than the pH of the separation membrane are collected in the compartment at the anodic side of the membrane. The pH of the membrane is between the pI of the most basic pI marker in the anodic separation compartment and the pI of the most acidic pI marker in the cathodic separation

compartment. In the most advanced version of this method, UV-absorbing carrier ampholytes, obtained either from derivatization of commercial stock or synthesis from pentaethylenehexamine, are used as the pI marker mixture followed by capillary IEF (cIEF) analysis of the two fractions [53]. Since both of these carrier ampholyte mixtures contain hundreds of ampholytes per pH unit, the pH value of the membrane can be very precisely determined as the spacing between the most basic pI marker in the anodic separation compartment and the most acidic pI marker in the cathodic separation compartment should be very small. Unfortunately, there are a few problems with using these carrier ampholyte mixtures: derivatization of commercial carrier ampholytes only generates a mixture with an estimated pI range of $6 < pI < 9$, the addition of significant amounts of UV-absorbing carrier ampholytes disrupts the linearity of the pH gradient in the cIEF analysis, and these materials require laborious, multi-step synthesis and/or processing.

Thus, all current methods for the determination of the buffering pH inside buffering-membranes suffer from significant limitations and it is an area ripe for additional development.

2.2 Limitations of current preparative IET devices

Current preparative IET devices suffer from limitations due to the serial arrangement of the separation compartments, difficulties in the selection of appropriate buffering membranes and the effect of Joule heating on separation selectivity.

2.2.1 Limitations associated with a serially arranged MCE

Though IET in MCEs with serially arranged separation compartments has become a useful technique for fractionation of complex protein or peptide mixtures and purification of single protein targets [54-62], all present serially arranged MCE systems suffer from a collection of intrinsic flaws. The most troublesome are: (*i*) an increase in the size of the collection chamber decreases the field strength, (*ii*) an increase in the number of collection chambers decreases the field strength, and *(iii)* the majority of system potential is dropped across the chambers where conductivity is low.

2.2.2 Selection of appropriate buffering membranes for IET

2.2.2.1 Background and objective

Though extensive work on the determination of the pH inside immobilized buffering membranes will be presented in Section 3, any uncertainties in the pI values of the target ampholytes can limit the utility of these measurements. For this reason, if sufficient amounts of reference sample are available, a trial-and-error method is the most accurate method to screen for appropriate membranes. As an illustration of the limitations in trial-and-error membrane selection, especially when used in a preparative IET instrument such as the Twinflow or Biflow, a membrane selection for the isolation of a monoclonal antibody was performed.

2.2.2.2 Instrument setup, materials, and method

The separation was carried out in a Twinflow MCE that was set up for binary separation. The separation was repeated in four trials, using separation membranes with pH values of 8.7, 8.9, 9.1, and 9.2. Each trial used a pH 2 anodic membrane and a pH 12 cathodic membrane. 850 mL of a solution with an antibody concentration of ~4 mg/mL, carnosine concentration of 10 mM and sucrose concentration of 30 wt% was prepared fresh for each trial and used as the acidic feed solution. A stock solution of 10 mM arginine in 30 wt% sucrose was used as the basic feed solution for all separations. The anolyte was 30 mM methanesulfonic acid (MSA) and the catholyte was 180 mM NaOH, both in 30 wt% sucrose. Feed and collection solutions were recirculated at 30 mL/min. Anolyte and catholyte solutions were recirculated at 2 L/min. All solutions were circulated through individual water-cooled jacketed reservoirs. The system was operated at a constant 150 mA for 15 minutes and the content of the basic collection chamber was analyzed by capillary electrophoresis (CE). All CE runs were completed with a 50 μm internal diameter fused silica capillary (L_t = 26 cm; L_d = 19 cm), operated at 15 kV, using an ε-aminocaproic acid / acetic acid, pH 4.5 buffer as the background electrolyte. The polarity was plus-to-minus.

2.2.2.3 Results and discussion

Electropherograms for the solution in the basic collection chamber are shown in Figure 11. In the experiment, if the separation membrane allows the antibody to pass from the acidic feed stream to the basic collection stream, one can be sure that the membrane

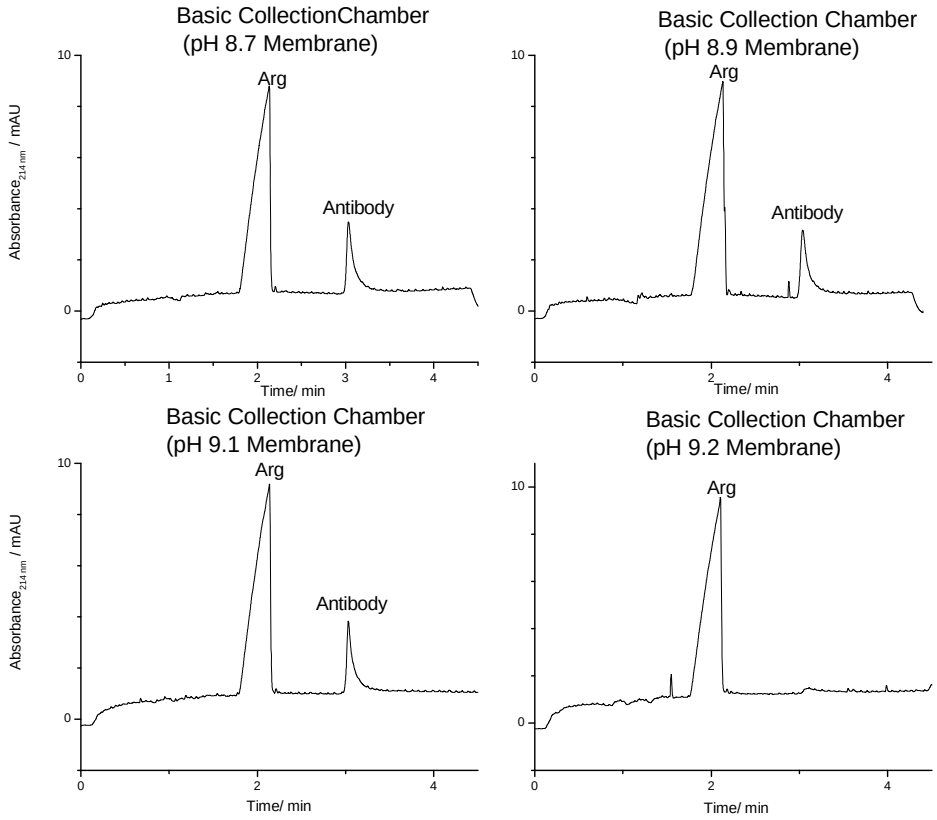

Figure 11. Electropherograms of samples taken from the basic collection chamber of the Twinflow after 15 minutes of IET. Arginine was used as cathodic pH biaser and was present in all samples.

buffers at a pH lower than the pI of the target compound. However, if the antibody remains trapped in the more acidic compartment, one can be sure that the membrane pH is higher than the pI of the target. In this case, the pH 8.7, 8.9, and 9.1 membranes were determined to buffer at a pH lower than the pI of the sample target. The pH 9.2 membrane buffers at a pH higher than the pI of the target. This indicates, that the membrane pair having pH 9.1 and 9.2 would be suitable for the IET isolation of the target antibody. Unfortunately, though accurate, this method is time-consuming for any IET instrument that can only test one membrane per trial; all other devices that can test

multiple membranes are limited by the serial arrangement of their separation compartments.

2.2.3 Effect of Joule heating on separation selectivity

2.2.3.1 Background and objective

Over the course of an IET separation, the power load needed to maintain an efficient separation may change. Since the amount of Joule heat generated is directly related to the electrical power load, the temperature inside the buffering membranes and in the sample compartments may change over the course of the run. This temperature effect may change the pK_a values of both the buffering species inside the membrane and/or the pK_a values (and in turn, the pI) of the target analyte. This can lead to loss of separation as the target leaves its intended collection compartment. In order to probe this temperature effect, the migration behavior of a single isoelectric point marker during a binary IET run was monitored.

2.2.3.2 Instrument setup, materials, and method

The separation was carried out in a Twinflow MCE that was set up for a binary separation. A pH 4.5 membrane was used as the separation membrane. pH 2 and pH 8.7 membranes were used as the anodic and cathodic membrane, respectively. The acidic feed stream contained 2 mM 3,4-diaminobenzoic acid and 10 mM aspartic acid. The basic collection stream contained 10 mM histidine. The anolyte and catholyte were 30 mM MSA and 30 mM lysine, respectively. Feed and collection solutions were

recirculated at 30 mL/min. Anolyte and catholyte solutions were recirculated at 2 L/min. All solutions were circulated through individual, jacketed reservoirs. The reservoirs were thermostated at 2.5 ˚C between 0 and 60 minutes and 25 ˚C between 60 and 140 minutes. The acidic feed and basic collection streams were sampled at 10-minute intervals. All samples were analyzed using CE.

2.2.3.3 Results and discussion

Electropherograms for the samples taken from the acidic feed and basic collection streams at 0, 20, 30, 60, 90, 110, 120, and 140 minutes are shown in Figures 12 and 13.

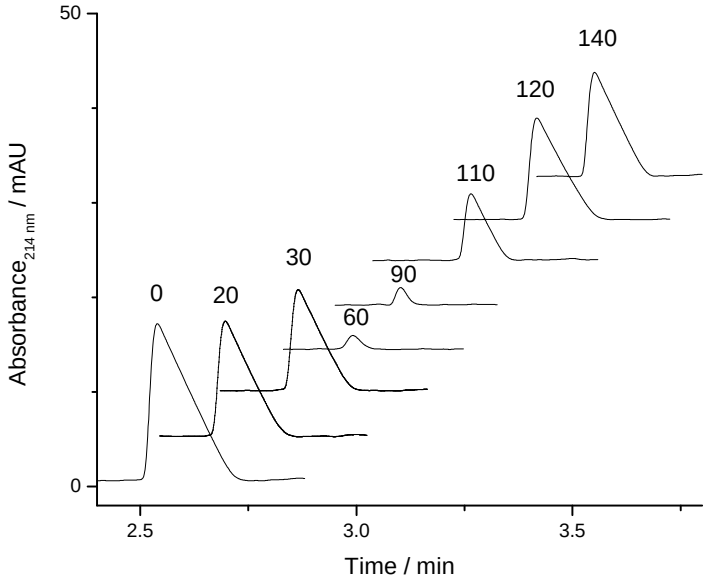

Figure 12. Electropherograms of the samples taken from the acidic separation chamber of the Twinflow over the course of 140 minutes of IET. Each sample has been offset on the absorbance and separation time axis for clarity.

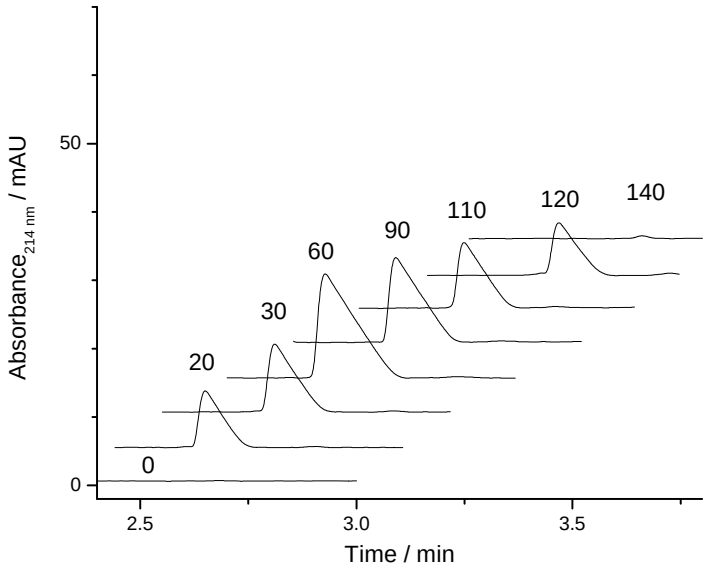

Figure 13. Electropherograms of the samples taken from the basic separation chamber of the Twinflow over the course of 140 minutes of IET. Each sample has been offset on the absorbance and time axes for clarity.

Over the first 60 minutes, while the solutions and the membranes were at a lower temperature, the concentration of the pI marker decreased in the anodic feed stream and increased in the basic collection stream. This demonstrates that under the initial, low temperature conditions, the pH of the separation membrane was appropriate for the separation of 3,4-diaminobenzoic acid and aspartic acid. Between 60 and 140 minutes, while the membranes and the solutions were at a raised temperature, the concentration of the pI marker increased in the anodic feed stream and decreased in the basic collection stream. This demonstrates that at the raised temperature the pH of the separation membrane was no longer suitable for the separation of 3,4-diaminobenzoic acid and

aspartic acid, i.e., separation selectivity was lost: the pH of the membrane was now higher than the pI of the marker. This shift could be due to a change in the pH of the buffering membrane, the pI of the marker, or a combination of both. Regardless of the underlying cause, the experiment demonstrates that a change in the operating temperature of the system can lead to a change in the separation selectivity during IET. This effect can lead to incomplete separations or transfer of ampholytes into unintended compartments. Unfortunately, current designs provide no solution to this problem.

3. DETERMINATION OF THE OPERATIONAL pH VALUE OF BUFFERING MEMBRANES BY ISOELECTRIC TRAPPING SEPARATIONS OF A CARRIER AMPHOLYTE MIXTURE*

3.1 pH determinations using fluorescent carrier ampholyte mixtures

3.1.1 Background and objective

Previous work has shown the utility of phenoxypropyl chromophore-containing UV-absorbing carrier ampholyte mixtures for the determination of the operational pH of buffering membranes [53]. However, if these chromophore-tagged CAs are present in segments of the capillary during isoelectric focusing (cIEF) at a relatively high concentration, they alter, locally, the pH gradient set up by the UV-transparent commercial CAs. Such an alteration would disrupt the linearity of the established pH gradient and affect the accuracy of the extrapolated membrane pH value. Therefore, the amount of UV-absorbing CAs taken from the membrane characterization IET experiment and added to the sample mixture subjected to cIEF analysis has to be minimal. In order to gain improved detection sensitivity, and reduce the load of chromophore-tagged CAs in the cIEF runs, a fluorescent CA mixture was synthesized.

3.1.2 Materials and methods

3.1.2.1 Synthesis and preparation of a fluorescent carrier ampholyte mixture from pentaethylenehexamine

The reaction scheme is presented in Figure 14. Briefly, to a round bottom flask, 1 g of the trisodium salt of 8-hydroxypyrene-1,3,6-trisulfonate, 3 mL of DMSO, 1 eq. of triethylamine and 2 eq. of epichlorohydrin were added. The reaction mixture was maintained at 75 °C with constant stirring in a dry nitrogen atmosphere. After 7 h, 1 eq of pentaethylenehexamine was added and the reaction mixture was maintained at 75 °C, with constant stirring, overnight, in a dry nitrogen atmosphere. The reaction products were desalted and purified by IET in a modified BF200IET unit (Gradipore, French's Forest, NSW, Australia).

3.1.2.2 Analysis of the fluorescent carrier ampholyte mixture obtained from pentaethylenehexamine

Fluorescence excitation and emission spectra of the purified carrier ampholytes were obtained with an Aminco-Bowman Series 2 luminescence spectrometer.

Additionally, cIEF analysis with laser induced fluorescent detection (cIEF-LIF) of the purified carrier ampholyte mixture was completed to confirm that a complex mixture of fluorescent ampholytes was generated. cIEF-LIF electropherograms were obtained with a Beckman PA800 with LIF detection (488 nm excitation). The fluorescent CAs were used in a 4% solution of $3 < pI < 10$ Pharmalyte CAs, with arginine as cathodic blocker.

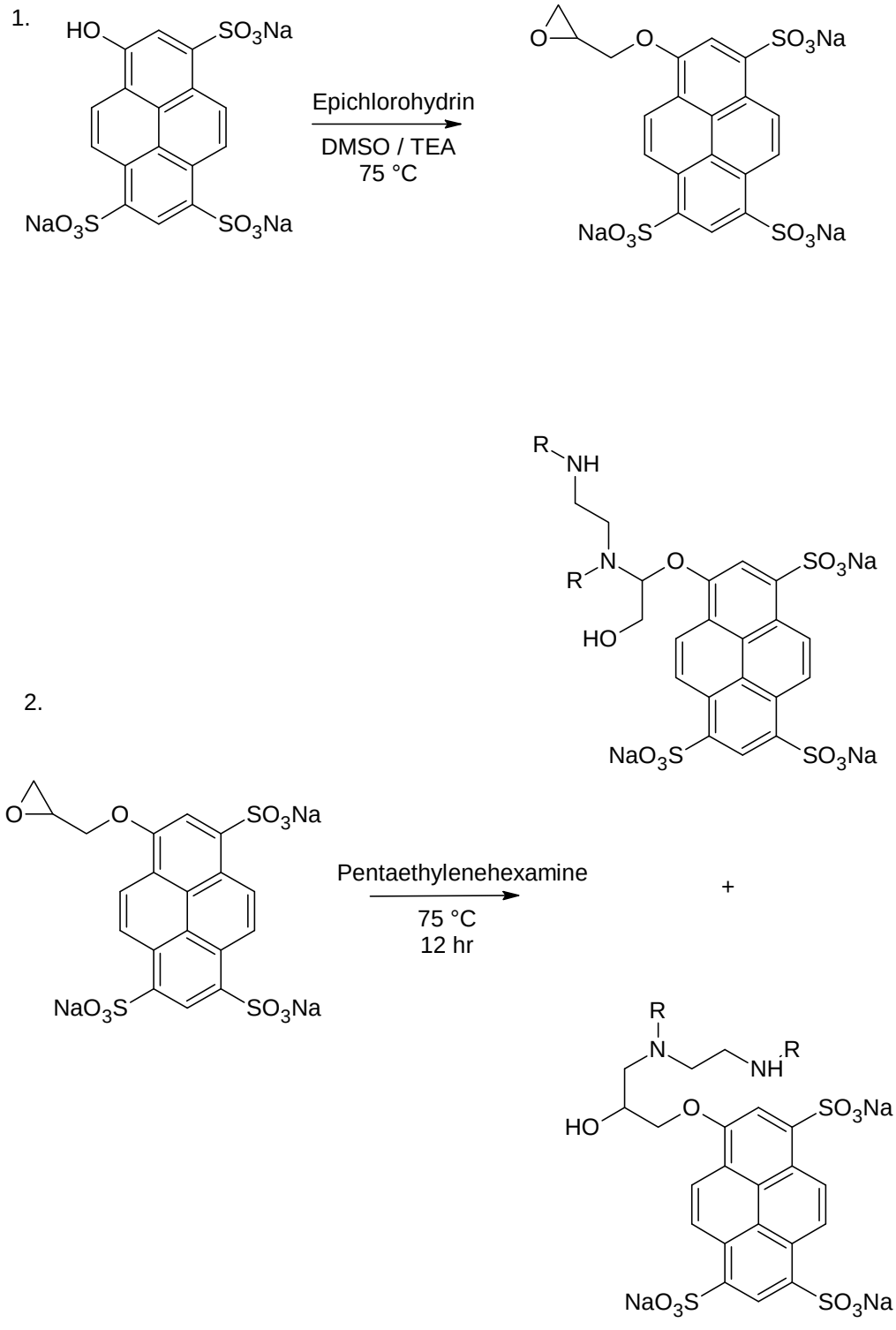

Figure 14. Reaction scheme for synthesis of fluorescent carrier ampholytes. R-hydrogen or additional aliphatic amines.

3.1.2.3 Binary IET fractionation of fluorescent carrier ampholytes

The carrier ampholyte fractionation was carried out in a Twinflow MCE, setup for binary separation. A PVA-based buffering membrane with pH ~2 was used as the anodic membrane. A PVA-based buffering membrane with pH ~12 was used as the cathodic membrane. The separation membrane was also a PVA-based buffering membrane with pH 8.1 < pH < 8.3. The buffering membranes had a nominal thickness of about 150 μm. The anolyte, catholyte and sample solutions were pumped from jacketed reservoirs that were thermostated by an antifreeze solution flowing through a Model 1106 chiller (VWR, Bristol, CT, USA). The anolyte and catholyte were recirculated through the respective compartments of the BF200IET unit at a flow rate of 2 L/min; the sample streams were pumped through the separation compartments at a flow rate of 20 mL/min. Typically, the anolyte was a 30 mM MSA solution and the catholyte was a 180 mM NaOH solution. The IET separation was run in constant current mode with 130 mA, for 1 h, with an initial potential of 400 V and final potential of 560 V. The separation potential was provided by a 900 V, 1200 mA dc power supply (E-C Apparatus, Holbrook, NY, USA).

3.1.2.4 cIEF analysis of the fluorescent carrier ampholyte fractions obtained by IET

The fluorescent CA fractions collected during the IET separations were analyzed by full-column imaging cIEF using an iCE280 unit (Convergent Biosciences, Toronto, Canada) that was equipped with an Alcott 718AL autoinjector and a 96-well microtiterplate adapter (Alcott, Norcross, GA, USA). The separation cartridge of the iCE280 contained

a 5 cm × 100 μm I.D. fluorocarbon-coated fused silica capillary (Convergent Biosciences). For the cIEF separations, the sample transfer time was 130–140 s, the potential was 3 kV, applied for 6–10 min. The analyzed samples were dissolved in a 4% solution of 3 < pI < 10 Pharmalyte CAs that also contained ElphoMark pI markers in 50–250 μM concentration. The electropherograms were processed by the EZ Chrom (Scientific Software, Pleasanton, CA, USA) and Origin 6.1 (OriginLab, Northhampton, MA, USA) software packages.

3.1.3 Results and discussion

Fluorescence excitation and emission spectra for the purified fluorescent CA mixture are shown in Figures 15 and 16. The excitation spectrum shows a broad excitation band with λ_{max} = 465 nm. This indicates that these CA are suitable for cIEF-LIF with a number or currently available laser sources.

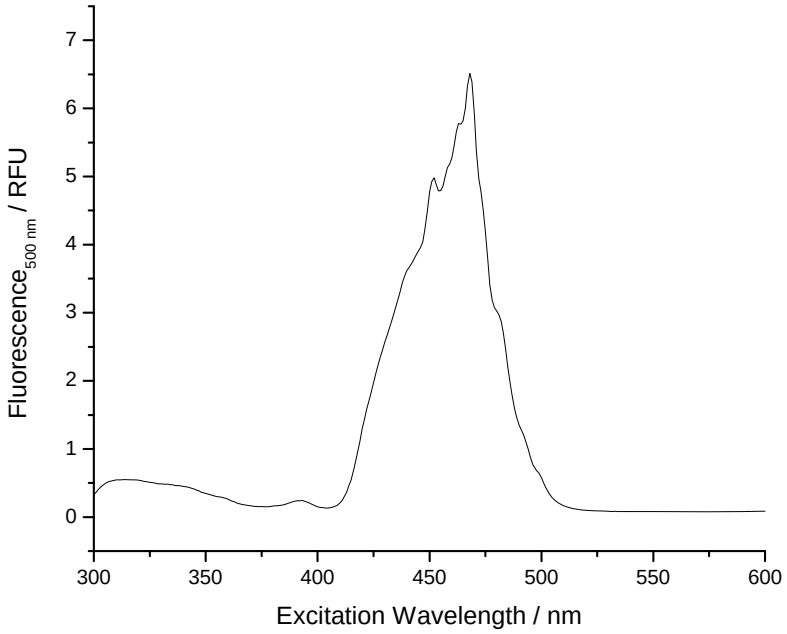

Figure 15. Fluorescence excitation spectrum for the purified fluorescent CA mixture.

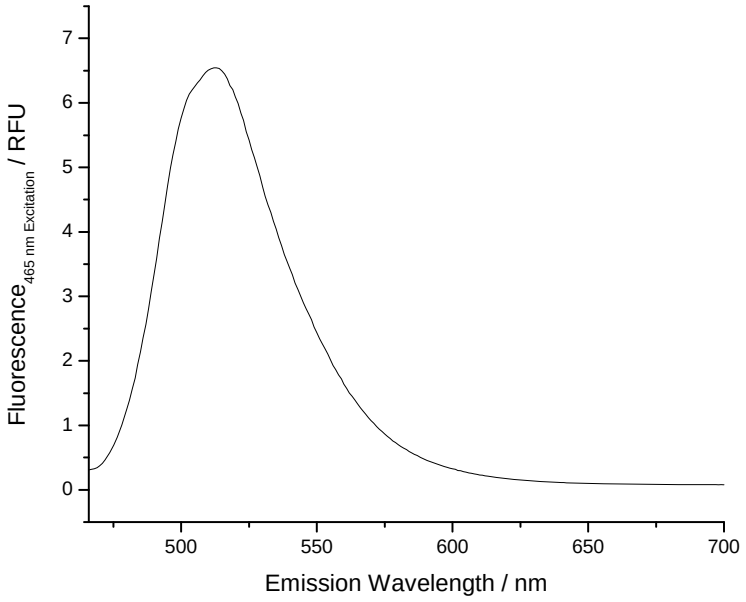

Figure 16. Fluorescence emission spectrum for the purified fluorescent CA mixture excited at 465 nm.

cIEF-LIF analysis of the purified fluorescent CA mixture is shown in Figure 17. It is important to note that this electropherogram was obtained using a single-point detector, and pressure was used to mobilize the focused carrier ampholytes past the detector. Therefore, the first 6 minutes of the electropherogram represent the focusing of the carrier ampholytes and may display transient peaks. Once focusing is completed and pressure is applied, a clear drop-off of the fluorescence at ~6 minutes is observed. This drop-off represents a focused band of arginine, added to ensure that none of the carrier ampholytes are focused beyond the detector window. The arginine band is followed by a plethora of focused bands spanning from ~20-70 minutes. These peaks confirm that a complex mixture of fluorescent ampholytes has been generated and should be suitable for use in determining the pH inside buffering membranes.

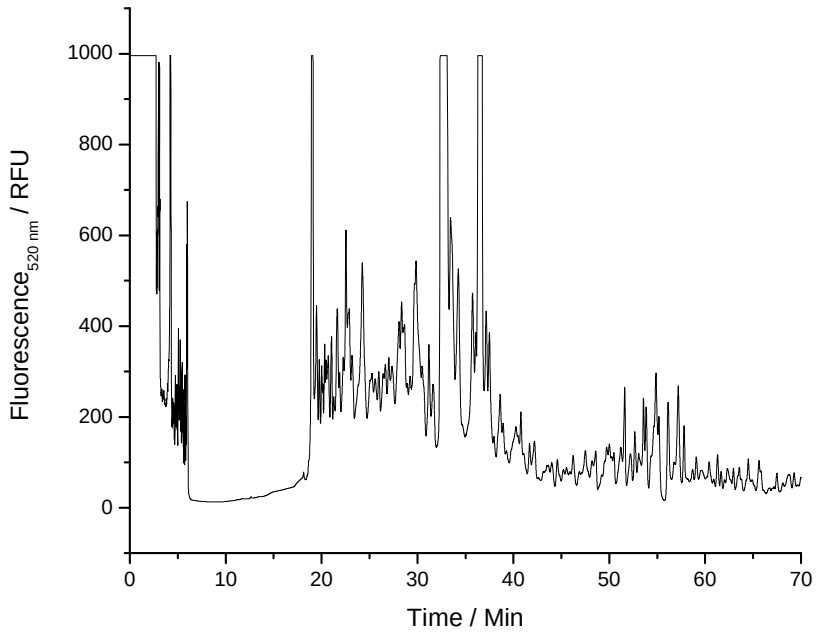

Figure 17. cIEF-LIF analysis of the purified fluorescent carrier ampholyte mixture.

Additionally, cIEF analysis using full-column imaging UV absorbance detection of the purified fluorescent CA mixture is shown in the top panel of Figure 18. Unlike in cIEF-LIF, where a single-point detector was used, full-column imaging detection does not need any type of mobilization and allows for near real-time monitoring of the progress of the separation. Based on fitting the focusing positions and the known pI values of the pI markers, the CAs are all in the $6 < pI < 9.75$ range. Unlike previous carrier ampholytes synthesized for membrane pH determinations, no acrylic acid was used in the synthesis and all the negative charges on the CAs came from the sulfonate groups of the fluorophore [53]. Consequently, only components with relatively high pI values are expected to be present in the tagged CA mixture.

In order to determine the pH of a buffering membrane, the membrane was installed in the BF200IET unit as the separation membrane. A 10 mL portion of a 10 mM solution of IDA was added to the solution reservoir of the anodic separation compartment. A 10 mL portion of an approximately 2% (w/w) solution of the purified, fluorescent CA mixture was added to the solution reservoir of the cathodic separation compartment. The separation potential was applied and IET was continued until the conductance and pH values in both the anodic and cathodic separation compartments reached their respective steady state values. Loading the fluorescent CA mixture only into the cathodic separation compartment simplified the analytical work: one only had to determine the pI value of the most basic labeled CA ampholyte that moved into the anodic separation compartment during the IET separation.

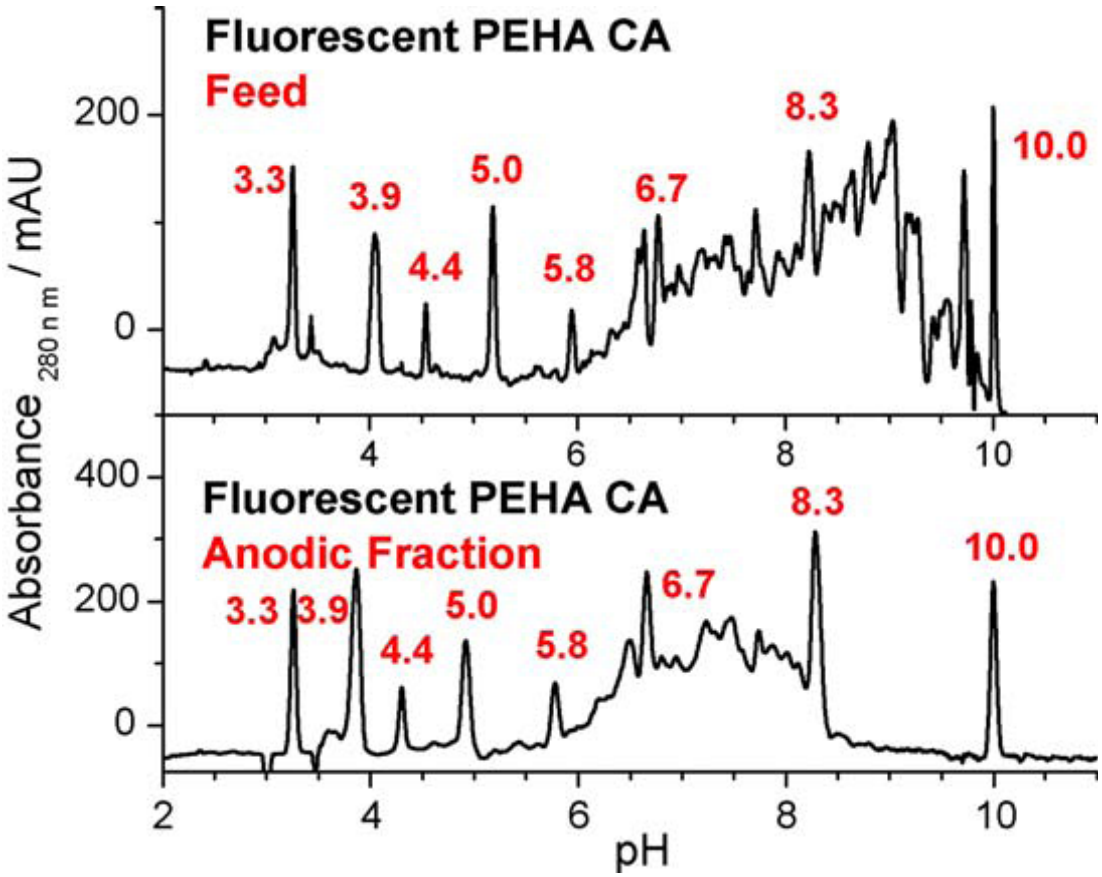

Figure 18. Full column imaging cIEF separation of (i) the tagged carrier ampholyte mixture synthesized from the sodium salt of 8-hydroxy-1,3,6-pyrenetrisulfonic acid, epichlorohydrin and PEHA, and used as the initial feed mixture in the IET experiment (top panel) and (ii) the fraction collected from the anodic separation compartment at the end of the IET separation (bottom panel). Nominal pH of the separation membrane: 8.1 < pH< 8.3.

Since the alkoxypyrenetrisulfonate group has a higher molar absorbance than the phenoxypropyl group, the concentration of the tagged CA required for the cIEF analysis was less than one half of what was required for the phenoxypropyl-tagged CAs.

The results of the cIEF analysis for the fraction collected from the anodic separation compartment at the end of the IET separation are presented in Figure 18. There is a very

clear drop off in the UV absorbance at the high pI side in the fraction taken from the anodic separation compartment indicating that the operational pH of the buffering membrane during IET was about 8.25 (just below the pI = 8.3 marker). It is expected that once full-column imaging fluorescence detection (see, e.g., Refs. 63, 64) becomes commercially available, the required tagged CA load can be reduced even further.

3.2 pH determinations using commercial UV-transparent carrier ampholyte mixtures

3.2.1 Background and objective

While the method shown in section 3.1 yielded accurate membrane pH values, it had a practical difficulty: preparation of the fluorescent CAs required considerable time and effort, which became a significant burden when the method was used daily for the characterization of a large number of buffering membranes. However, recently it was realized that the monotonity of the pH gradient, the foundation of every IEF separation can be exploited to develop a simple method for the determination of the operational pH value of a buffering membrane. This new membrane pH determination method is described here. In the first step (Figure 19a), a binary IET separation of a conventional, UV-transparent, commercially available $3 < pI < 10$ CA mixture is carried out in a two-separation compartment MCE with the membrane to be characterized installed as the separation membrane.

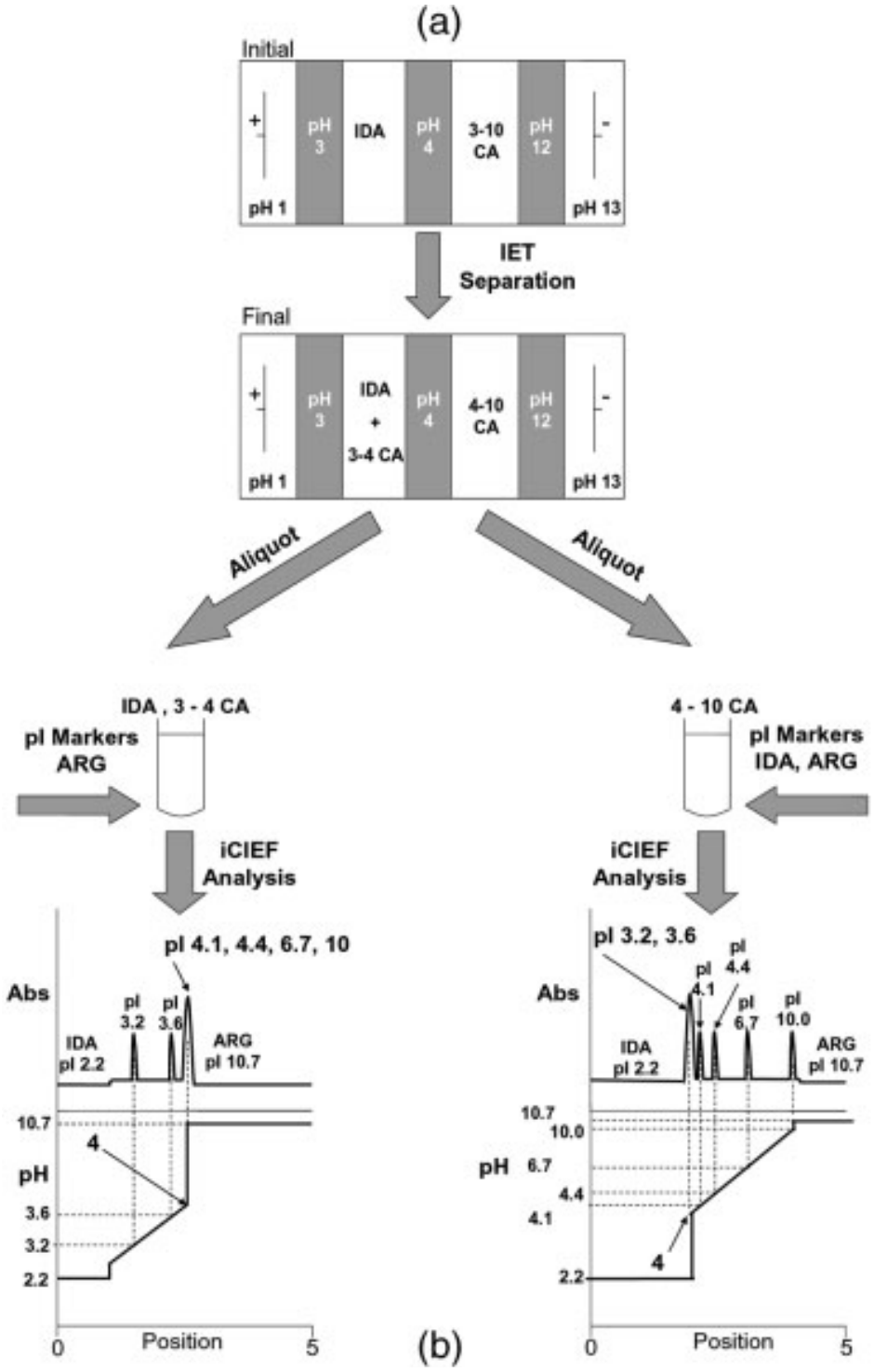

Figure 19. Schematic of the membrane pH determination method. Top panel: IET separation of the 3 < pI < 10 CA mixture in the BF200IET unit. Bottom panel: preparation of the low pI and high pI samples, cIEF analysis of the samples and schematic of the resulting electropherograms.

In the second step (Fig. 19b), a sufficient amount of a UV-transparent, acidic ampholyte (anodic blocker, pI < 3), a sufficient amount of a UV-transparent, basic ampholyte (cathodic blocker, 10 < pI), and a few, appropriately chosen pI markers are added to an aliquot of the CA mixture trapped in both the anodic and the cathodic separation compartments of the MCE. In the third step, both mixtures are then analyzed by cIEF and the electropherograms are evaluated as shown later to obtain the operational pH value of the buffering membrane.

3.2.2 Materials and methods

3.2.2.1 IET equipment and procedure

The operational pH value of the buffering membrane to be characterized was determined by carrying out a binary IET separation of a Pharmalyte 3 < pI < 10 CA mixture in a modified BF200IET unit (Gradipore, French's Forest, NSW, Australia) [38]. The membrane to be characterized was installed as the separation membrane. The BF200IET apparatus was thermostated by a Model 1106 chiller (VWR, Bristol, CT, USA) and powered by a 900 V, 1200 mA dc power supply (E–C Apparatus, Holbrook, NY, USA). In the IET experiments, the anolyte was always a 30 mM MSA solution; the catholyte was a 180 mM NaOH solution. The buffering membranes had an active surface area of about 15 cm^2 and a thickness of about 0.15 mm. The intermembrane distances were about 1 mm. The separation compartments had a volume of about 1.5 mL each. Solutions in the separation compartments were recirculated at a flow rate of 30 mL/min.

The anolyte and catholyte solutions were recirculated at flow rates of 2000 mL/min. All solutions were pumped from jacketed glass reservoirs that were thermostated at about 15 ˚C. All buffering membranes were PVA-based membranes synthesized in our laboratory [21-23, 25]. Their nominal pH values were as follows: anodic membranes, $1.5 < pH < 2$; cathodic membranes, $11.5 < pH < 13$; separation membranes about pH 3.9, 4.2, and 8.9. The reservoirs connected to the anode and cathode compartments contained 100 mL of the anolyte and catholyte, respectively. For the characterization of the pH 3.9 and 4.2 buffering membranes, the reservoir connected to the anodic separation compartment was filled with 30 mL of a 20 mM iminodiacetic acid (IDA) solution, the reservoir connected to the cathodic separation compartment was filled with 30 mL of an 8% w/w solution of a $3 < pI < 10$ CA mixture. For the characterization of the pH 8.9 buffering membrane, the reservoir connected to the anodic separation compartment was filled with 30 mL of an 8% w/w solution of a $3 < pI < 10$ CA mixture, the reservoir connected to the cathodic separation compartment was filled with 30 mL of a 20 mM arginine (ARG) solution. These arrangements insured that (i) the receiving separation compartment always had an adequate initial conductivity and (ii) that as the separation progressed, more and more of the applied voltage dropped across the separation compartment that contained the feed CA solution (this helped the timely completion of the IET separation). The IET separations were continued for 2 h at 500 mA, in constant current mode. At the end of the separation, aliquots were taken both from the anodic and cathodic separation compartments of the BF200IET and analyzed by cIEF as described in the next section.

3.2.2.2 Analytical equipment and procedure

An appropriate volume of a stock solution containing anodic and cathodic blockers, ElphoMark pI markers and methylcellulose were added directly to the aliquots taken from the anodic and cathodic separation compartments of the BF200IET at the end of the IET separation. The two samples thus obtained were then analyzed by an iCE280 full-column imaging capillary electrophoretic device (Convergent Biosciences, Toronto, Canada). The separation capillary was a 5 cm long, 100 mm i.d. fluorocarbon-coated fused-silica capillary (Convergent Biosciences). In the analytical IEF separations, the anolyte was always a phosphoric acid solution, the catholyte a sodium hydroxide solution. The samples were injected by an Alcott 718AL autoinjector (Alcott, Norcross, GA, USA) using a sample transfer time of 140 s and analyzed by applying an initial potential of 500 V for 30 s and a separation potential of 3 kV for 600 s. The electropherograms were processed by the EZ Chrom (Scientific Software, Pleasanton, CA, USA) and Origin 6.1 (OriginLab, Northhampton, MA, USA) software packages.

3.2.3 Results and discussion

3.2.3.1 The membrane pH determination method

The new membrane pH determination method is shown schematically in Figure 19a and 19b. In the first step, an MCE containing two separation compartments (such as the BF200IET unit) is assembled and the buffering membrane whose pH is to be determined is installed as the separation membrane. Next, if the expected pH of the membrane is below 7, the anodic separation compartment of the MCE is filled with a 20 mM solution

of an acidic (pI < 3), single-component ampholyte (e.g., IDA). The cathodic separation compartment is filled with an 8% w/w solution of a 3 < pI < 10 CA mixture. Then, an IET separation is carried out, in constant current mode (e.g., at 500 mA), for a time long enough (e.g., for 2 h) to complete the transfer of the movable CAs. During this time, CAs with 3 < pI < $pH_{membrane}$ pass through the separation membrane and accumulate in the IDA solution that is recirculated through the anodic separation compartment of the MCE. CAs with $pH_{membrane}$ < pI < 10 remain in the solution that is recirculated through the cathodic separation compartment of the MCE. At the end of the IET separation, an aliquot is collected from the anodic separation compartment of the MCE. This aliquot is then mixed with (i) a set of UV-absorbing pI markers (e.g., pI 3.2; 3.6; 4.1; 4.4; 6.7; 9.6; and 10.0) and (ii) enough ARG to make the solution at least 20 mM in ARG. This mixture is referred to as the low pI sample. Another aliquot is collected from the cathodic separation compartment of the MCE. This second aliquot is mixed with (i) enough IDA to make the solution at least 20 mM in IDA, (ii) with the same (or different) set of UV-absorbing pI markers, and (iii) enough ARG to make the solution at least 20 mM in ARG. This mixture is referred to as the high pI sample.

The low- and high-pI samples thus prepared are then analyzed by cIEF yielding a train of bands that contiguously fill the capillary from its anodic end to its cathodic end. For the low pI sample, the train of adjacent bands (starting from the anode) is formed by: (i) IDA (originally added to the anodic separation compartment of the MCE), (ii) CAs with 3 < pI < $pH_{membrane}$ (CAs that moved through the separation membrane and into the

anodic separation compartment of the MCE), interspersed with the separated pI markers having $3 < pI < pH_{membrane}$ (added in the sample preparation step), (iii) pI markers with $pH_{membrane} < pI < 10$ (added in the sample preparation step), and (iv) ARG (added in the sample preparation step). Since the pI markers having 3 < pI < pH-membrane are in what is in fact a "narrow-range" CA mix (CA mix with $3 < pI < pH_{membrane}$), they are separated from each other (as they would be in a normal cIEF run) allowing for the construction of a conventional pI versus focusing position calibration curve. Since the pI markers with $pH_{membrane} < pI < 10$ are outside the pI range of the CAs present in the low-pI sample, the bands of these pI markers are adjacent to each other and appear as a tightly squeezed, "unresolved" UV-absorbing band between the last CA (CA with $pI = pH_{membrane}$) and ARG. The focusing position of this "unresolved band", according to the acidic range calibration curve, yields the $pH_{membrane}$ value sought. For the high-pI sample, the train of adjacent bands (starting from the anode) is formed by: (i) IDA (added in the sample preparation step), (ii) pI markers with $3 < pI < pH_{membrane}$ (added in the sample preparation step), (iii) CAs with $pH_{membrane} < pI < 10$ (CAs that did not move through the separation membrane and remained in the cathodic separation compartment of the MCE), interspersed with the separated pI markers having $pH_{membrane} < pI < 10$ (added in the sample preparation step), and (iv) ARG (added in the sample preparation step). Since the pI markers with $pH_{membrane} < pI < 10$ are in what is in fact another "narrow-range" CA mix (CA mix with $pH_{membrane} < pI < 10$), they are separated from each other allowing for the construction of another conventional pI versus position calibration curve. Since the pI markers having $3 < pI < pH_{membrane}$ are outside the pI

range of the CAs present in the high pI sample, the bands of these pI markers are adjacent to each other and appear as a tightly squeezed, "unresolved", UV-absorbing band between IDA and the first CA (CA with pI = $pH_{membrane}$). The focusing position of this "unresolved" band, according to the basic range calibration curve, again yields the $pH_{membrane}$ value sought. If the expected membrane pH is above 7, the anodic separation compartment is filled with a solution that contains an 8% w/w solution of $3 < pI < 10$ CAs. The cathodic separation compartment of the MCE is filled with a 20 mM solution of a basic, single-component ampholyte that has a pI value higher than 10 (e.g., ARG). Then, an IET separation is carried out, in constant current mode, at 500 mA, for 2 h. During this time, the $pH_{membrane} < pI < 10$ CAs pass through the buffering membrane and accumulate in the ARG solution that is recirculated through the cathodic separation compartment. The $3 < pI < pH_{membrane}$ CAs remain in the solution that is recirculated through the anodic separation compartment. At the end of the IET separation, an aliquot is collected from the anodic separation compartment and it is mixed with (i) enough IDA to make the solution at least 20 mM in IDA, (ii) a set of UV-absorbing pI markers (e.g., pI 3.2; 3.6; 4.1; 4.4; 6.7; 9.6; and 10.0), and (iii) enough ARG to make the solution at least 20 mM in ARG. This solution is known as the low pI sample. Another aliquot is collected from the cathodic separation compartment and it is mixed with (i) enough IDA to make the solution at least 20 mM in IDA and (ii) the same (or different) set of UV-absorbing pI markers. This solution is known as the high-pI sample. The two samples thus prepared are then analyzed by cIEF and the results interpreted as described above for the characterization of the $pH < 7$ membrane.

3.2.3.2 Use of the new membrane pH determination method

A nominal pH 4.2 membrane was selected for the first test. During 500 mA constant current IET, the initial potential was 44 V, the final potential (at the end of 2 h) was 110 V. To prepare the low-pI sample, the aliquot taken from the anodic separation compartment was mixed with pI markers 3.2, 3.6, 4.1, and 4.4, and ARG. To prepare the high-pI sample, the aliquot taken from the cathodic separation compartment was mixed with IDA, pI markers 3.6, 4.1, 4.4, and 10.0, and ARG. Figure 20 shows the results of the cIEF analysis of the low-pI (top panel) and high-pI (bottom panel) samples. The 3-point low pI calibration curve yields pI 4.21 for the most basic peak (marked by *). The 4-point high pI calibration curve yields pI 4.27 for the most acidic peak (marked by *). Three parallel experiments using membranes cut from the same stock sheet yielded an average membrane pH value of 4.24 ± 0.03 (based on the anodic separation compartment samples) and 4.29 ± 0.03 (based on the cathodic separation compartment samples). Similar tests for a nominal pH 3.9 (Figure 21) and a nominal pH 8.9 (Figure 22) buffering membrane yielded 3.93 ± 0.01 (anodic separation compartment samples) and 3.98 ± 0.01 (cathodic separation compartment samples) as well as 8.86 ± 0.07 (anodic separation compartment samples) and 8.99 ± 0.04 (cathodic separation compartment samples), respectively (three parallel experiments each). The membrane pH values determined with the help of the anodic separation compartment samples are typically slightly lower than the pH values determined with the help of the cathodic separation compartment samples. We have found that this systematic error can be as low

as 0.02 when only one pI marker is used outside the pI range of the CA fraction, and it can be as high as 0.05 when multiple pI markers are used outside the pI range of the CA fraction. Convenience calls for the use of a pI marker mixture with multiple components; the price for this convenience is a slight decrease in accuracy.

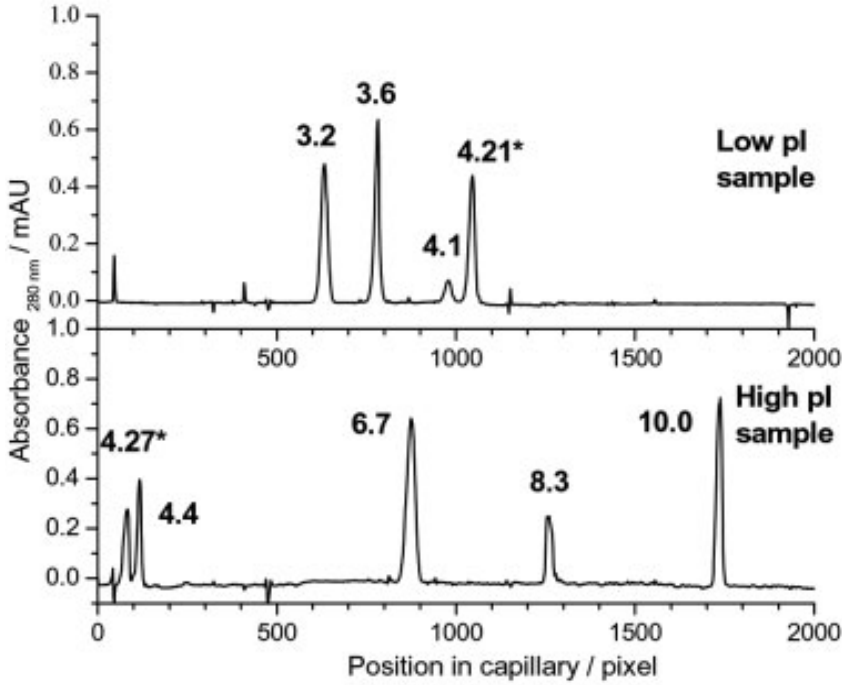

Figure 20. Full column imaging cIEF separation of the low pI sample (top panel) and high pI sample (bottom panel) obtained during the determination of the operating pH value of a nominal pH 4.2 buffering membrane.

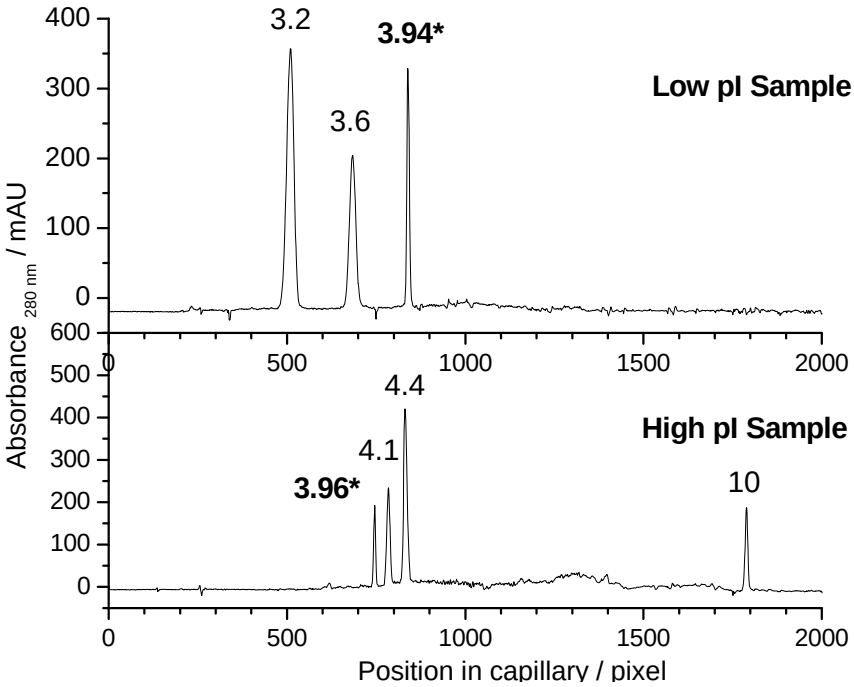

Figure 21. Full column imaging cIEF separation of the low pI sample (top panel) and high pI sample (bottom panel) obtained during the determination of the operating pH value of a nominal pH 3.9 buffering membrane.

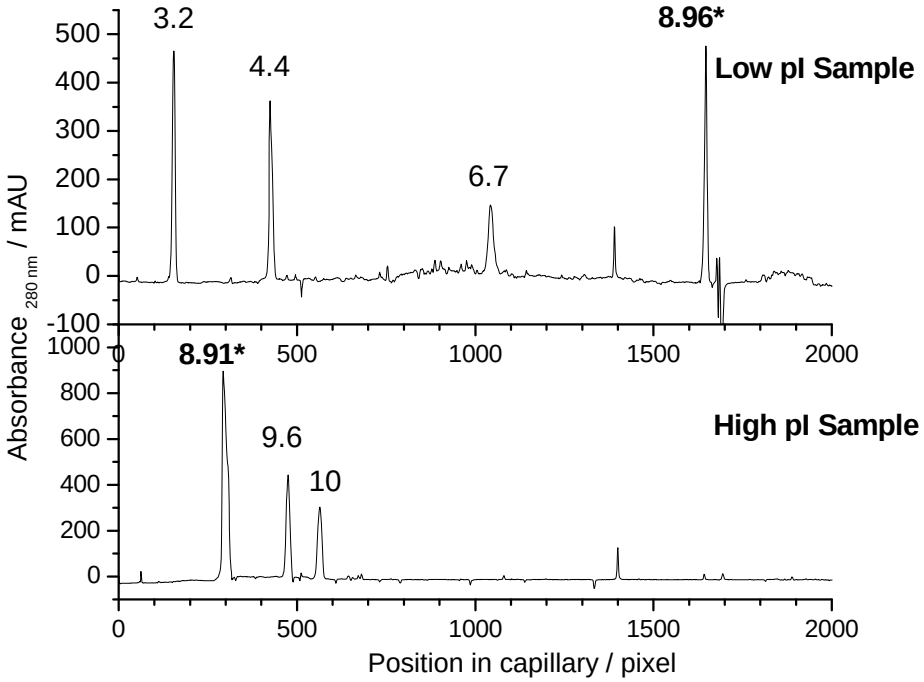

Figure 22. Full column imaging cIEF separation of the low pI sample (top panel) and high pI sample (bottom panel) obtained during the determination of the operating pH value of a nominal pH 8.9 buffering membrane.

4. DESIGN AND MANUFACTURE OF A NEW, PREPARATIVE-SCALE ISOELECTRIC TRAPPING DEVICE

4.1 Objectives for a new preparative-scale IET device

In light of the limitations of the current preparative MCEs, it is simple to form a set of objectives for the design of a new system. Key factors in the design of a new preparative MCE include: (i) improve scalability in terms of number of fractions, power input, and amounts processed, (ii) replace electrophoretic chamber-to-chamber transport with convective delivery, (iii) create an orthogonal delivery and harvesting scheme, (iv) provide multiple destinations to correct for temperature-induced selectivity changes, (v) avoid parasitic potential drops that don't have separative value.

4.2 Means to achieve the objectives for a new preparative-scale IET device

The following sections describe the specifics for the design and manufacture of the parallel-arranged preparative-scale MCE that has countercurrent sample flow paths past a co-directional pH gradient. This device is called T-RECS for ***t***rapping by ***r***ecursive ***e***lectrophoresis in a ***c***ompartmentalized ***s***ystem. The main design elements used to meet the objectives for the system were: (i) parallel arrangement for the electrodes and collection compartments, (ii) directionally-controlled convection system for delivery of analytes, (iii) short anode-to-cathode distance, (iv) short intermembrane distances, (v) an external cooling system, (vi) use of hydrolysis-resistant structural materials.

4.3 T-RECS: design overview

Figure 23 shows a schematic for a system that incorporates all six of the design elements described in Section 2.2. This system utilizes four separation heads, each head containing the following chambers: anodic chamber, cathodic chamber, acidic flow-through channel, basic flow-through channel, and a collection channel. Each chamber/channel is delimited by either one (anodic and cathodic chambers) or two buffering membranes (collection and feed channels). The four collection channels are bracketed by five different buffering membranes. The most acidic of these five membranes forms the low pH barrier for trapping in the first collection channel. Conversely, the most basic of the five membranes forms the high pH barrier for trapping in the fourth collection channel. The remaining membranes are arranged in such a way that the more basic membrane bracketing a collection channel has the same pH as the more acidic membrane bracketing the collection channel in the next separation head. This way, one forms a continuous pH gradient orthogonal to the segmented pH gradient of each separation head. The use of a continuous pH gradient in one dimension guarantees that all ampholytic compounds will have a final destination. If one were to leave "gaps" in either of the pH gradients, ampholytes whose pI values fall into the gaps would be continuously recirculated through the flow-through channels and would transiently pass through various collection channels. The acidic flow-through channels are bracketed by a low pH anodic membrane (on the anodic side) and by the lower pH separation membrane that encompasses the adjacent collection channel (on the other side). The basic flow-through channels are bracketed by a high pH cathodic membrane

(on the cathodic side) and by the higher-pH separation membrane that encompasses the adjacent collection channel (on the other side). The system operates by directing two common feed solutions, one acidic (red) and one basic (blue), through the four separation heads, while the electrode and collection channels of each head are recirculated independently of the other heads. This process allows for directionally controlled delivery of sample, paired with orthogonal harvesting.

4.4 Design and manufacture of the separation heads

4.4.1 Design and manufacture of electrode chambers

The chambers that contain the electrodes consist of a PVC housing, Tefzel® aligning rods, a platinum-coated titanium grid-electrode, a PVC shoulder washer, rubber gaskets, and threaded port-to-barb connectors. The electrode chamber was designed using AutoCAD 2006 software (Autodesk, Inc., San Rafael, CA 94903). All manufacturing was done using conventional machine tools.

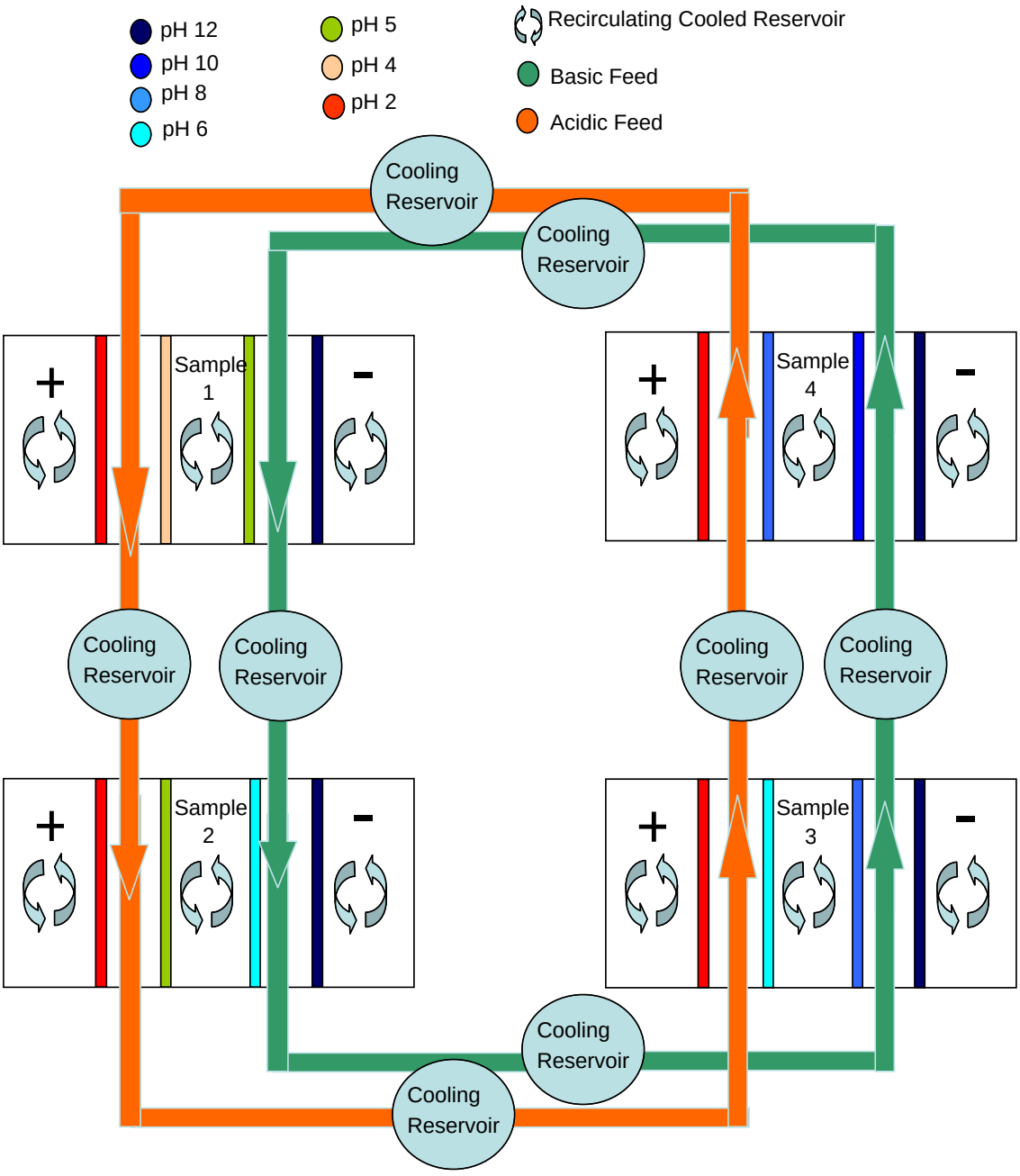

Figure 23. Schematic of the T-RECS.

4.4.1.1 Electrode chamber

3-D rendered representations of the two versions, one with outlets for the flow-through channels and collection channel and the other having inlets for the flow-through channels and collection channel, are shown in Figures 24 and 25. The external dimensions of the housing are 13.2 cm long, 4 cm wide, and 3.2 cm deep. The housing is built from a solid poly(vinyl chloride) block (PVC block). PVC block was chosen as the structural material due to its chemical resistance (particularly for acid and base), ease of machining, electrical resistance, dielectric strength and low cost. Working from the internal face (which will mate with the flow-through and separation channels), a 10 cm long, 1.5 cm wide, and 0.5 cm deep, centered electrolyte channel was milled into each block using a 1/2" milling tool. 1/8" by 0.5" deep blind holes, for holding the aligning rods, were drilled and reamed to 0.126" to ensure a slip fit of the 1/8" Tefzel® dowel pins. A pair of 1" deep blind holes, at opposite ends of the electrolyte channel, one 1/8", the other 0.2460" (used for securing and aligning the electrode) were drilled from the electrolyte channel. Through holes of 1/8" for the flow-through channel and collection inlets/outlets, 1/4" for the electrolyte inlets, and 3/8" for the electrolyte outlets were drilled. The inlet and outlet holes were threaded to fit the commercially available barbed connectors. Additionally, a 3/8"-to-0.1770" wide hole was drilled from the top of the block to allow for connection of the electrode to a banana plug socket. Finally, 0.1065" blind holes were drilled and tapped to make 4 threaded holes on the electrode compartment to affix the block to an external cradle. This last step was done working from the external face of the element.

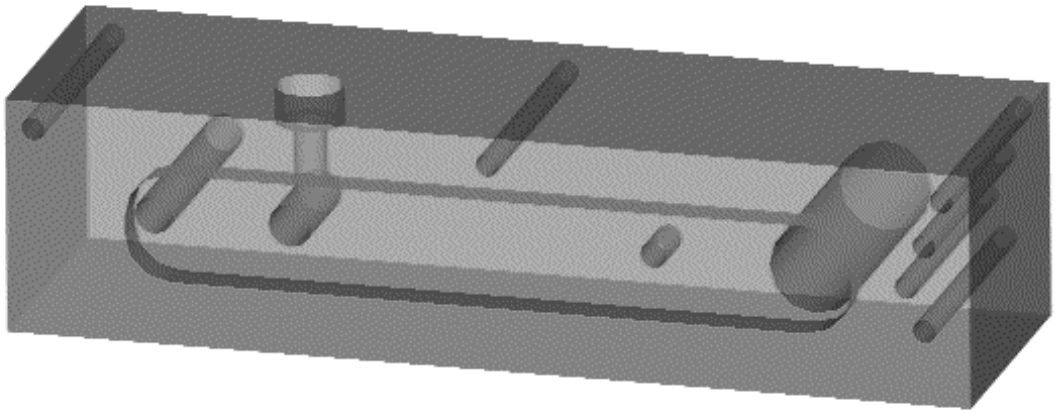

Figure 24. 3-D rendering of the electrolyte housing having flow-through and collection outlets.

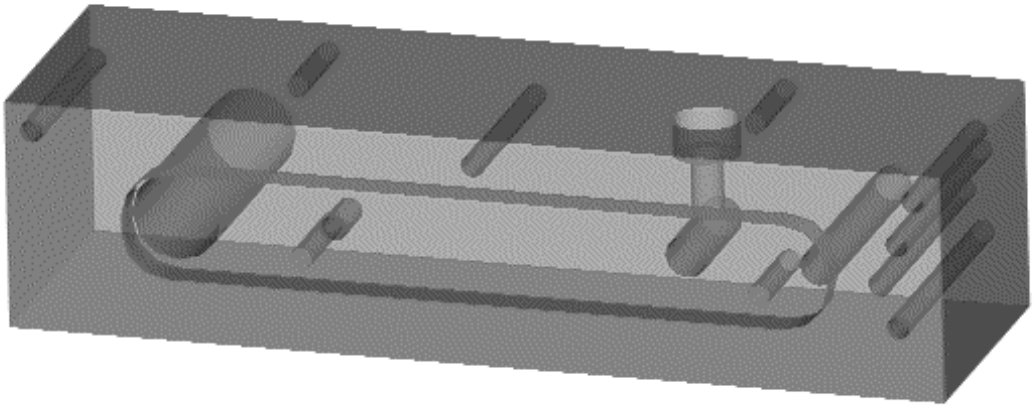

Figure 25. 3-D rendering of the electrolyte housing having flow-through and collection inlets.

4.4.1.2 Tefzel® aligning rods, platinum coated titanium electrode, PVC shoulder washer, rubber gaskets, and threaded port-to-barbed connectors

The remaining pieces of the electrode chambers included custom-made parts and modified commercial parts. The commercially available threaded port-to-barb connectors were resized to fit the instrument. The platinum electrode, made of platinum-coated titanium mesh, was a modified version of the electrodes used in the Twinflow system [39]. A PVC shoulder washer and rubber gasket were used to secure the electrode, prevent contact of the electrode with membranes, and guarantee a constant anode-to-cathode distance for the entire chamber. Tefzel® aligning rods were cut to 1.5" length from 1/8" rod stock and used to ensure proper alignment of the anodic chamber, cathodic chamber, acidic flow-through channel, basic flow-through channel, collection channel, and membranes. Tefzel® was chosen due to its mechanical toughness, chemical inertness, and low coefficient of friction.

4.4.2 Design and manufacture of the flow-through channels, collection channels, and silicone gaskets

The flow-through channels, collection channels, and silicone gaskets were designed using AutoCAD 2006 software (Autodesk, Inc., San Rafael, CA 94903). All manufacturing was done using a CO_2 laser cutter (Universal Laser Systems Inc., Scottsdale, AZ). The laser cutter was controlled using AutoCAD software with the laser cutter set as a plotter.

4.4.2.1 Flow-through and collection channels

3-D representations of two versions of the flow-through channels and two versions of the collection channels are shown in Figures 26-29. Both the flow-through channels and the collection channels have external dimensions that are 13.2 cm long, 4 cm wide, and 0.040” deep and are cut from a solid poly(vinyl acetate) sheet (PVAC sheet). In all versions of the channels, a centered channel, 10 cm long and 1.5 cm wide, tapering down to 1/8” at the inlet/outlet, was cut from the stock sheet and three 1/8” holes were cut to receive the Tefzel® aligning rods. Two versions of each type of channel were built and tested in the instrument. Version 1 (Figures 26 and 28) utilized a smooth, gentle, double curve to transition the channel between 1.5 cm at the middle of the channel to 1/8” at the inlets/outlets. The gentle transition prevented capturing of bubbles inside the channel but provided a limited amount of solid PVAC material between the inlet/outlets of the flow-through channels and the inlet/outlets of the collection channel. A lesser amount of material limits the area of the sealing surface and made adequate sealing more difficult to achieve. Version 2 (Figures 27 and 29) has an extended 1/8” wide channel and a more aggressive double curve transition between 1.5 cm and 1/8”. Version 2 provided a significant increase in the sealing surface area and improved sealing. However, due to the more constricted flow path, an increase in backpressure was observed and additional compression was used for sealing.

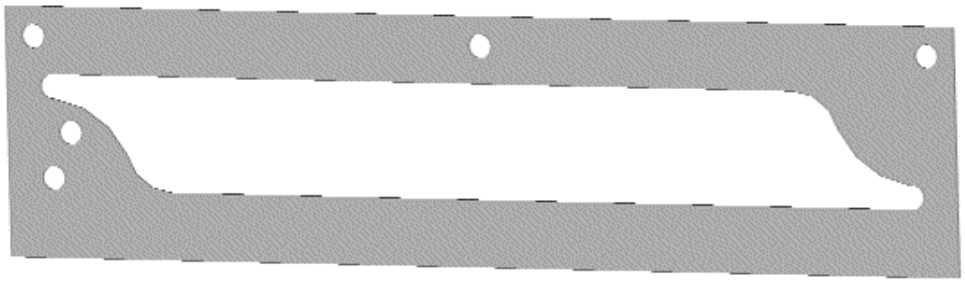

Figure 26. 3-D rendering for version 1 of the flow-through channels.

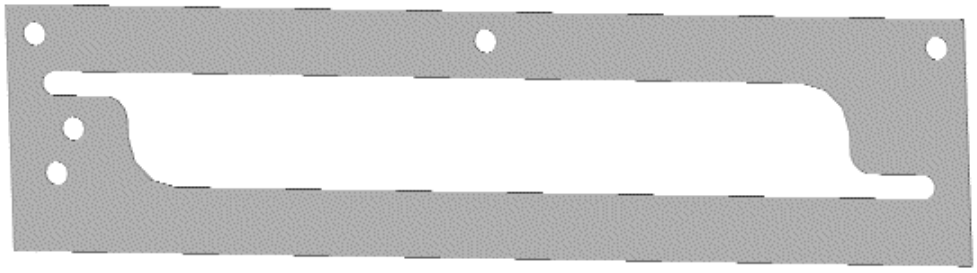

Figure 27. 3-D rendering for version 2 of the flow-through channels.

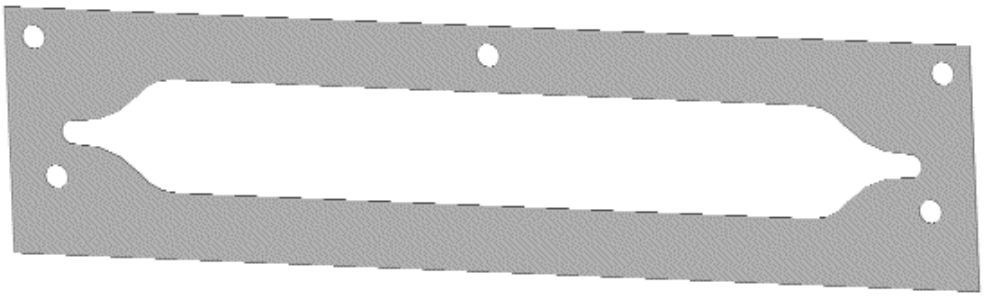

Figure 28. 3-D rendering for version 1 of the collection channels.

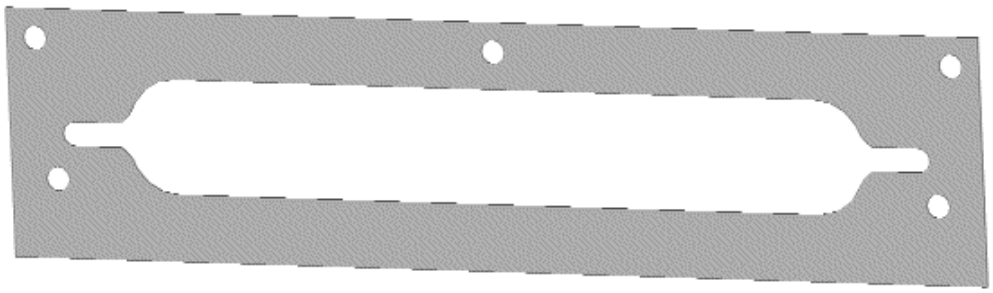

Figure 29. 3-D rendering for version 2 of the collection channels.

4.4.2.2 Silicone gaskets

3-D representations of two types of gaskets used to obtain a seal between the membranes and the channels are shown in Figures 30 and 31. Of the two types, Figure 30 gaskets are used to seal between the anodic/cathodic membranes and the electrode chamber and Figure 31 gaskets are used to seal between the separation membranes and the flow-through or collection channels. Each gasket is 13.2 cm long, 4 cm wide, and 0.020" deep and are cut from a solid silicone sheet. A centered channel, 10 cm long and 1.5 cm wide, which tapers to a double curve, was cut from the stock sheet. Six 1/8" holes were cut, three for the inlet and outlets and three to receive the Tefzel® aligning rods.

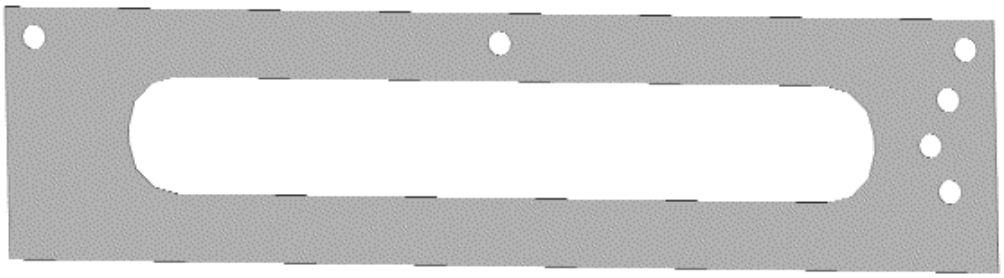

Figure 30. 3-D rendering of the gaskets used to seal the anodic/cathodic membranes.

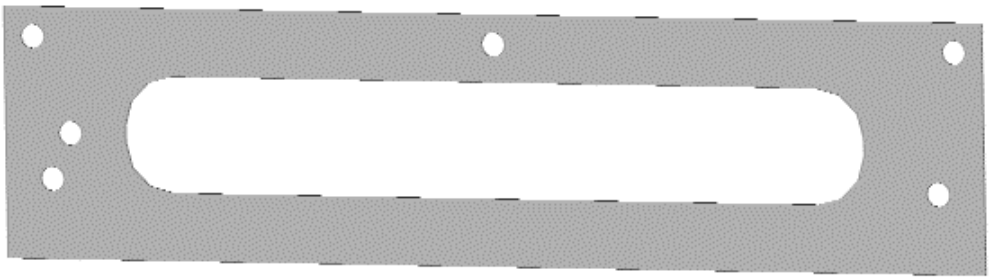

Figure 31. 3-D rendering of the gaskets used to seal the separation membranes.

4.4.3 Design and manufacture of a cradle for the assembled separation head

A 3-D representation of a cradle used to hold the electrode chambers is shown in Figure 32. The cradle is constructed of three aluminum blocks. Two 2.75” long, 1.275” wide, and 0.5” deep blocks form the walls of the cradle and a 5” long, 2.75” wide, and 0.5”

deep block forms the floor. Each wall has four or five 6-32 threaded holes for securing the walls to the floor. One wall contains four 9/64” through holes that allow for attachment of the electrode compartments to the cradle. The second wall contains two 1/4”-20 threaded holes for thumbscrews which provide the compression needed for sealing.

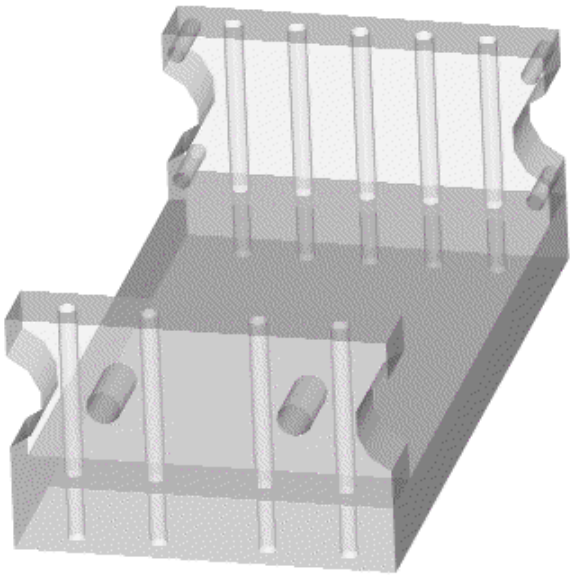

Figure 32. 3-D rendering of the aluminum cradle.

4.4.4 Assembled separation head

A 3-D rendering and photograph of an assembled separation head are shown in Figures 33 and 34.

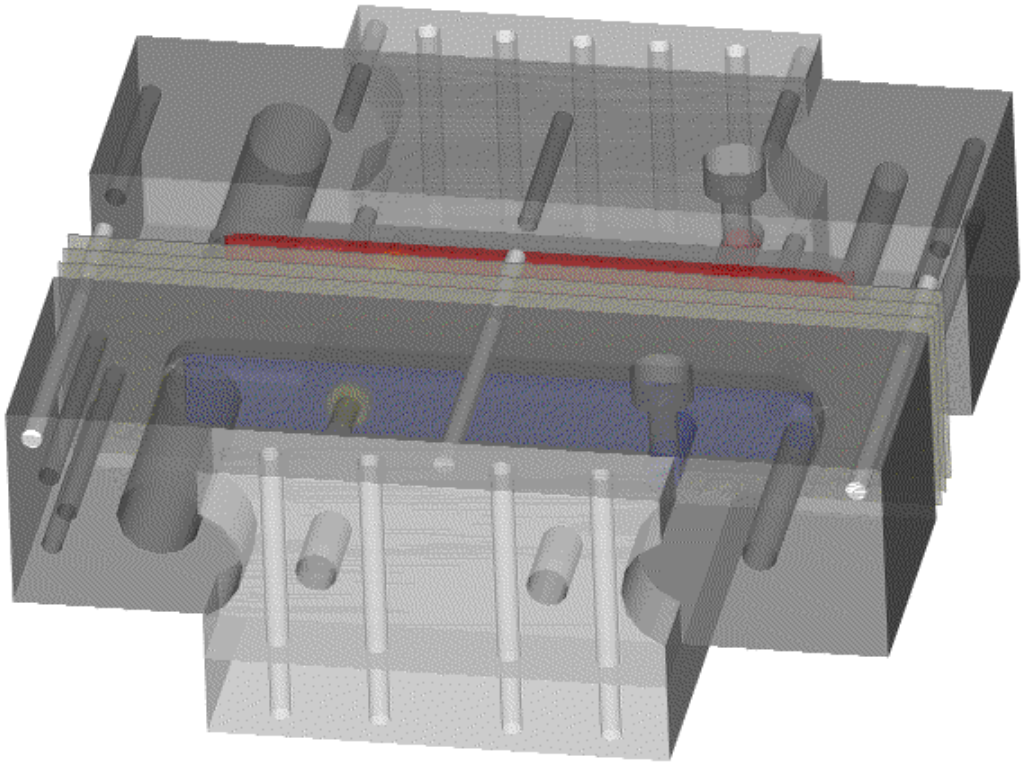

Figure 33. Assembled separation head including the electrode chamber, flow-through channels, collection channel, electrodes (blue for cathode, red for anode), aligning rods, shoulder washers, and rubber gaskets.

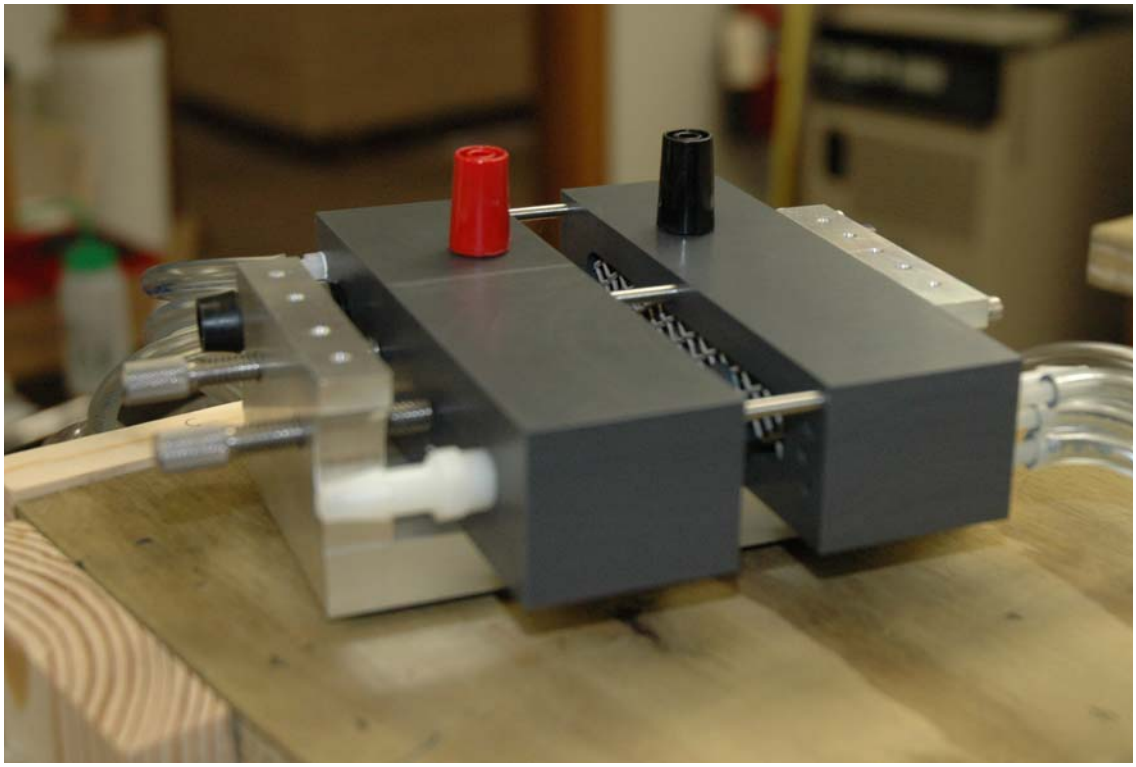

Figure 34. Photograph of the assembled separation head including the electrode chamber, aligning rods, shoulder washers, rubber gaskets, threaded port-to-barb connectors, and tubing.

4.5 Design and manufacture of the external support system and the jacketed reservoirs

4.5.1 External support

An external support system was designed to house the four separation heads, sample and electrolyte reservoirs, and the tubing necessary for fluid delivery. A 3-D rendering of the support system is shown in Figure 35. The entire support was constructed of weather-proof, treated lumber. Wood was chosen as the structural material due to its electrical resistance, workability and low cost. The support was constructed of two 3/4” sheets

forming two tiers with 1” dowel rods as pillar supports between the two tiers. A series of blocks with points to attach nylon ties were used to hang the liquid reservoirs.

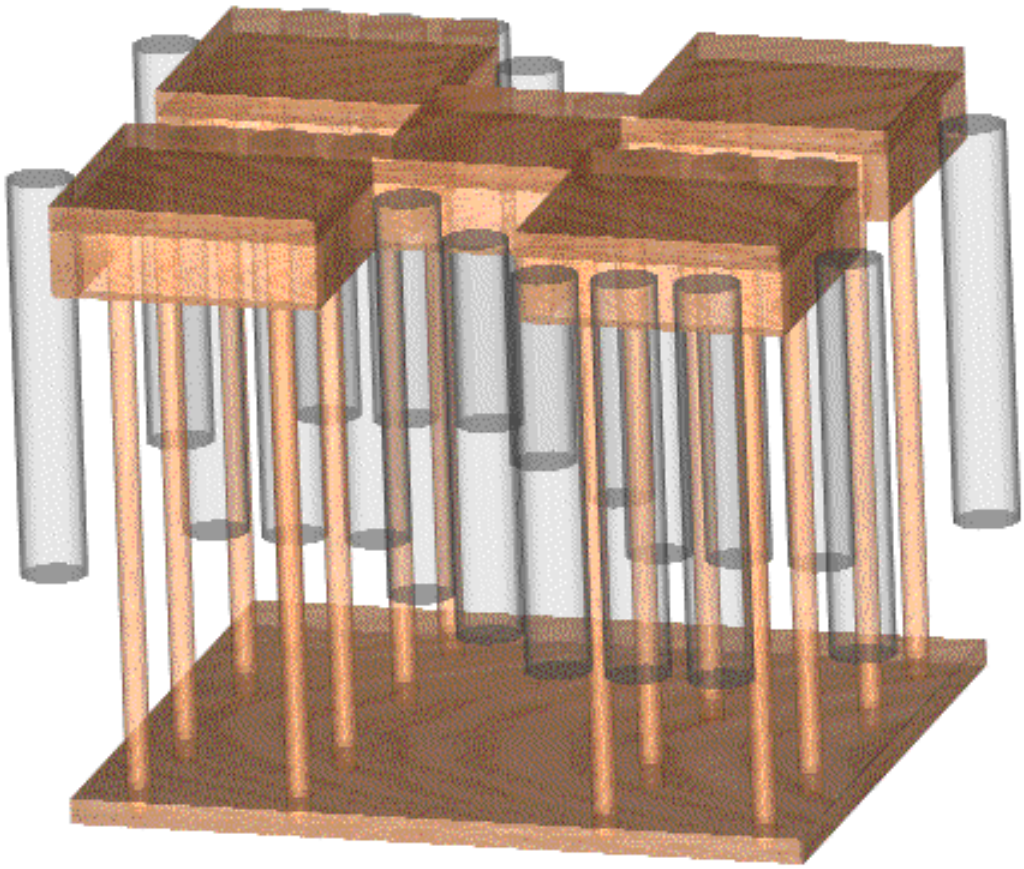

Figure 35. 3-D rendering of the external support system showing locations of the pillars and the liquid reservoirs.

4.5.2 Jacketed reservoirs

Fifteen 100 mL graduated, jacketed glass cylinders were used as reservoirs for the solutions. The reservoir jackets and a Coolflow CFT-33 refrigerated recirculator were connected serially to provide temperature control.

4.6 Fluid delivery

Two types of pumps were employed to provide delivery of the electrolyte, flow-through, and collection solutions. For the electrolyte solutions, Eheim Universal 1046 centrifugal pumps that deliver 2 L /min were used. One pump was used for each electrolyte reservoir, for a total of 8 pumps. For the flow-through and feed solutions, a 12-channel Ismatec peristaltic pump was used. The peristaltic pump was able to deliver flow rates between 0.35 and 35 mL / min. Electrolyte solutions were delivered with ¼" inlet tubing and ½" outlet tubing. Flow-through and collection solutions were delivered with 1/8" inlet and 3/16" outlet tubing. The larger diameter tubing was selected for the outlets in order to reduce back pressure. All flow-through and collection solutions were setup to have an air gap before reaching the return reservoir to prevent any electrical current from flowing through tubing.

4.7 Arrangement of the completed system

The 3-D AutoCAD rendering and the photograph of the completed system are shown in Figures 36 and 37. One of the key advantages of this arrangement is flexibility. The system can be adapted to run in a number of modes including; (i) a single isolated

separation head (ii) 4 isolated separation heads (iii) 4 heads connected and arranged as in Figure 23 (iv) a 4-head system that does serial binary cuts to form a cascade.

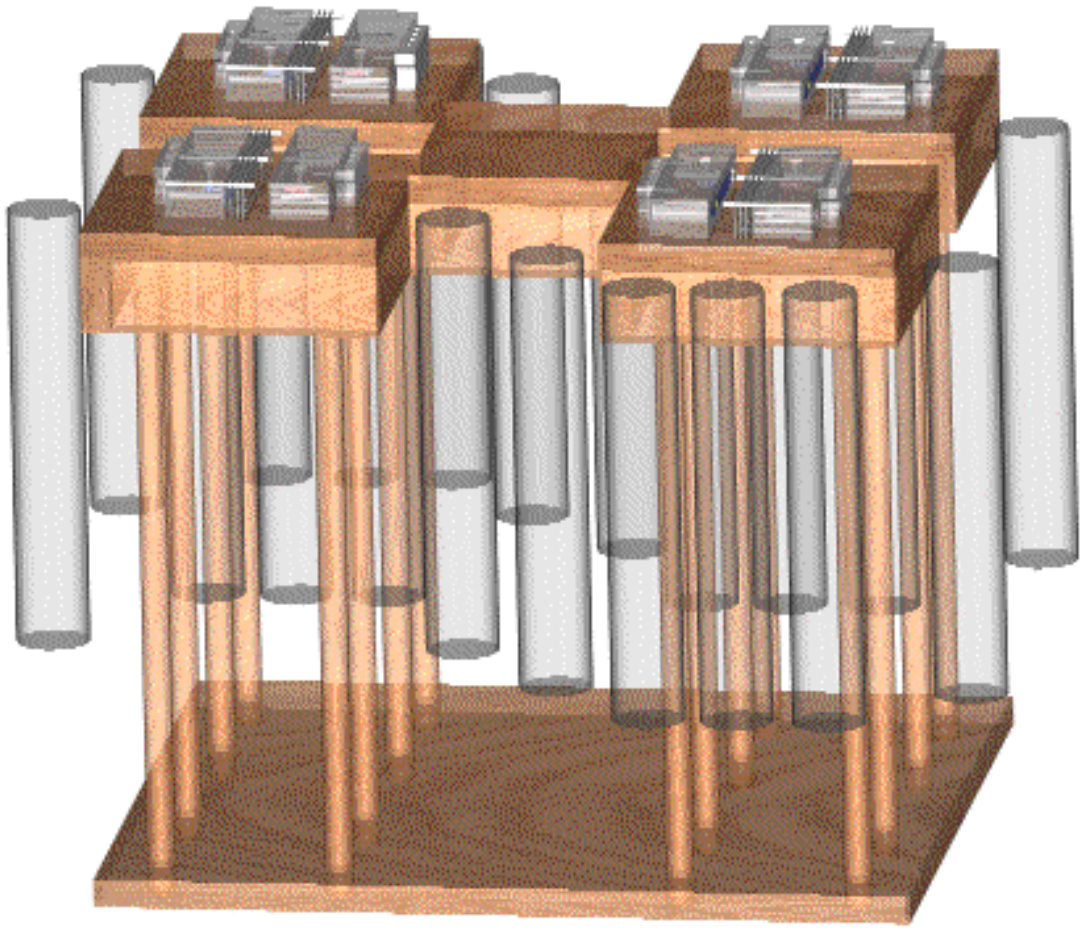

Figure 36. 3-D AutoCAD rendering of the arranged separation heads, external support system, and fluid reservoirs.

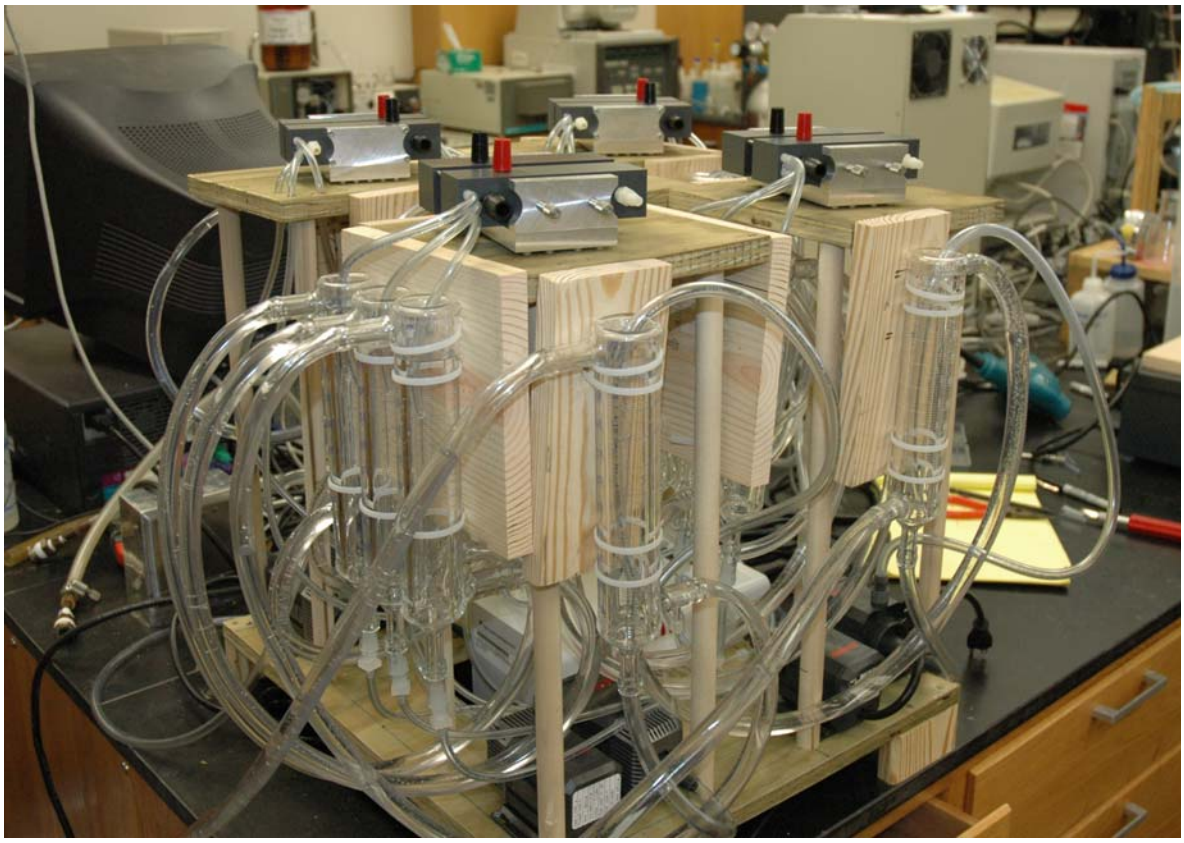

Figure 37. Photograph of the arranged separation heads, external support system, and the fluid reservoirs.

5. OPERATION OF THE T-RECS

5.1. Optimization of the flow-through and collection stream flow rates

5.1.1 Background and objective

The first experimental task for the new device was to determine the appropriate flow rates. Since the T-RECS system was designed with an air-break between each liquid reservoir and separation head (to provide for electrical and hydraulic decoupling of the heads), each reservoir requires its own pump for liquid delivery. A consequence of this is, when operated as a parallel MCE with four connected heads, any differences in flow rates between adjacent pumps will cause a buildup / depletion for the pair of reservoirs associated with the two mismatched pumps. This becomes problematic as empty reservoirs will force air into the separation head, depleted reservoir volumes reduce the system's cooling ability, and large solvent buildups may cause loss of sample due to overflow of the reservoirs. A 12-channel peristaltic pump was selected to minimize the differences in flow rate from pump to pump. However, variations in the tube internal diameter, degree of tube compression, imperfections on the roller surfaces and uneven wear of the tubing can lead to different channel-to-channel flow rates. For the particular pump used in the T-RECS system, it has been noted that the channel-to-channel flow rate differences are minimized when operating at RPM rates near the higher end of the pumps' capabilities [personal communication with Ismatec, Inc., Zurich, Switzerland]. In light of this, it was important to evaluate the channel-to-channel variability for various flow rates. Additionally, once true flow rates for each channel have been determined,

flow rate differences for adjacent pumps can be minimized by grouping pumps having the most similar flow rates.

5.1.2 Materials, method, and instrument setup

Flow rates for each channel were determined by measuring the total mass of deionized water transferred in 10 minutes. Briefly, on a level surface, the inlet tubing of a single pump channel was immersed into a large volume of water and the outlet tubing was set to drip freely into a dried, pre-weighed glass beaker. Inlet depth and outlet height were held constant for each channel tested.

5.1.3 Results and discussion

The results for operation at 45, 30, 22.5, and 4.5 RPM are tabulated in Table 1. The lowest coefficient of variation for the delivered mass of water, 2.28%, was found for operation at 30 RPM. Thus, 30 RPM, corresponding to a flow rate of approximately 23 mL/min was selected as the flow rate for the flow-through and collection channels. Additionally, one can use this table to determine which pump channels to use for adjacent pumps. For example, any of the 4 channels that delivered the flow rates furthest from the average, channel 1, 2, 3, and 12 can be used for the collection streams, because each collection stream is recirculated by only one pump. The remaining channels, used for the flow-through streams, can be divided into two groups of four: (i) channels 4, 6, 7 and 11 and (ii) channels 5, 8, 9 and 10.

Table 1. Total mass of deionized water transferred in 10 minutes by the peristaltic pump.

	Mass of water (g) delivered at			
	45 RPM	**30 RPM**	**22.5 RPM**	**4.5 RPM**
Channel 1	300.313	222.132	149.130	28.394
Channel 2	320.154	224.216	159.730	30.638
Channel 3	312.417	224.590	155.469	29.936
Channel 4	307.433	233.453	152.120	29.375
Channel 5	305.425	226.136	149.470	28.770
Channel 6	300.750	230.615	146.584	28.263
Channel 7	299.373	230.569	145.411	28.161
Channel 8	301.811	228.702	146.610	28.679
Channel 9	290.256	230.716	140.460	27.211
Channel 10	299.206	227.022	141.138	27.523
Channel 11	295.882	230.953	142.868	27.588
Channel 12	312.391	242.038	148.934	29.085
Average	303.784	229.262	148.160	28.635
Standard Deviation	8.222	5.244	5.683	1.011
CV (%)	**2.707**	**2.287**	**3.836**	**3.533**

5.2 Operation of a single separation head

5.2.1 Probing the effect of the electrical power load on the temperature of the flow-through and collection streams

5.2.1.1 Background and objective

In addition to affecting the processing rate, the total electrical power load applied to the system will have an effect on the temperature of the streams. Since Joule heat scales according to Equation 3, an increased power load should cause an increase in the temperature of the solutions (assuming the same degree of cooling).

$$\frac{Q}{t} = I \cdot V$$

Operation at increased temperatures can become problematic for heat sensitive analytes, such as proteins. Thus, because of the importance of operating at moderate temperatures, the effect of changing power load on the temperature of the flow-through and collection streams was investigated.

5.2.1.2 Materials, method, and instrument setup

Figure 38 illustrates the arrangement for the IET experiment. 10 mM glutamic acid and 10 mM lysine were used as the acidic and basic flow-through solutions. The anolyte was 30 mM MSA, the catholyte was 60 mM NaOH. The anodic and cathodic membranes buffered at pH 2 and pH 10.5, the separation membranes at pH 4.2 and pH 9, respectively. The flow-through and collection streams were delivered at 23 mL/min (30 RPM) and the system was operated at 5, 10, 20, 40, and 60W. Power was varied sequentially, i.e., 5 W for the first 20 minutes, then 10 W for 20 minutes, and so on. Preliminary experiments indicated that the streams reached a constant temperature after about 15 minutes. Therefore, temperature was monitored at the outlets for the collection and flow-through streams after 20 minutes at a given power load. Additionally, the pH and conductivity values of each stream were measured: pH was measured by a VWR SB70P meter equipped with an Accumet glass pH probe, conductivity was measured by a Thermo Orion meter equipped with a MI-915 conductivity probe (Microelectrodes, Inc., Bedford, NH,).

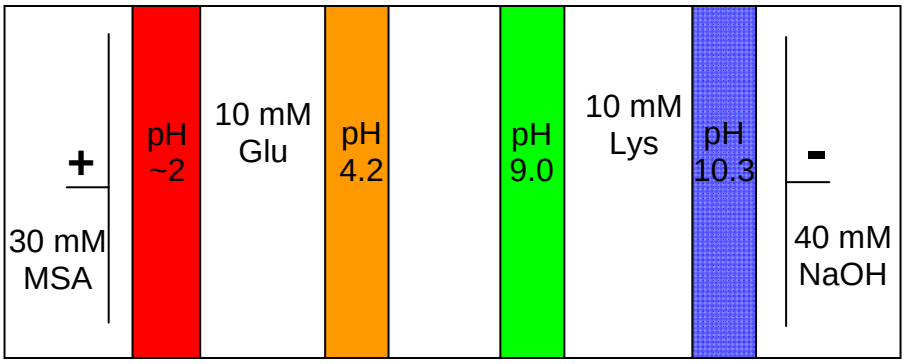

Figure 38. IET setup for monitoring the stream temperatures at various applied power.

5.2.1.3 Results and discussion

The outlet temperatures are plotted against the power load in Figure 39. As expected, the temperature of each stream varies with the power load. The temperature was highest in the collection stream, followed by the basic flow-through stream and the acidic flow-through stream. This observation can be explained by the relative conductivities of the different streams. Initial conductivity values for the streams were typically as follows: around 5 μS/cm for the collection stream, 60 μS/cm for the basic flow-through stream, and 250 μS/cm for the acidic flow-through stream. Since each stream can be thought of as an individual circuit element in a serial circuit, all sharing the same current, the least conductive (most resistive) stream would experience the greatest Joule heating and should have the highest temperature. The slope of the temperature *vs.* applied power line is the steepest for the collection stream, followed by the basic flow-through stream and the acidic flow-through stream. At 5 watts, there is no difference between the temperatures of the flow-through streams and there is only a 0.5 ˚C difference between

the flow-through streams and the collection streams. At the high end, even at 60W, the highest outlet temperature was only 27.5 ˚C.

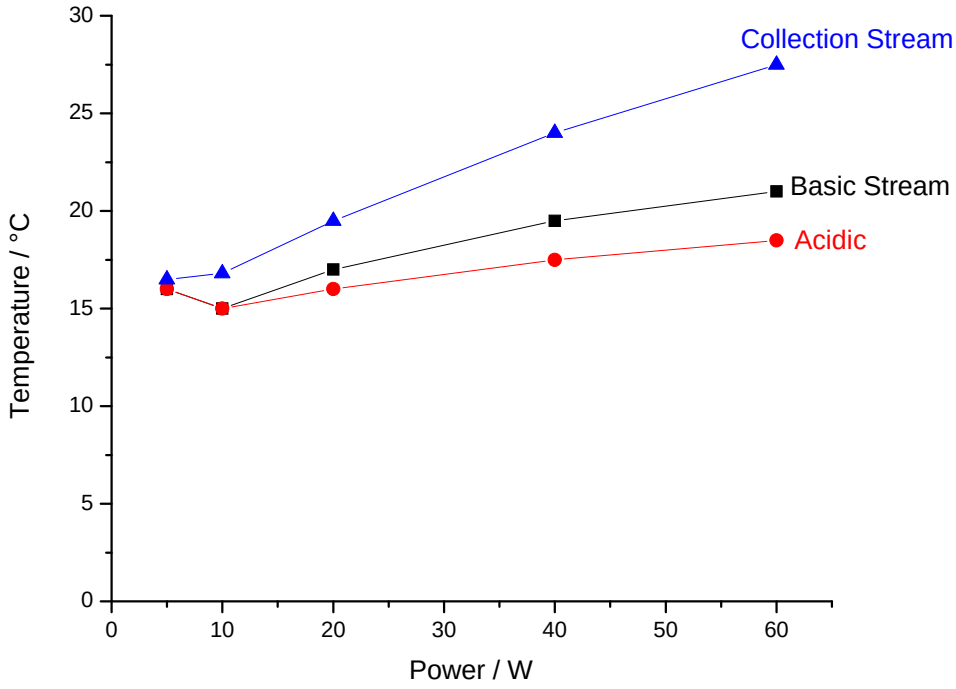

Figure 39. Outlet solution temperature vs. applied power for a single T-RECS separation head. Blue, red and black lines represent the collection, the acidic flow-through and the basic collection streams, respectively.

The pH and conductivity profiles are plotted in Figures 40 and 41. Zero power represents the initial conditions before the experiment began. Initially, in the basic flow-through stream, there is an increase in both the conductivity and pH. This change is likely caused by diffusion of Na^+ into the chamber because the rate of electrophoretic ion removal, at low power loads such as 5 and 10 W, is less than the rate of diffusion into the channel. For increased power loads (increased current), one can see a decline in the conductivity

and pH of the basic flow-through stream indicating removal of the invading Na^+ ions. After 20 minutes, at 60 W, pH and conductivity returned to levels similar to the initial conditions. Similarly, but to a lesser degree, the conductivity of the acidic flow-through stream rises - and its pH decreases – when the power loads are low, 5 and 10 W, and decreases when the power loads are high. As in the basic flow-through stream, this is likely caused by diffusion of the strong electrolyte, in this case MSA, into the channel. For the collection stream, conductivity is steady while the pH varies between 5 and 7. One could argue that a small amount of either glutamic acid or MSA diffused into the collection stream and the aliquot analyzed was taken before the invading acid was electrophoretically removed. Calculations indicate that a glutamic acid concentration of about 0.015 mM would decrease the pH down to the lowest observed pH. The pH and conductivity results indicate that invasion by the electrode liquids can cause significant changes in the separation. Thus, any experiment that requires a low power needs to be done with a lower concentration of the electrolytes. Based on the pH of the electrode membranes, much lower concentrations could have been used for the previous experiment: 2 mM for MSA and 3 mM for NaOH would have been sufficient. These low concentrations should significantly lower the rate of diffusion into the flow-through chambers and prevent invasion-related pH and conductivity changes.

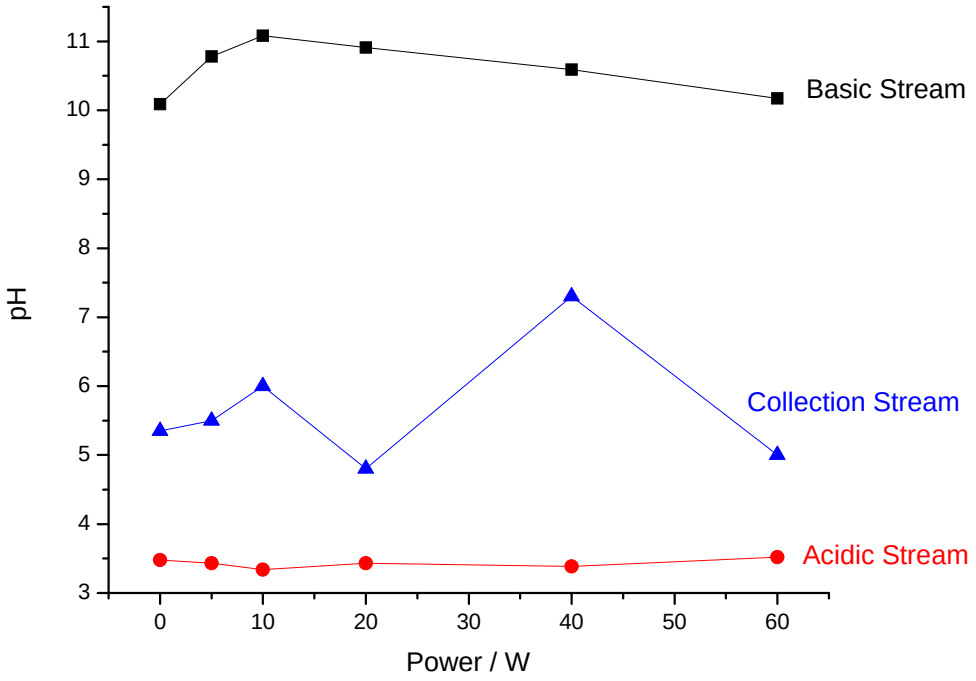

Figure 40. pH vs. applied power for a single T-RECS separation head. Blue, red and black lines represent the collection, the acidic flow-through and the basic collection streams, respectively.

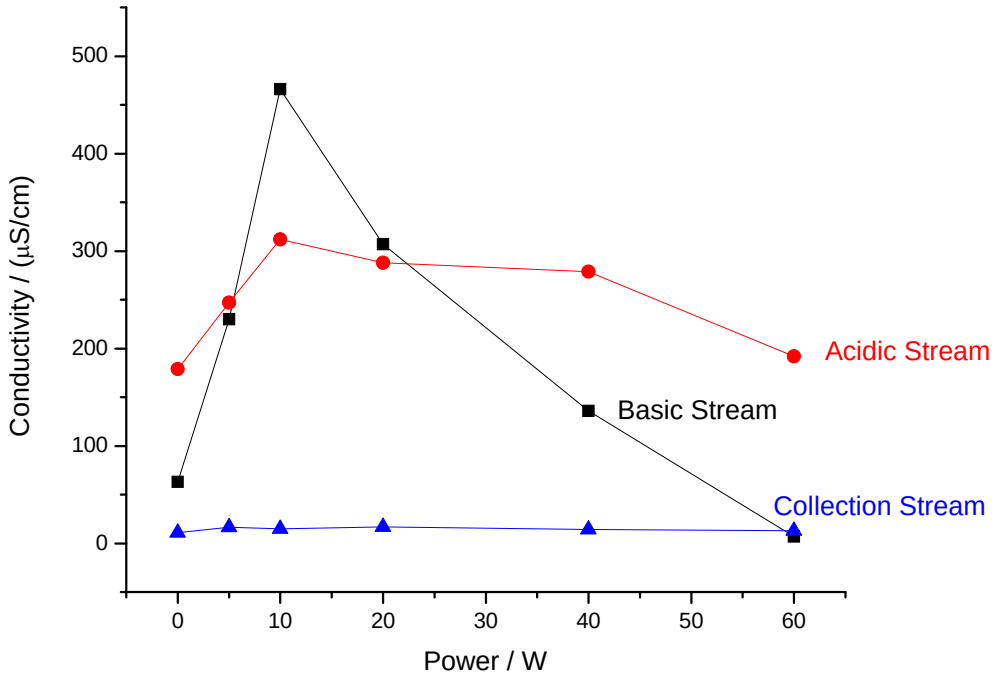

Figure 41. Conductivity vs. applied power for a single T-RECS separation head. Blue, red and black lines represent the collection, the acidic flow-through and the basic collection streams, respectively.

5.2.2 Desalting of strong electrolytes

5.2.2.1 Background and objective

Removing unwanted salts from samples is an important concern, especially for preparative separations of protein and peptide samples. Since ammonium sulfate precipitation and ion-exchange chromatography - often used in the preparation of protein-based materials – add large amounts of salts to the samples, a number of methods have been devised to remove the added salts. The classical salt removal techniques include passive dialysis, electrodialysis, tangential flow filtration, and

centrifugal filtration. More recently, IET has been used as a desalting technique [26,27,65]. In light of this use of an IET device, the desalting properties of a single T-RECS separation head were probed. In order to be able to monitor the desalting process, UV-absorbing histidine was used as a model ampholyte and UV-absorbing strong electrolytes were used as salt.

5.2.2.2 Materials, method, and instrument setup

Figure 42 illustrates the arrangement for the IET experiment. The T-RECS was setup with a single collection chamber, bracketed by a pH 4 membrane on the anodic side and a pH 10 membrane on the cathodic side. The anolyte was a 2 mM benzenesulfonic acid solution ($BzSO_3H$); the catholyte was 3.5 mM benzyltriethylammonium hydroxide (BzTEAOH) solution. The collection stream initially contained 2 mM histidine and 10 mM benzyltrimethyl ammonium *p*-toluenesulfonate ($BzTMA^+$ / $PTSA^-$), allowing for easy differentiation of the invading electrolytes and the initial salt. The anolyte and catholyte were delivered at a flow rate of about 2 L/min, the collection stream was delivered at 23 mL/min (30 RPM). The system was operated for 60 minutes: the initial current was 200 mA at 33 V, the final current was 114 mA at 600 V. Aliquots were taken from the collection stream at short intervals, initially at 1 minute, then at 5 minutes for the last 30 minutes. The pH and conductivity values were measured for each stream. The pH was measured by a VWR SB70P meter equipped with an Accumet glass pH probe, conductivity was measured by a Thermo Orion meter equipped with a MI-915 conductivity probe (Microelectrodes, Inc.). The aliquots were also analyzed by CE, the

UV detector was set at 214 nm. An internal standard, phthalic acid, was added to correct for variations in the injected volumes.

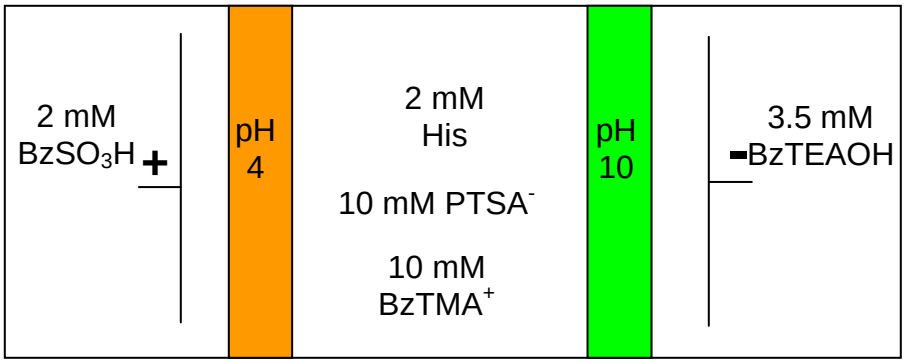

Figure 42. IET setup for probing the desalting ability of a T-RECS separation head.

5.2.2.3 Results and discussion

Representative electropherograms are shown in Figure 43 for the anolyte stream (at 0 and 60 minutes), in Figure 44 for the catholyte stream (at 0 and 60 minutes), and in Figure 45 for the collection stream (at 0, 6, 12, 20, 26, 35, 50, and 60 minutes). There is no evidence of invasion of the collection stream by either benzenesulfonic acid or benzyltriethylammonium hydroxide, nor is loss of histidine observed in any of the electropherograms. As expected, the strong electrolyte salt is removed from the collection stream and its ions are transferred into the respective electrolyte streams. After about 25 minutes, benzyltrimethylammonium ions are no longer detectable in the collection stream. *p*-Toluenesulfonate ions do not disappear until about 35 minutes. Due to dilution, the relative signal strength for benzyltrimethylammonium ions and *p*-

toluenesulfonate ions is smaller in the electrolyte streams than their initial values in the collection stream.

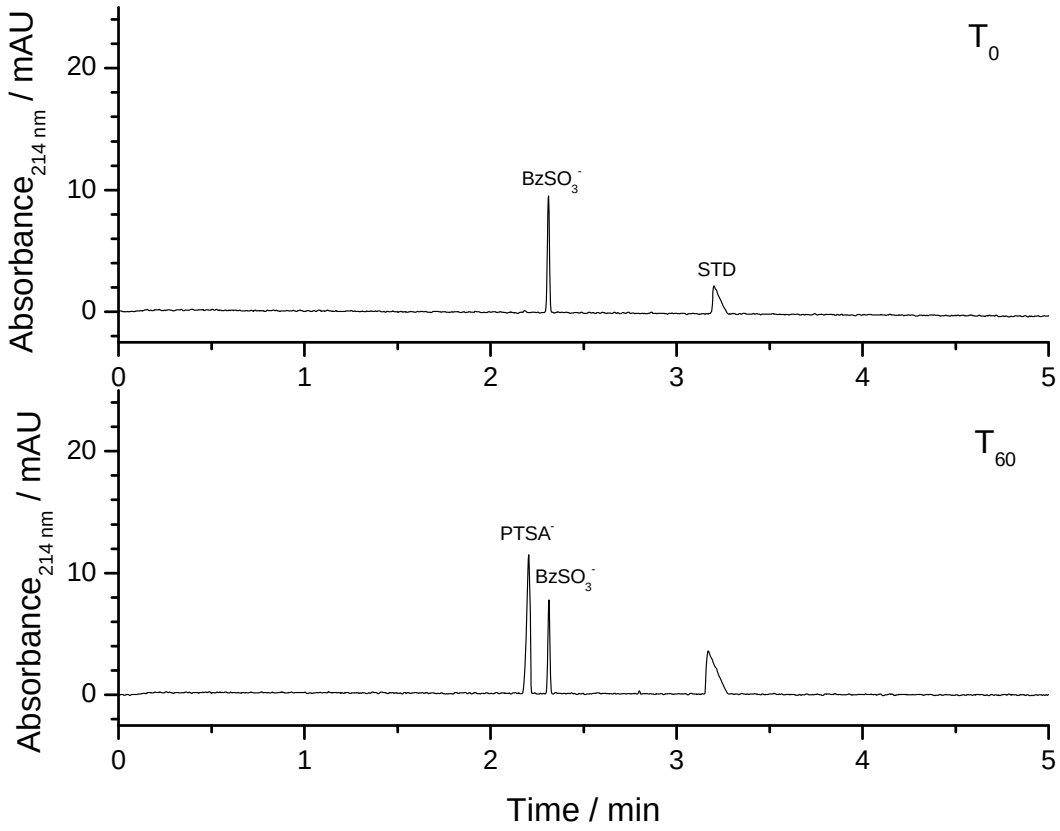

Figure 43. Electropherograms for the anolyte at 0 and 60 minutes. Peaks corresponding to benzenesulfonate ($BzSO_3^-$), *p*-toluenesulfonate ($PTSA^-$), and phthalate (STD) are labeled.

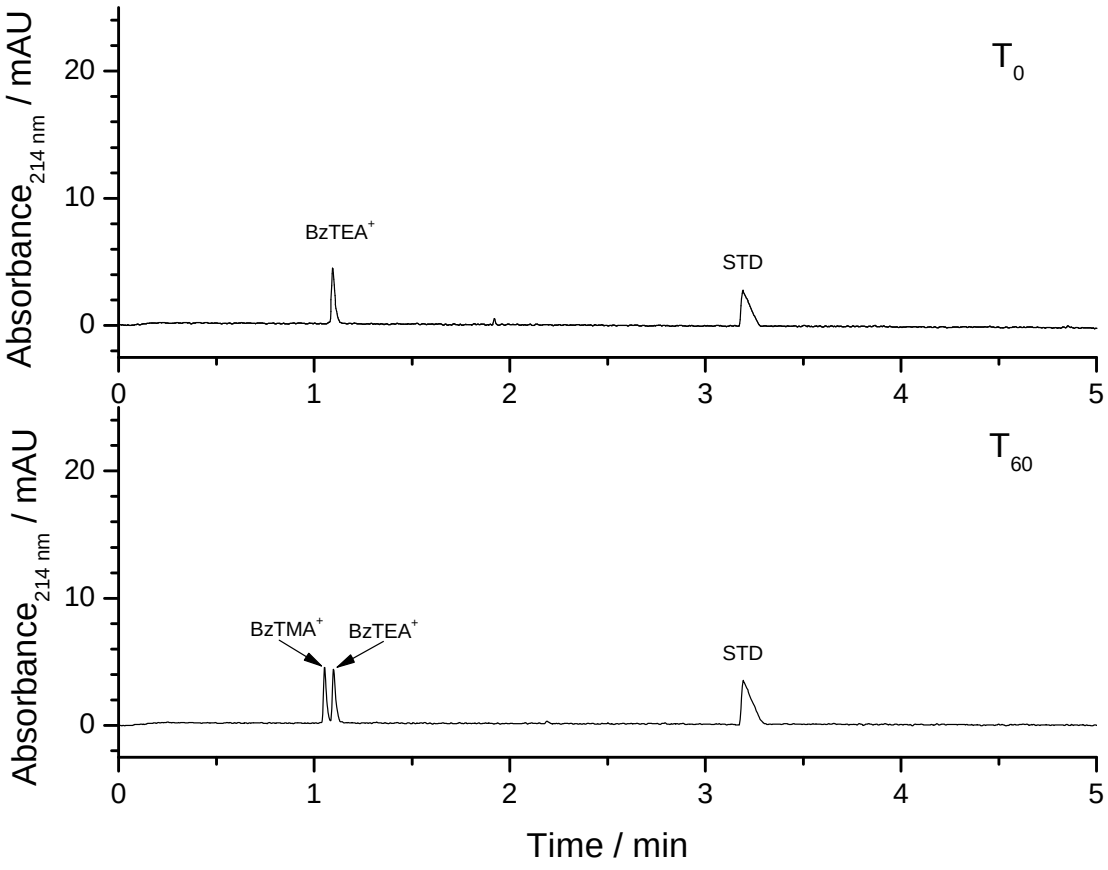

Figure 44. Electropherograms for the catholyte at 0 and 60 minutes. Peaks corresponding to benzyltriethylammonium ions ($BzTEA^+$), benzyltrimethylammonium ions ($BzTMA^+$), and phthalate ions (STD) are labeled.

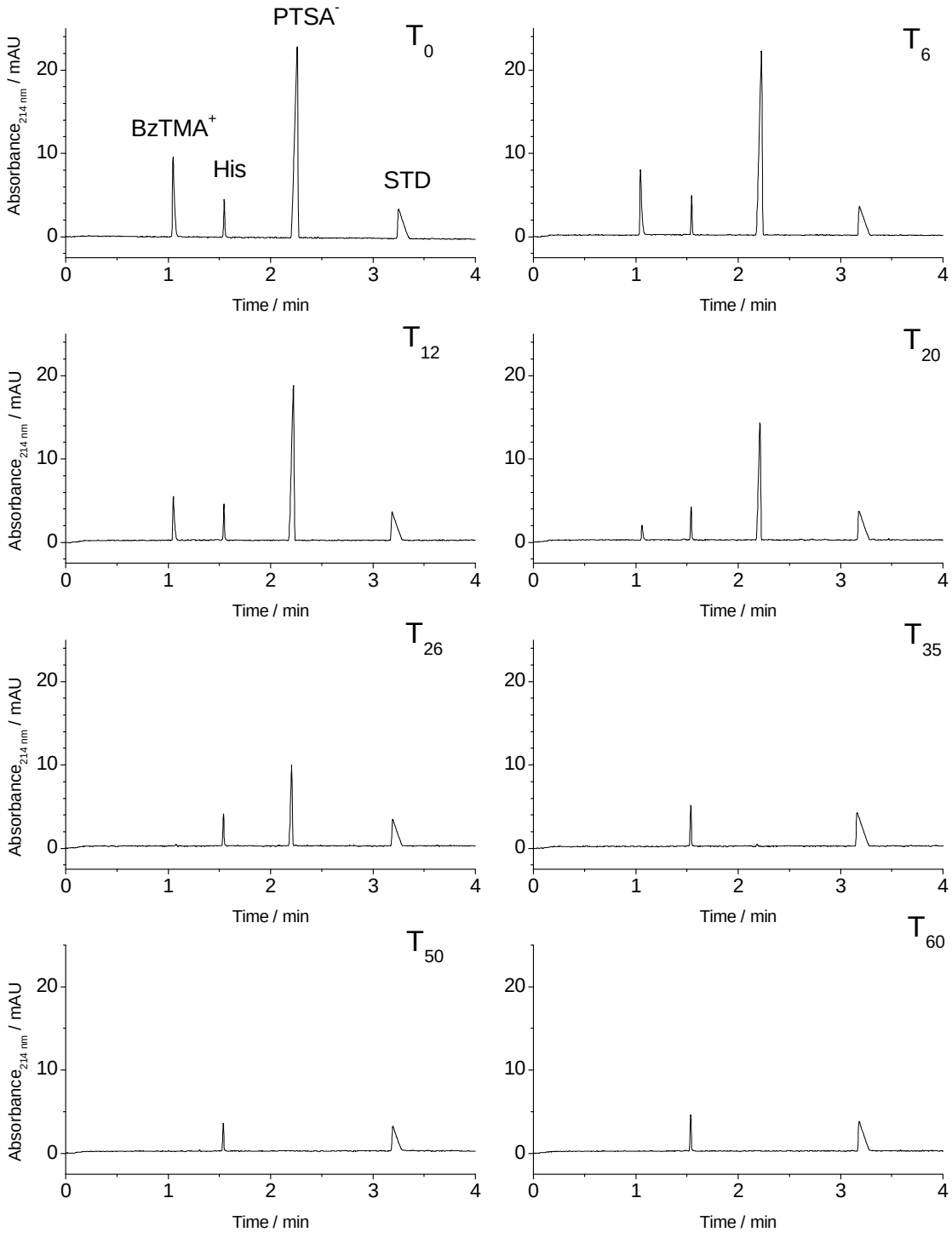

Figure 45. Electropherograms for the collection stream at 0-60 minutes. Peaks corresponding to the benzyltrimethylammonium ions ($BzTMA^+$), *p*-toluenesulfonate ions ($PTSA^-$), histidine (His), and phthalate ions (STD) are labeled.

The pH and conductivity profiles for the collection stream are plotted in Figures 46 and 47. An acidic pH transient was observed with a pH minimum of 3.02 at 23 minutes. This is likely caused by the different removal rates for the electrolyte pair as reported by Shave and Vigh, because $BzSO_3^-$ invasion from the anolyte was not observed [65]. Since the mobility of $BzTMA^+$ is larger than that of $PTSA^-$, $BzTMA^+$ was removed at a faster rate than $PTSA^-$. Thus, the H^+ concentration had to increase in order to preserve electroneutrality, causing the pH of the solution to decrease. Interestingly, the conductivity profile revealed a previously unreported transient of increased conductivity. This increase in conductivity is due to the ionic mobility differences of hydronium ions, $362.5 \times 10^{-5} \frac{cm^2}{V \cdot S}$, and benzyltrimethylammonium ions, $35.6 \times 10^{-5} \frac{cm^2}{V \cdot S}$. Essentially, during electrophoresis, one is exchanging a relatively slow cation with an extremely fast cation which causes an increase in conductivity even though the total salt concentration is rapidly decreasing.

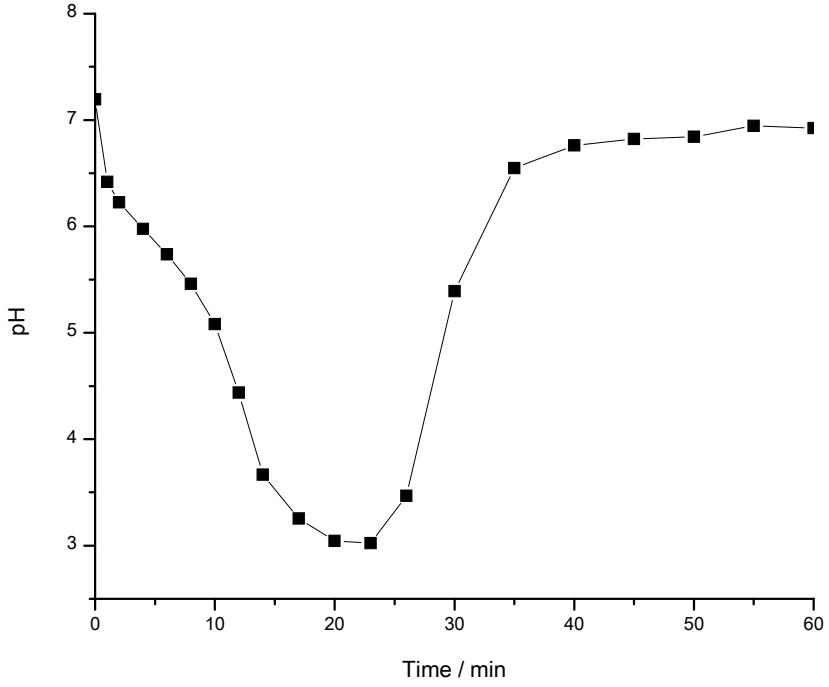

Figure 46. pH profile for the collection stream.

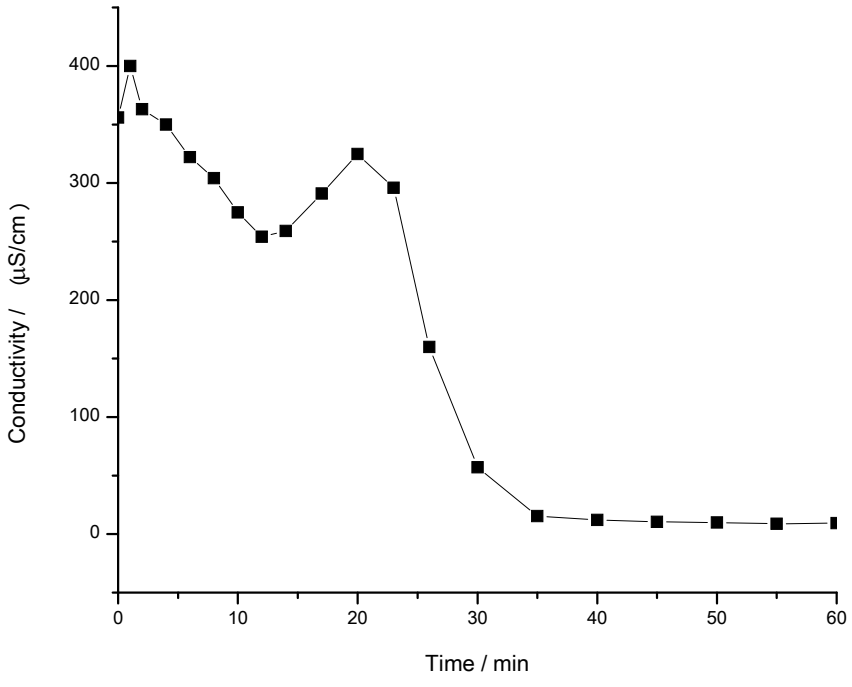

Figure 47. Conductivity profile for the collection stream.

In order to confirm that the observed pH and conductivity changes are explained by the different removal rates for $PTSA^-$ and $BzTMA^+$, the concentration of each constituent is plotted in Figure 48 and the concentration differences of the two are plotted in Figure 49. Figure 48 confirms that the rate of removal for $BzTMA^+$ is higher than for $PTSA^-$. Figure 49 indicates that the concentration of excess $PTSA^-$ reaches a maximum of about 3 mM at 23 minutes. This correlates well with the time when the minimum pH was detected and would give a calculated pH of 3.11 which is very close to the observed pH minimum. Additionally, Figure 48 indicates that there is little to no loss of histidine over the course of the experiment. The results of the desalting experiments indicate that the T-RECS separation head is a well-behaved system that operates as expected for the removal of unwanted salts and trapping of the ampholytic target.

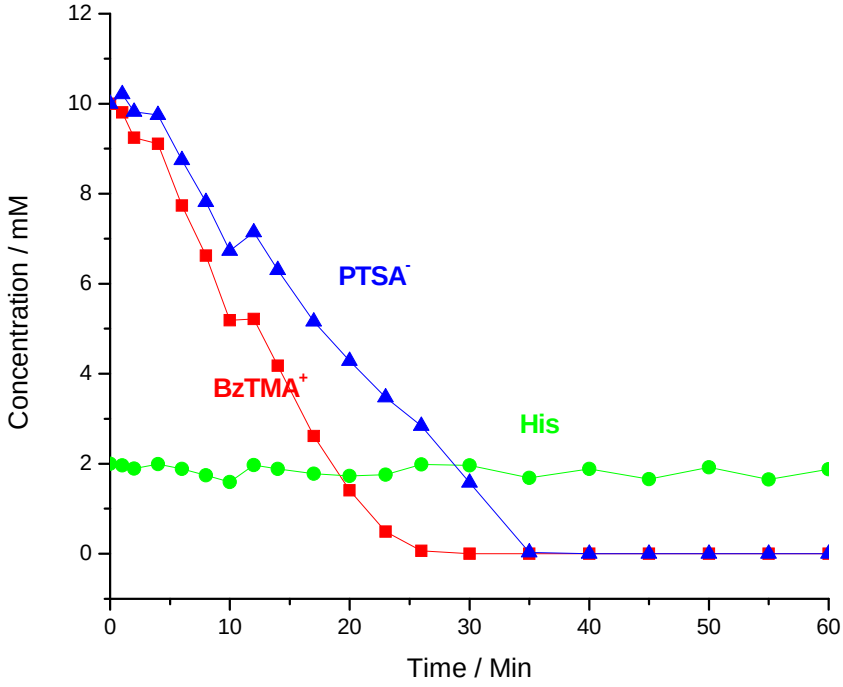

Figure 48. Concentration profiles for *p*-toluenesulfonate ($PTSA^-$), benzyltrimethylammonium ($BzTMA^+$), and histidine (His) in the collection stream.

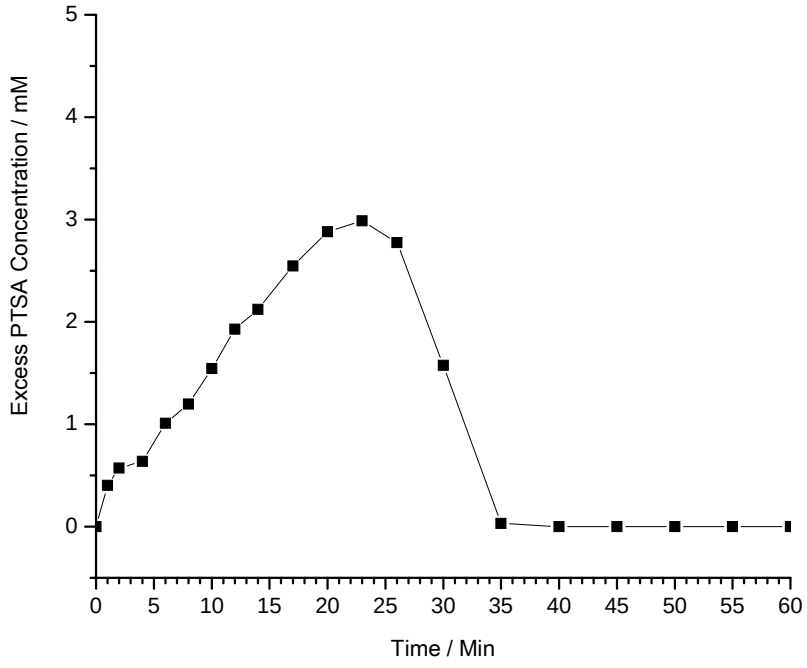

Figure 49. Plot of the difference in $PTSA^-$ and $BzTMA^+$ concentrations over time.

5.2.3 IET separation of small ampholytic molecules

5.2.3.1 Background and objective

Small ampholytes are often used to probe the properties of new IET devices [43,44]. Small molecules are chosen due to their well understood physicochemical properties, ease of analysis and handling, commercial availability and low cost. Using a simple ampholyte mixture paired with an optimized CE method and pH / conductivity measurements allows one to confirm, with relative ease, the proper operation of the separation head, the membranes, the electrolytes and the pH biasers. In this experiment the objective was to demonstrate effective separation of the ampholytes and trap them in their destination stream for an extended period of time.

5.2.3.2 Materials, method, and instrument setup

Except for the composition of the flow-through and collection solutions, the same IET arrangement was used as in Section 5.2.1.2 (Figure 38). A stock solution containing lysine, histidine, glutamic acid and nicotinic acid (each at 2 mM) was used for both the acidic and basic flow-through solutions. Initially, the collection solution was deionized water. The anolyte and catholyte streams were delivered at a flow rate of about 2 L/min, the collection stream was delivered at a flow rate of 23 mL/min. The system was operated for 240 minutes at 40 W, with an initial current of 211 mA at 190 V and a final current of 58 mA at 691 V. Aliquots were taken from the collection stream at 5, 10, 20, 30, 60, 120, and 240 minutes. The pH and conductivity values were measured for each stream. pH was measured by a VWR SB70P meter equipped with an Accumet glass pH

probe, conductivity was measured by a Thermo Orion meter equipped with a MI-915 conductivity probe (Microelectrodes, Inc.). Aliquots were also analyzed by CE, with absorbance detection at 190 nm. DMSO was used as the electroosmotic flow marker.

5.2.3.3 Results and discussion

Electropherograms for aliquots taken from the collection stream, the acidic flow-through stream and the basic flow-through stream are shown in Figures 50, 51 and 52, respectively. Lysine and histidine are quickly removed from the acidic flow-through stream, while nicotinic acid remains there for the entire time course. Similarly, histidine and nicotinic acid are removed from the basic flow-through stream while lysine remains there. However, after about 120 minutes, the size of the lysine peak decreases. This may be caused by a failure of the cathodic membrane that allows lysine to escape out to the catholyte chamber. Analysis of the catholyte after 240 minutes (Figure 53) confirms a slow loss of lysine to the catholyte. As for the collection in the appropriate streams, histidine builds up in the collection stream, lysine in the basic flow-through stream, and nicotinic acid in the acidic flow-through stream, as expected.

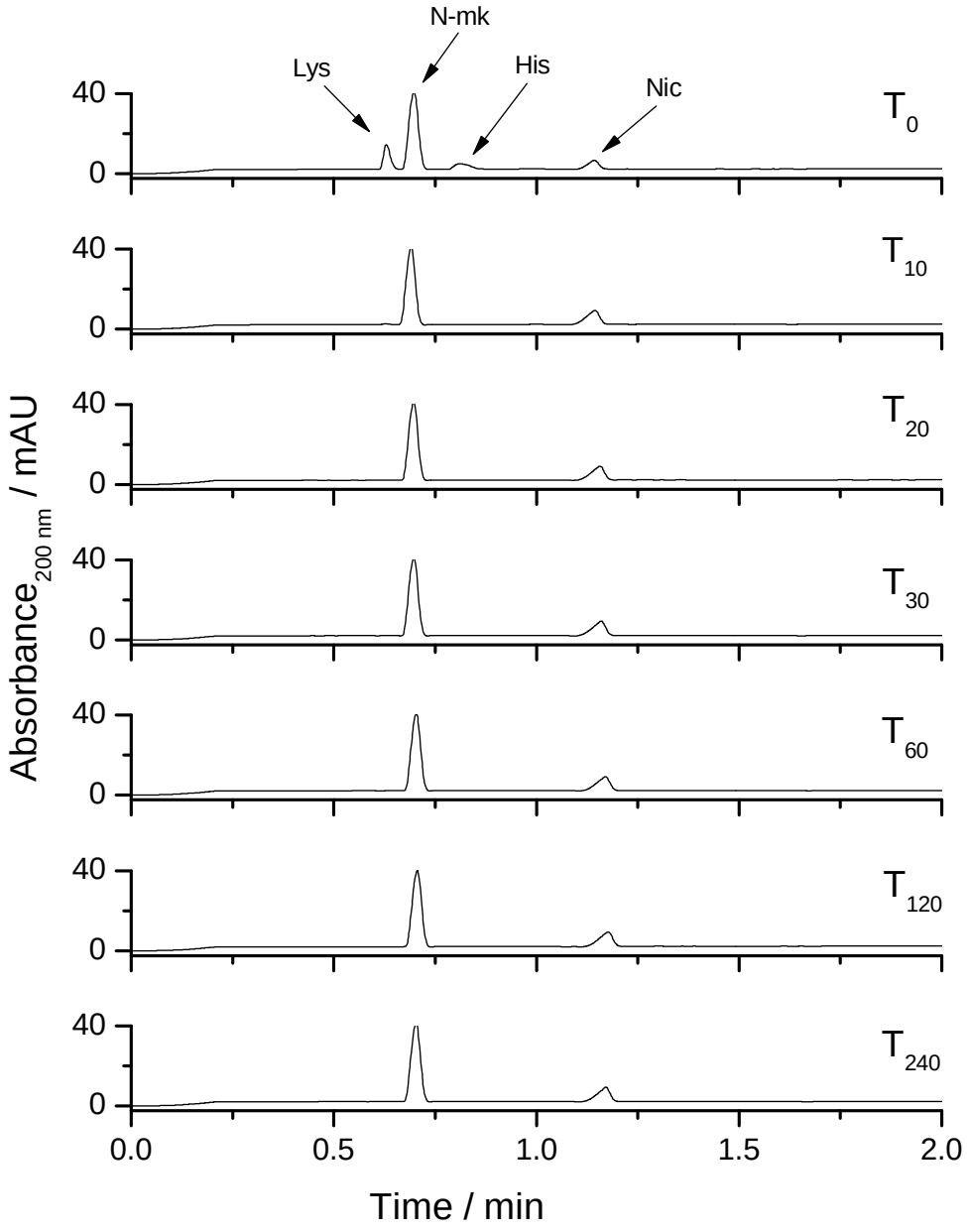

Figure 50. Electropherograms for aliquots taken from the acidic flow-through stream in the 0-240 min time interval (N-mk: electroosmotic flow marker).

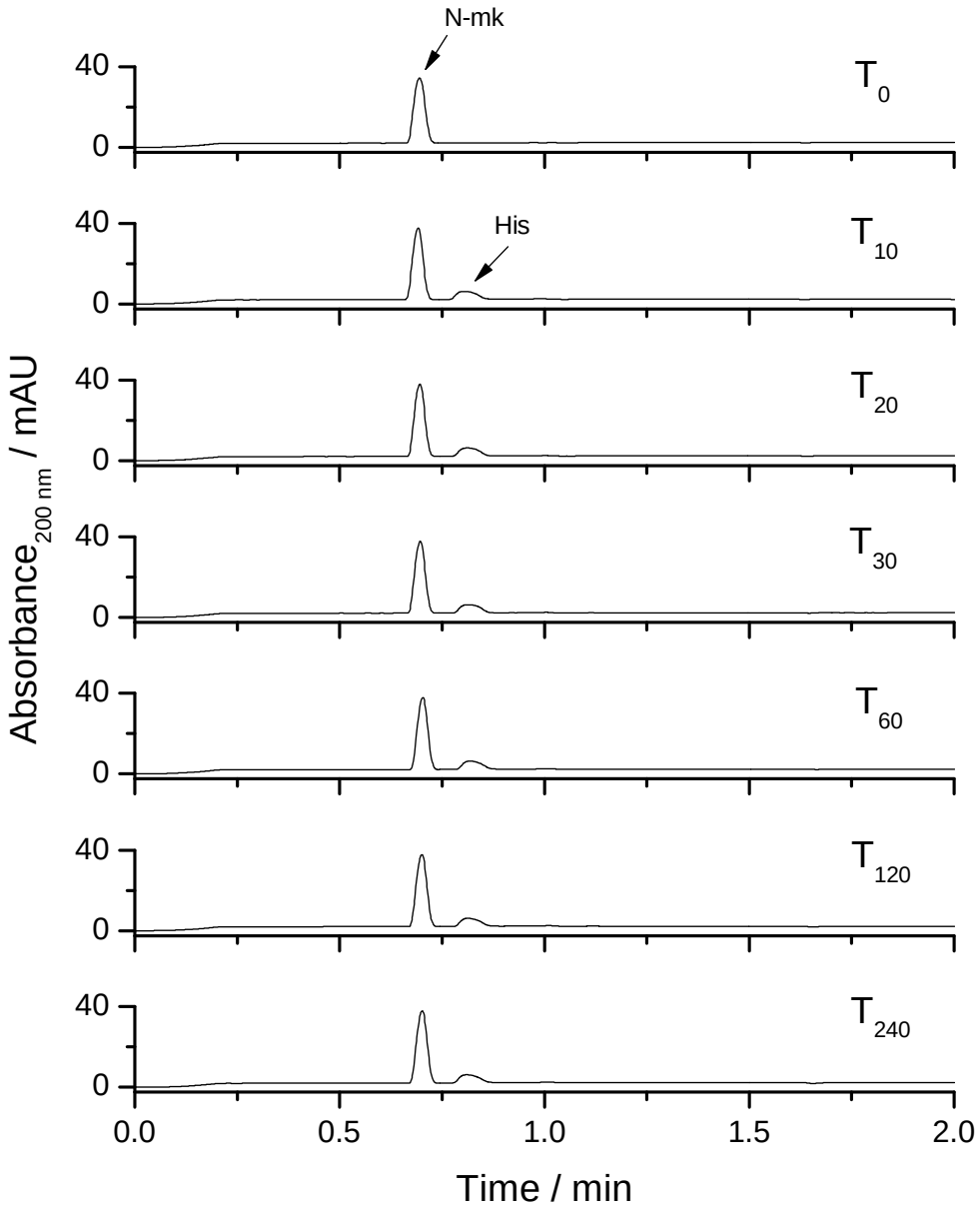

Figure 51. Electropherograms for aliquots taken from the collection stream in the 0-240 min time interval (N-mk: electroosmotic flow marker).

.

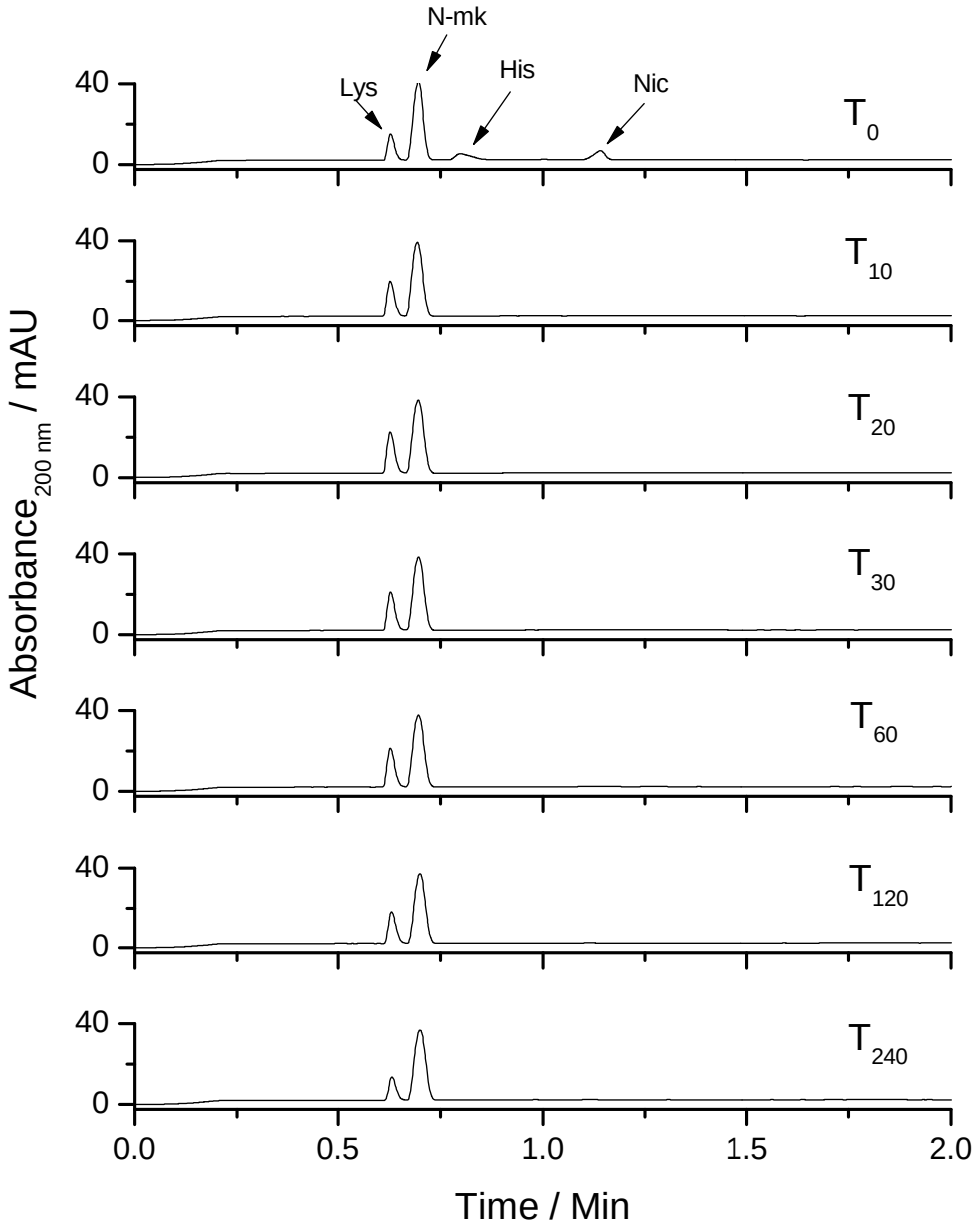

Figure 52. Electropherograms for aliquots taken from the basic flow-through stream in the 0-240 min time interval (N-mk: electroosmotic flow marker).

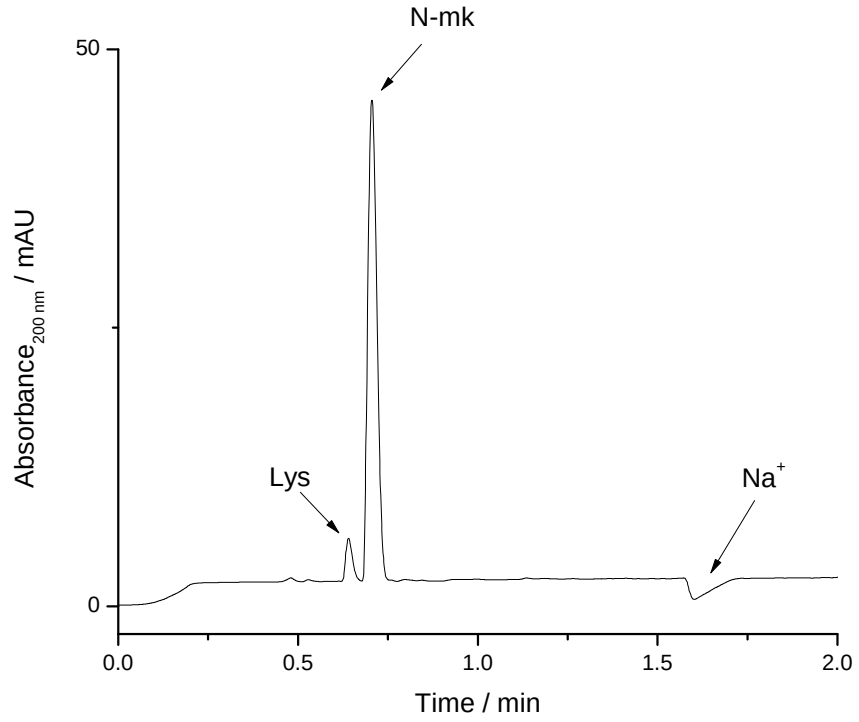

Figure 53. Electropherogram for an aliquot of the catholyte at 240 min (N-mk: electroosmotic flow marker).

The pH and conductivity profiles for the collection and flow-through streams are plotted in Figures 54 and 55. All streams started at $5 < pH < 6$, rapidly approached a pH that approximated the pI of the trapped small ampholyte, and remained relatively constant for the duration of the 4 hour long experiment. The conductivity profiles show a significant decrease in the conductivity in the basic flow-through stream and relatively small changes in the acidic flow-through and collection streams. As in Section 5.2.2, this is likely due to the high mobility of hydronium ion. In the basic flow-through stream, the conductivity contribution of the increased hydroxide ion concentration is much lower than the conductivity contribution of nicotinic acid and glutamic acid under the initial

conditions. Finally, the conductivity increase in the collection stream is small, because (i) histidine will establish a pH very near 7 (with little contribution to conductivity by either hydronium ions or hydroxide ions) and (ii) histidine is a relatively poor carrier ampholyte (ΔpK_a ~3.1).

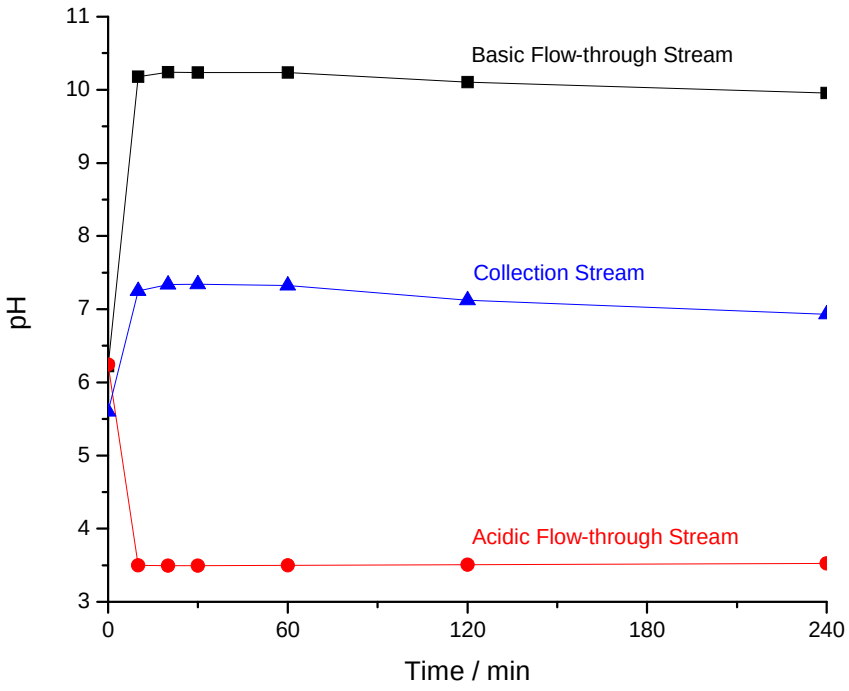

Figure 54. pH profiles during trapping of small ampholytes in a single separation head.

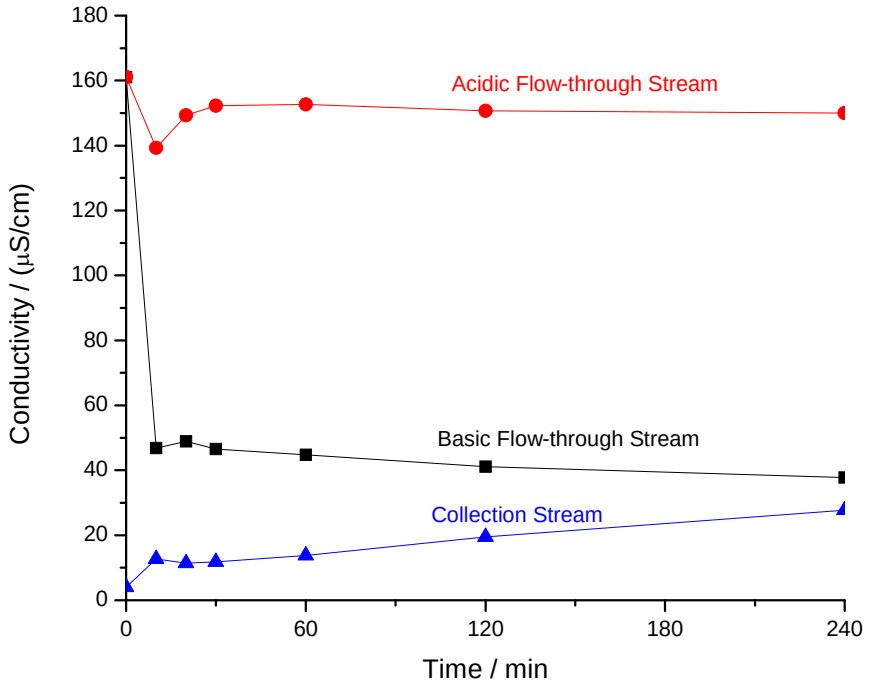

Figure 55. Conductivity profiles during trapping of small ampholytes in a single separation head.

5.3 Simultaneous operation of four isolated separation heads

5.3.1 Separation of small molecule ampholytes

5.3.1.1 Background and objective

As in section 5.2.3, UV-absorbing small molecule ampholytes were used to confirm the proper functioning of T-RECS when the four separation heads were operated simultaneously. In this case, the heads were isolated from each other, with each head having its own acidic and basic feed. In addition to confirming the proper operation of the 3 separation heads not tested in section 5.2, keeping the heads independent from each other is the simplest way to test the external support and tubing. Advantageously, this operating mode allows for screening of four IET arrangements simultaneously rather

than having to test them sequentially. A successful demonstration would show harvest of a single UV-absorbing small molecule ampholyte in each of the four collection chambers (with each collection chamber trapping a different species) and the depletion of this species from the acidic and basic flow-through streams.

5.3.1.2 Materials, method, and instrument setup

Figure 56 illustrates the IET arrangement for the experiment. A 500 mL stock solution of UV-absorbing ampholytes containing 1mM 3-aminobenzoic acid (pI 3.9), 1mM 4-(4-aminophenyl)-butyric acid (pI 4.8), 1mM 3-hydroxypyridine (pI 6.7) and 1mM carnosine (pI 8.1) was prepared. The UV-absorbing stock solution was divided into two aliquots. Lysine (pI 9.9) was added to one aliquot and glutamic acid (pI 3.2) to the other to reach final concentrations of 25mM and 8mM, respectively. The entire volume of these solutions was used as the basic (lysine containing) flow-through stream and the acidic (glutamic acid containing) flow-through stream for the experiment. The catholyte was a 10mM NaOH solution, the anolyte was a 15mM methanesulfonic acid solution. A 50/50 mixture of 10mM NaOH and 10mM methanesulfonic acid was loaded into the collection compartments to provide initial conductivity. The anodic and cathodic membranes for all separation heads were pH 2 and pH 10.5 membranes, respectively. Head 1 utilized pH 3.3 and pH 4.2 membranes as the acidic and basic separation membranes, respectively: this head should harvest 3-aminobenzoic acid (pI 3.9). Head 2 utilized pH 4.2 and 6.5 pH membranes and should harvest 4-(4-aminophenyl)-butyric acid (pI 4.8). Head 3 utilized pH 6.5 and 7.2 pH membranes and should harvest 3-

hydroxypyridine (pI 6.7). Head 4 utilized pH 7.2 and 8.9 pH membranes and should harvest carnosine (pI 8.1). The separation was run for 240 minutes with a maximum power load setting of 30 watts per separation head. Samples were taken from the acidic feed, basic feed, and collection streams of each head at 15, 30, 45, 60, 90, 120, 180, and 240 minutes. The pH and conductivity values were measured as in the previous experiments. The samples taken were diluted 50 / 50 with a pH 2.6 buffer (prepared by adding 50mmol formic acid and 5 mmol LiOH to 1 L of double-deionized water) that contained imidazole and dansylphenyalanine as mobility markers and internal standards. Each diluted sample was analyzed by capillary electrophoresis with a PDA detector monitoring absorbance at 214 nm. All CE runs were completed with a 50 μm internal diameter fused silica capillary (L_t = 30.6 cm; L_d = 20.3 cm), operated at 25 kV, using the pH 2.6 formic acid / lithium formate buffer as the background electrolyte. The polarity was plus-to-minus.

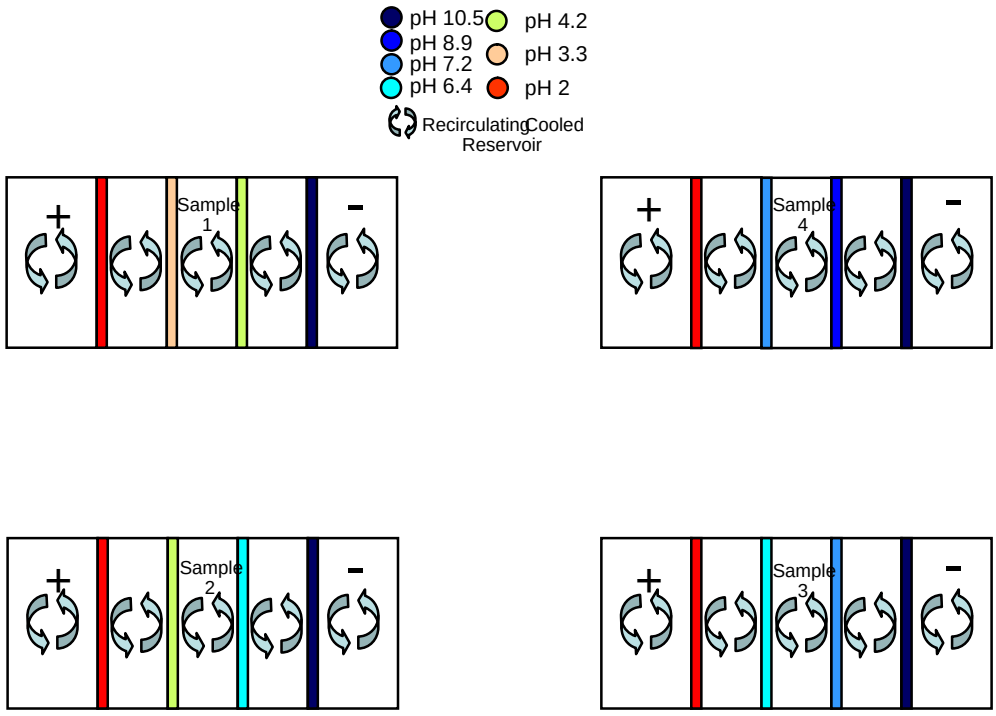

Figure 56. IET arrangement for harvesting small molecule ampholytes in the T-RECS operated as four isolated MCEs.

5.3.1.3 Results and discussion

The results of the CE analysis of the samples taken are displayed in Figures 57-60. Distortion of the peak shape for carnosine (pI 8.1) in electropherograms for the basic flow-through streams is due to co-migration with the lysine biaser. As such, estimated carnosine concentrations in the basic flow-through were determined using a different standard curve that was spiked with 25 mM lysine. Figure 57 shows that by 240 minutes, 3-aminobenzoic acid (pI 3.9) has been completely removed from the acidic and basic feed streams and has been isolated in the collection chamber of separation head 1 while

the other UV-absorbing markers are sequestered into the basic feed stream. Figure 58 shows that by 240 minutes, 4-(4-aminophenyl)-butyric acid (pI 4.8) has been removed from the acidic and basic feed streams and has been isolated in the collection chamber of separation head 2. Figure 58 also indicates that 3-aminobenzoic acid (pI 3.9) is trapped in the acidic feed stream and both 3-hydroxypyridine (pI 6.7) and carnosine (pI 8.1) are trapped in the basic feed stream. Figure 59 shows that by 240 minutes, 3-hydroxypyridine (pI 6.7) has been completely removed from the acidic and basic feed streams and has been isolated in the collection chamber of separation head 3. Figure 59 also indicates that both 3-aminobenzoic acid (pI 3.9) and 4-(4-aminophenyl)-butyric acid (pI 4.8) are trapped in the acidic feed stream and carnosine (pI 8.1) is trapped in the basic feed stream. Figure 60 shows that by 240 minutes, carnosine (pI 8.1) has been completely removed from the acidic and basic feed streams and has been isolated in the collection chamber of separation head 4 while the other UV-absorbing ampholytes are sequestered into the acidic feed stream. Since *(i)* a single UV-absorbing small molecule ampholyte was harvested in each collection stream, *(ii)* each collection stream trapped a different ampholyte, and *(iii)* ampholytes not trapped in a collection stream were found in the acidic or basic flow-through streams as would be expected based on their pI and the membrane pH values, it can be concluded that each separation head performed properly.

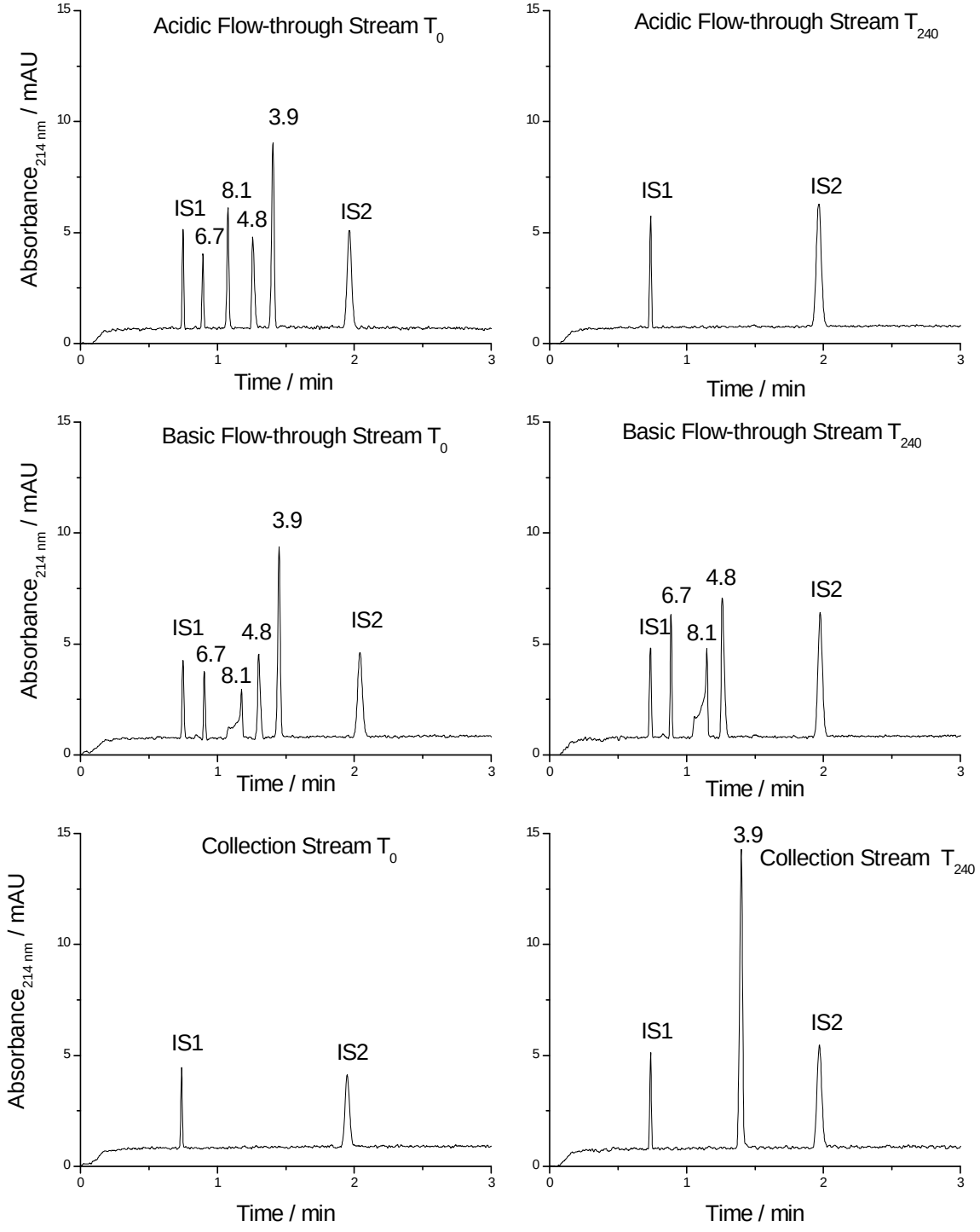

Figure 57. Electropherograms for the samples taken from the flow-through streams and the collection stream for separation head 1.

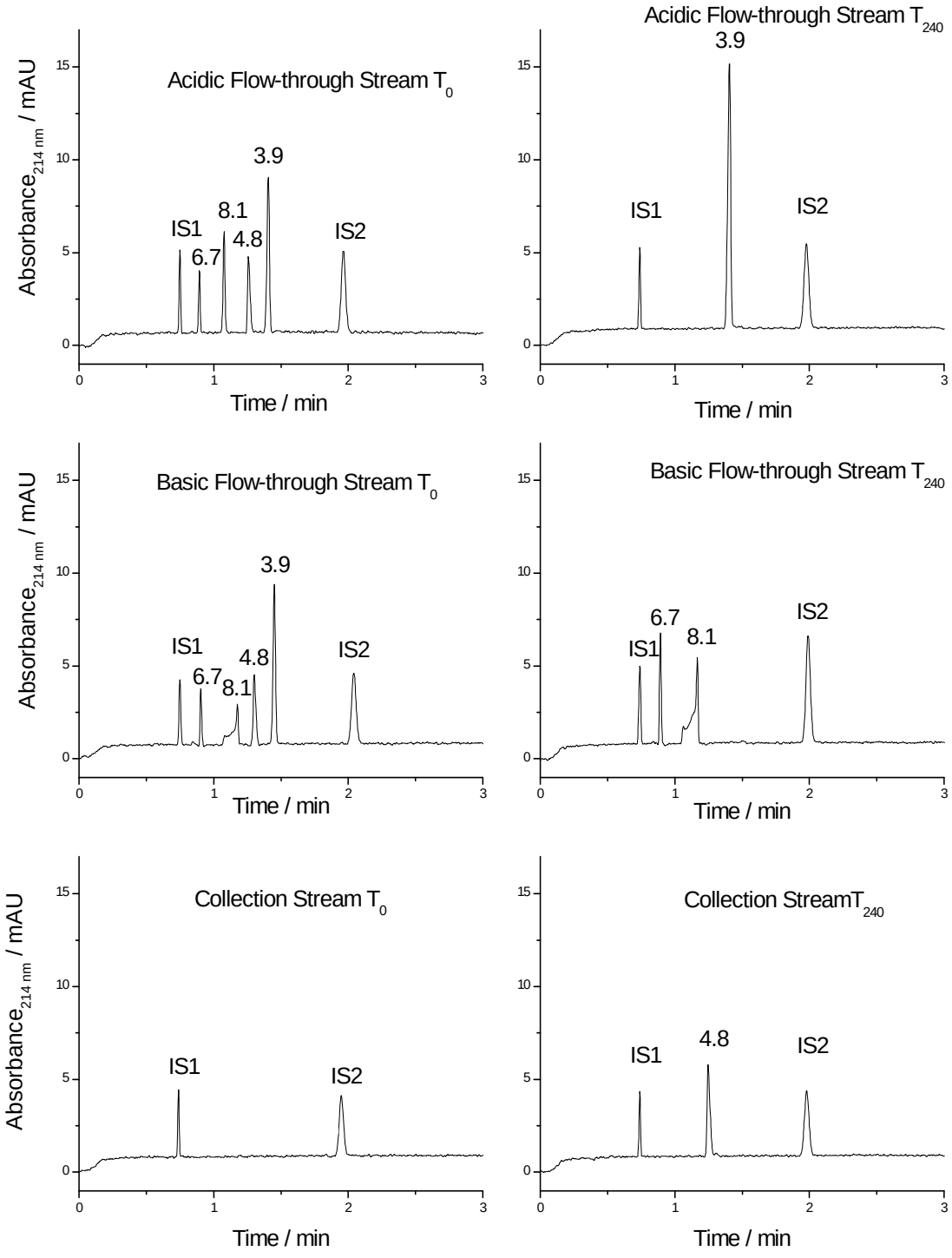

Figure 58. Electropherograms for the samples taken from the flow-through streams and the collection stream for separation head 2.

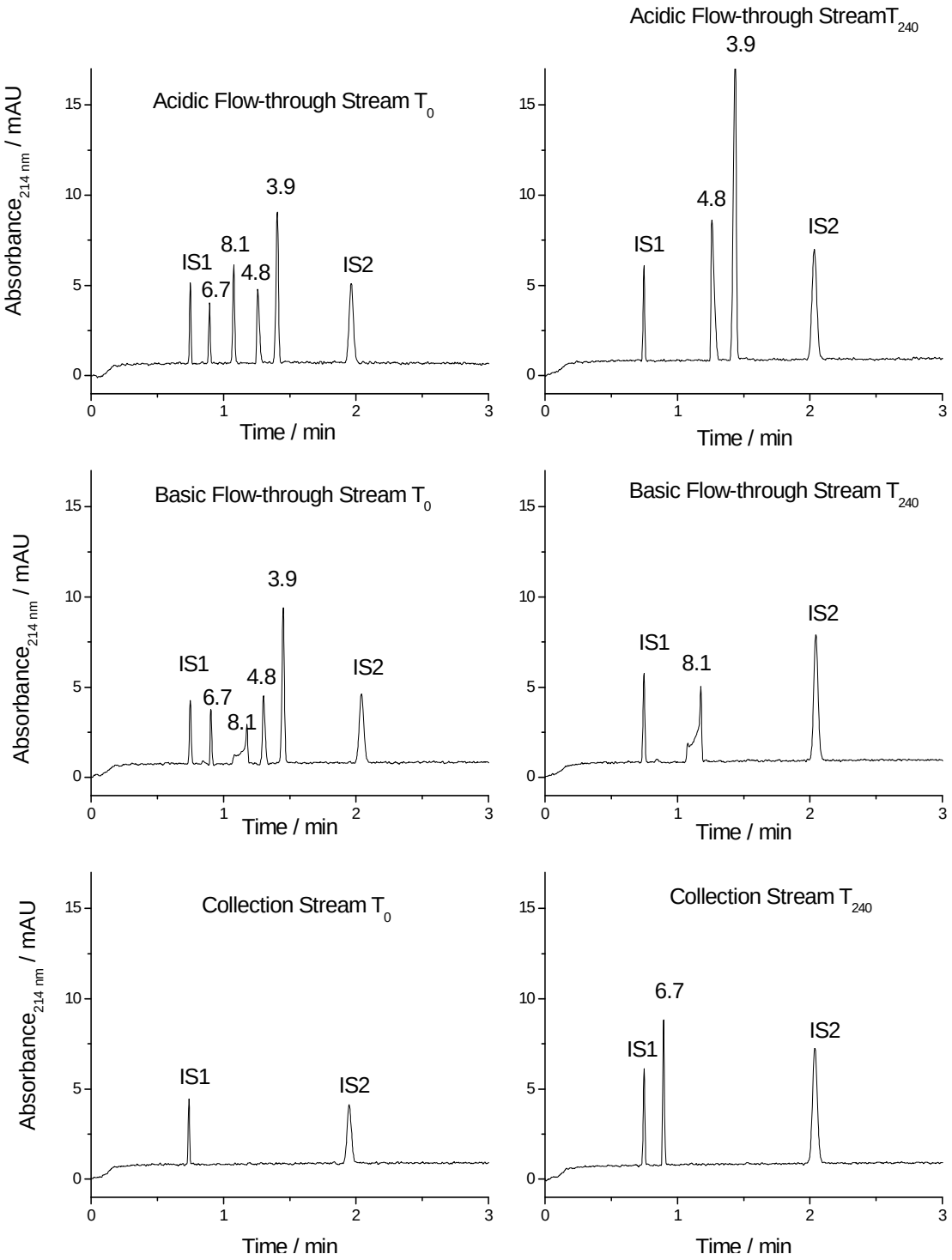

Figure 59. Electropherograms for the samples taken from the flow-through streams and the collection stream for separation head 3.

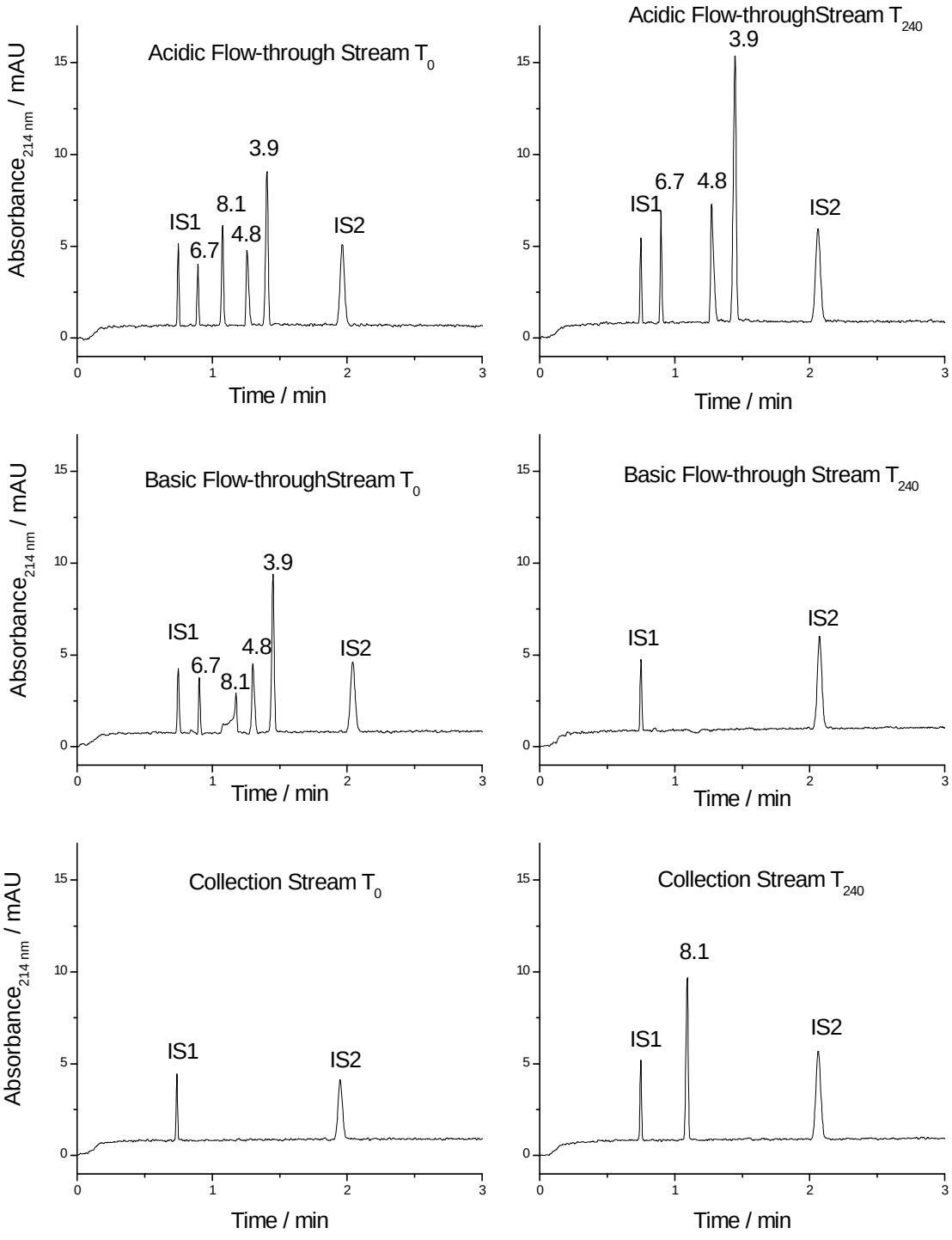

Figure 60. Electropherograms for the samples taken from the flow-through streams and the collection stream for separation head 4.

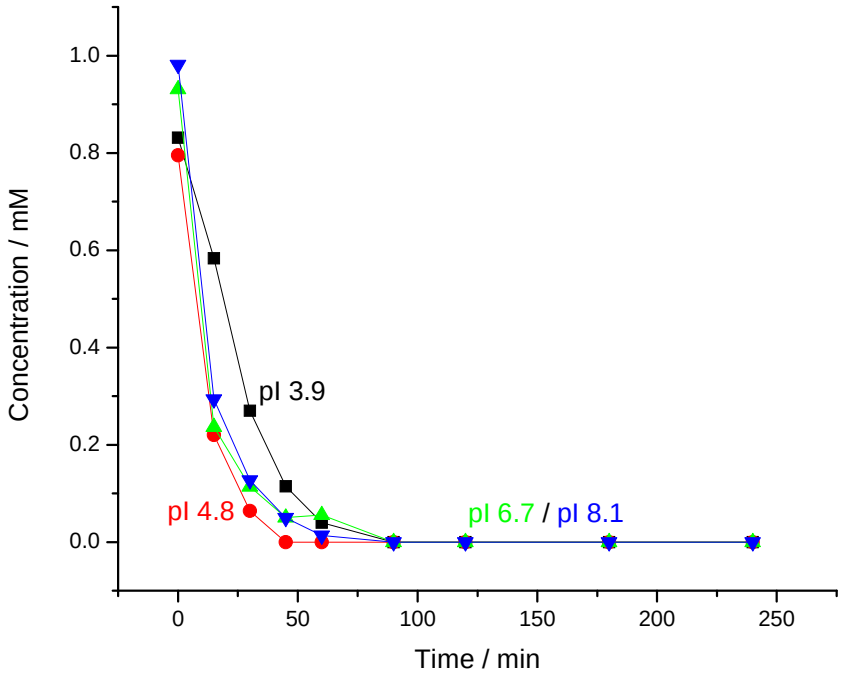

Figure 61. Concentration profiles for 3-aminobenzoic acid (pI 3.9), 4-(4-aminophenyl)-butyric acid (pI 4.8), 3-hydroxypyridine (pI 6.7) and carnosine (pI 8.1) in the acidic flow-through streams.

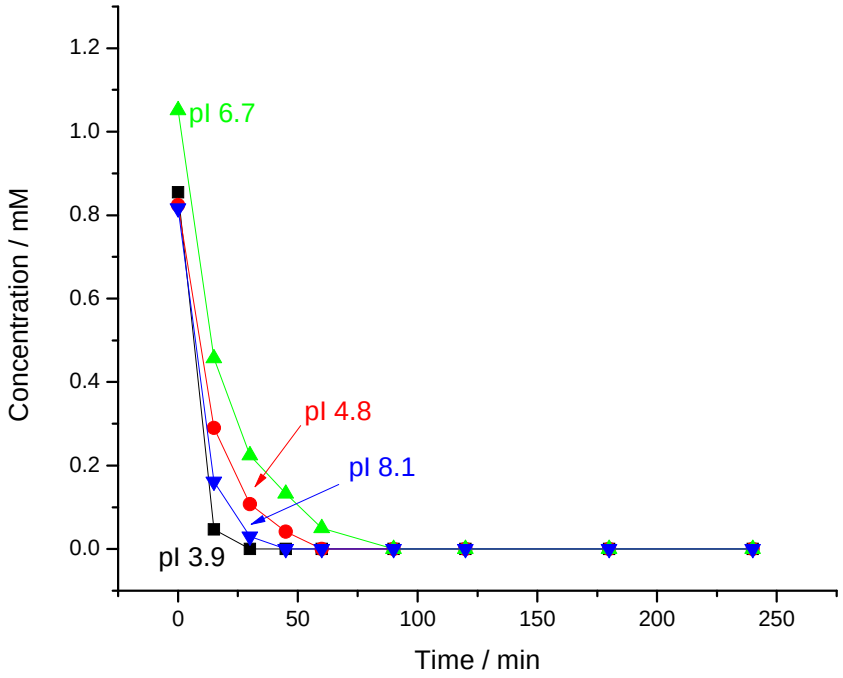

Figure 62. Concentration profiles for 3-aminobenzoic acid (pI 3.9), 4-(4-aminophenyl)-butyric acid (pI 4.8), 3-hydroxypyridine (pI 6.7) and carnosine (pI 8.1) in the basic flow-through streams.

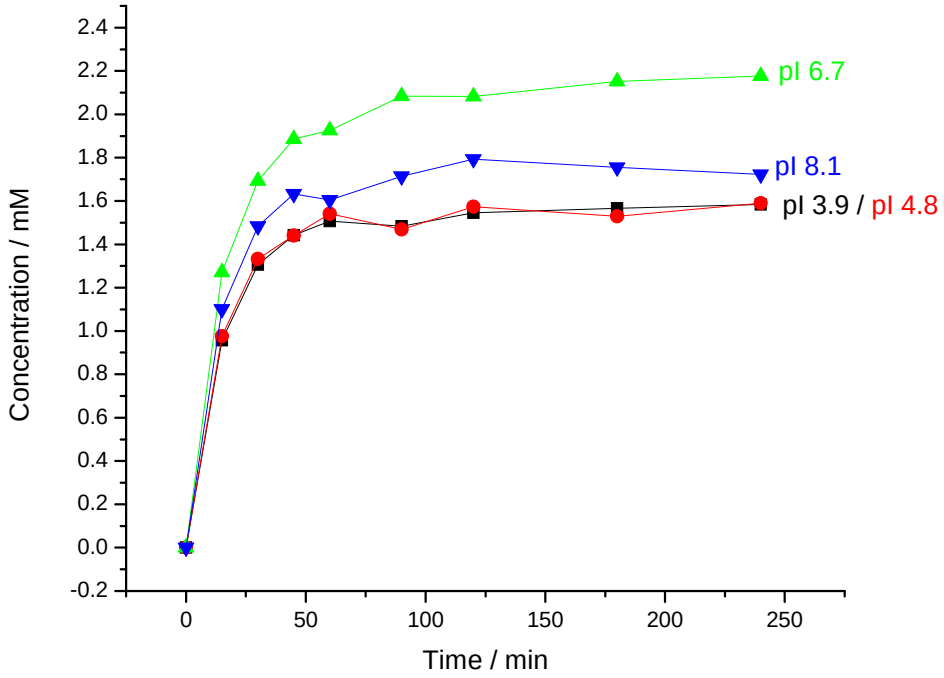

Figure 63. Concentration profiles for 3-aminobenzoic acid (pI 3.9), 4-(4-aminophenyl)-butyric acid (pI 4.8), 3-hydroxypyridine (pI 6.7) and carnosine (pI 8.1) in the collection streams.

The concentration of each ampholyte in the acidic, basic, and collection streams in each separation head is plotted as a function of the harvesting time in Figures 61-63, e.g., 3-hydroxypyridine concentrations are plotted for the compartments of separation head 3 in Figure 63. The ampholyte concentrations were estimated from the time-corrected relative peak areas (normalized to the imidazole internal standard, IS1) obtained by CE analysis. Electrophoretic depletion of each ampholyte from both the acidic and basic feed streams follows an exponential decay curve as depletion approaches completion. It appears that the separation is complete by 90 minutes, as none of the ampholytes remain detectable in either the acidic or basic feed streams. Additionally, by 90 min, the harvested target concentrations approach a final value and remain relatively constant for

the remainder of the separation. Finally, the pH and conductivity values, plotted in Figures 64 and 65, all approach steady state final values by the end of the separation. All pH plots are in good agreement with the results of the CE analysis, i.e., that the separation is complete in approximately 90 minutes. However, careful examination of the conductivity profile of separation head 3 indicates that the separation in fact may not be completed until approximately 120 minutes, because conductivity in this chamber doesn't reach a steady value until after this time point. Based on a completion time of 2 hours, the total processing and target production rates for T-RECS, operated as 4 isolated MCEs, are about 160 mg/hour and 40 mg/hour, respectively.

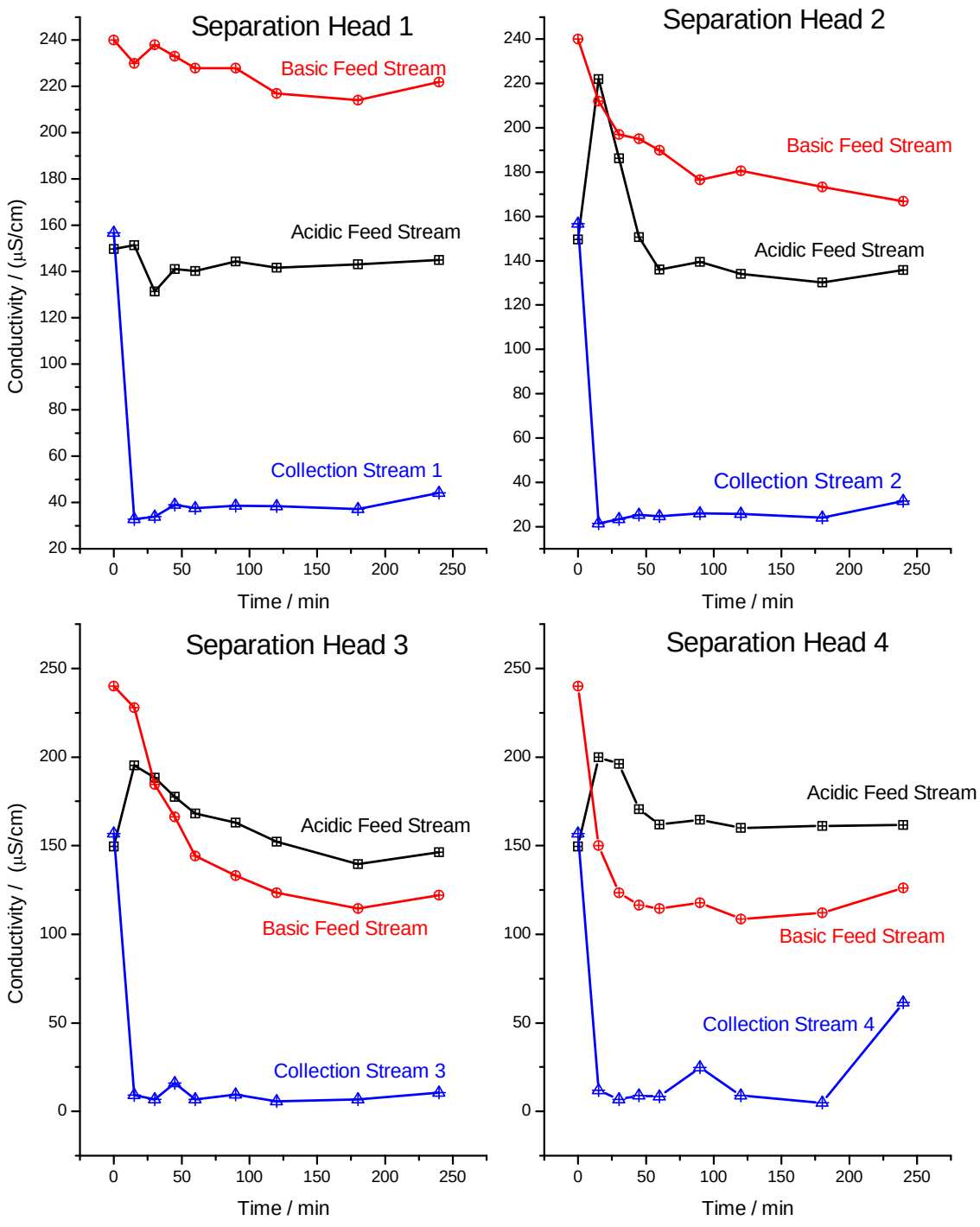

Figure 64. Conductivity profiles for each separation head for the separation of small molecule ampholytes.

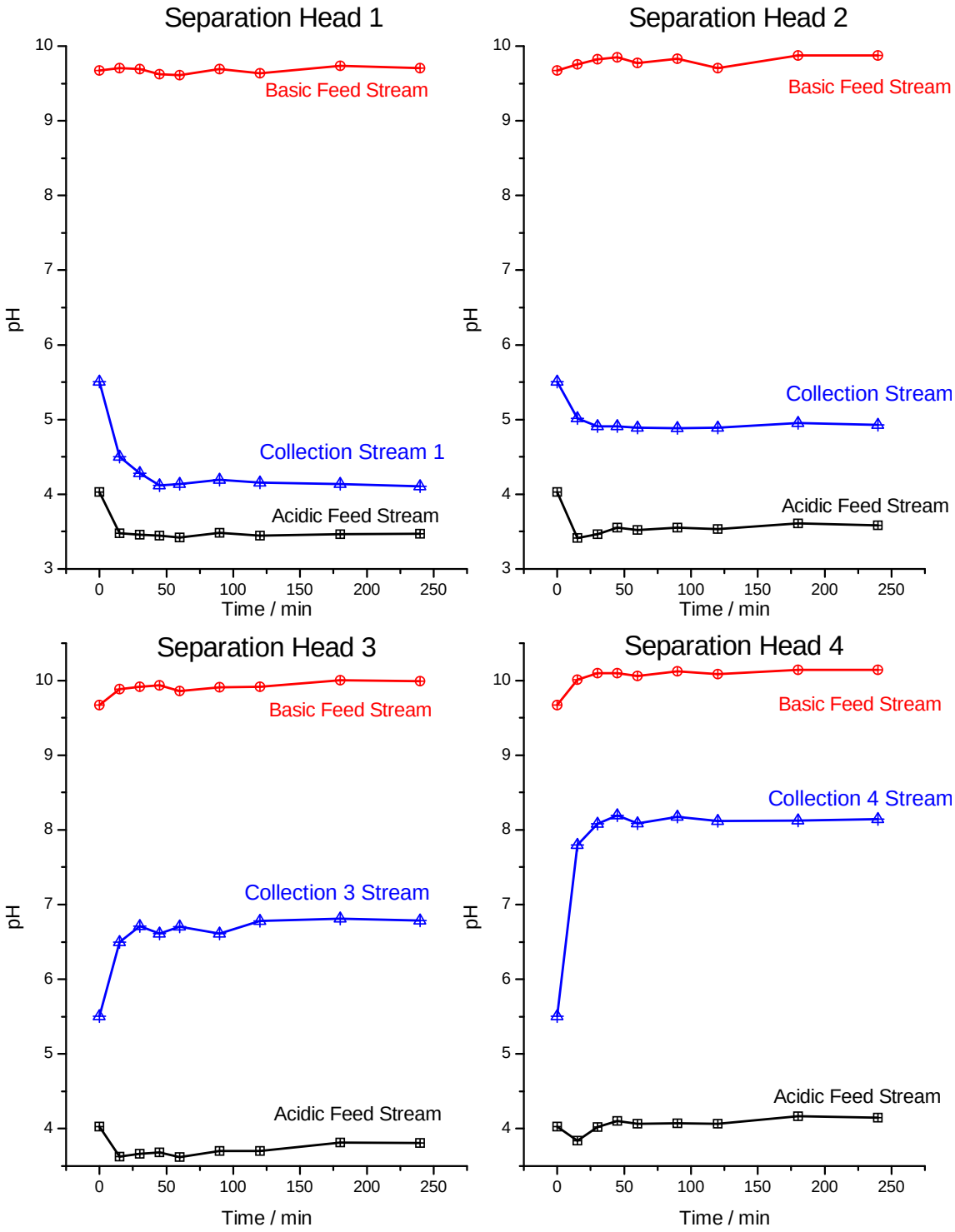

Figure 65. pH profiles for each separation head for the separation of small molecule ampholytes.

5.3.2 Separation of the isoforms of a diagnostic monoclonal antibody

5.3.2.1 Background and objective

One of the most attractive applications of preparative-scale IET is the purification of protein targets from complex mixtures. Monoclonal antibodies, because of their value in research, diagnostics, and therapeutics are of particular interest. Their preparative-scale IET separation has been studied previously [33]. Because of that, monoclonal antibody separations by T-RECS can provide a benchmark for comparison with previous work and demonstrate the suitability of T-RECS for protein separations.

5.3.2.2 Materials, method, and instrument setup

Figure 66 illustrates the IET arrangement for the experiment. A process pool of antibody pre-separated by ion-exchange chromatography and stored in 4-(2-hydroxyethyl)-1-piperazineethanesulfonic acid (HEPES) buffer (antibody concentration: 6.8 mg/mL, pH 8.06, conductivity of 2.6 mS/cm) was diluted to a final antibody concentration of about 2 mg/mL in a 5 mM histidine solution that also contained 30% w/w sucrose. 250 mL of this stock solution was used as the acidic flow-through streams. The basic flow streams contained 5 mM lysine and 30% w/w sucrose. The catholyte was a 10 mM NaOH solution, the anolyte was a 15 mM MSA solution and both solutions contained 30% w/w sucrose. An approximately 2 mM sodium methanesulfonate solution was used as the initial collection stream. The separation was run for 24 hours, at a maximum power load of 10 W in each separation head. Samples were taken from the acidic feed, basic feed, and collection streams in each head at 30, 60, 90, 120, 180, 360, 900, 1080, and 1440

minutes. The pH and conductivity values were measured as in the previous experiments. Samples taken from each collection stream at 1440 minutes were also analyzed by HPLC using a WCX-exchange column, a pH 6, 20 mM BisTRIS eluent in which the NaCl concentration was increased linearly from 50 to 200 mM in 60 minutes. Absorbance of the effluent was monitored at 280 nm. Additionally, 1440 minute samples taken from collection streams 3 and 4 were analyzed by cIEF using pI 8-10.5 carrier ampholytes.

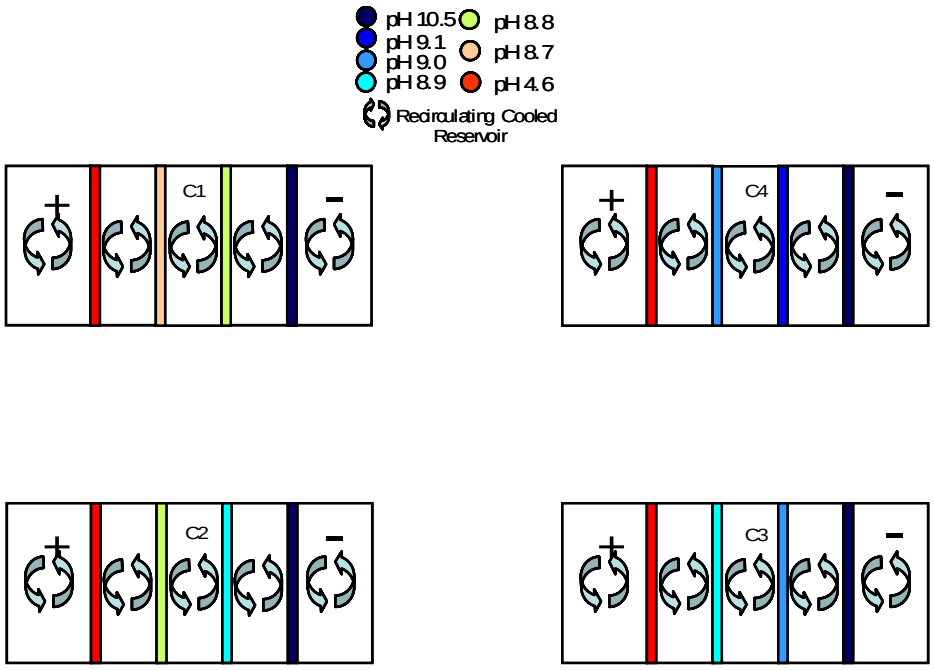

Figure 66. IET arrangement for separation of the diagnostic antibody isoforms with T-RECS operated as four isolated MCEs.

5.3.2.3 Results and discussion

The pH, conductivity, potential, and current profiles are plotted in Figures 67-70. Separation was halted after 24 hours as the potential and current values leveled off to constant values. An initial decrease in current and increase in potential caused by loss of

conductivity in the streams was observed for each separation head. These changes were attributed to removal of salt from the collection and acidic flow-through streams in agreement with the conductivity profiles for the streams (Figure 70). For the basic flow-through streams, salt removal caused a transient increase of conductivity as cations moved through the chamber and into the catholyte. For the acidic flow-through streams, a rapid decrease in conductivity over the first 60 minutes confirmed the fast removal of the initial HEPES buffer. Apart from the initial conductivity decrease confirming the removal of sodium methanesulfonate, little information could be discerned from the pH and conductivity profiles of the collection streams: they could be assigned as belonging to pure water or a very dilute solution of antibodies having a narrow pI range. Chromatograms for the samples taken from the collection stream are shown in Figure 71. By comparing the chromatograms for samples taken from the initial acidic flow-through stream and the 1440 min collection streams, it appears that antibodies were not trapped in the collection streams of separation heads 1 and 2. However, in the collection stream of separation head 3, one can observe a broad peak that has an elution time and peak shape similar to that of the acidic antibody variant, with little or none of the main antibody peak observed. In the collection stream of separation head 4, there is a sharp peak that correlates closely with the main antibody peak but also has a shoulder that overlaps with the elution time of the acidic variants. These results indicate that at least a partial separation of the acidic variants from the main antibody peak has been achieved in separation head 3, and that further separation of some of the acidic antibody variants from the main peak may have occurred in separation head 4. To more closely determine

the extent of separation between the acidic antibody isoforms and the main isoforms, cIEF, providing an orthogonal separation based on differences in pI rather than in chromatographic binding, was performed on the 1440 min samples taken from the collection streams of separation heads 3 and 4. The resulting electropherograms are shown in Figure 72. When the electropherograms for the collection streams of separation heads 3 and 4 are compared with the electropherograms of the antibody standard, it appears that the standard is slightly shifted toward more basic pI values. This shift is likely caused by HEPES (pK_a ~7.5), the buffer in which the standard is stored in, that distorts the pH gradient. Therefore, the antibody distributions can only be compared for the HEPES-free samples taken at 1440 min. The electropherogram for the sample taken from the collection stream in separation head 3 confirms that the acidic variants were mostly separated from the main and basic variants, because there is only a small peak that corresponds to the main variant, while there is significant enrichment for the acidic variants, especially the lowest pI acidic variants. Given a longer run time, complete separation of the acidic variants from the main peak would likely have been achieved. In the sample taken from the collection stream in separation head 4 the main peak is still present with significant enrichment for the two highest pI acidic variants. This indicates that separation head 4 is isolating a slightly higher pI fraction of the antibody variants, as would be expected. Finally, one can compare the processing rates for the new T-RECS system and a previous preparative-scale MCE, the Isoprime. In a similar experiment, the separation of the isoforms of a monoclonal HIV-1 antibody, the Isoprime was able to process a 235 mg sample in 11 days [33]. This indicates that the T-RECS system, which

was able to process a 750 mg of sample in only 24 hours, represents a significant improvement in the preparative-scale IET separation of monoclonal antibodies.

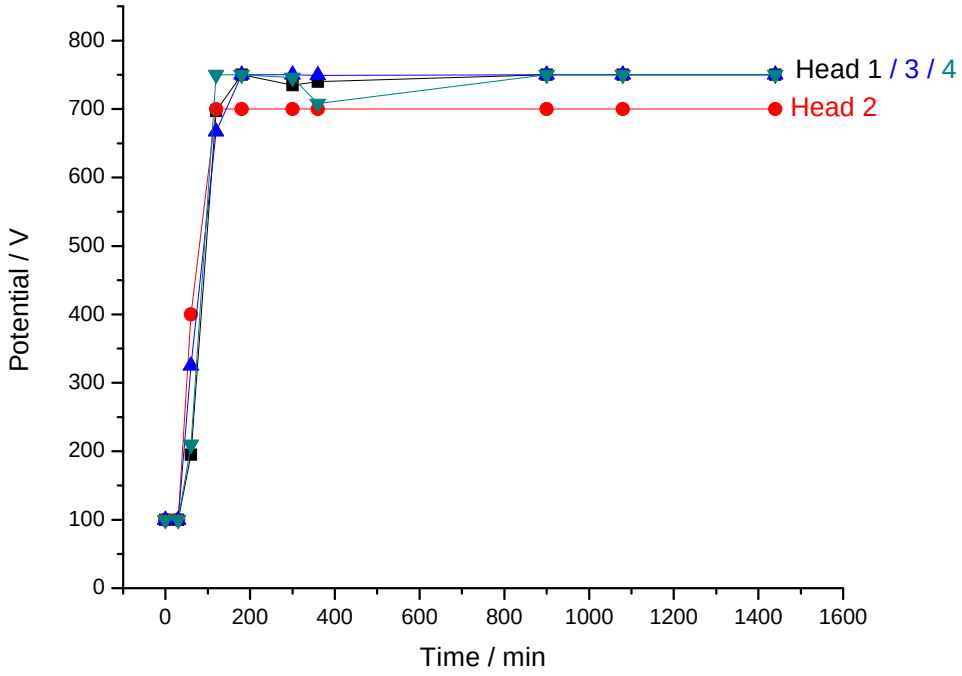

Figure 67. Potential profiles for the four separation heads for the separation of the isoforms of a diagnostic monoclonal antibody.

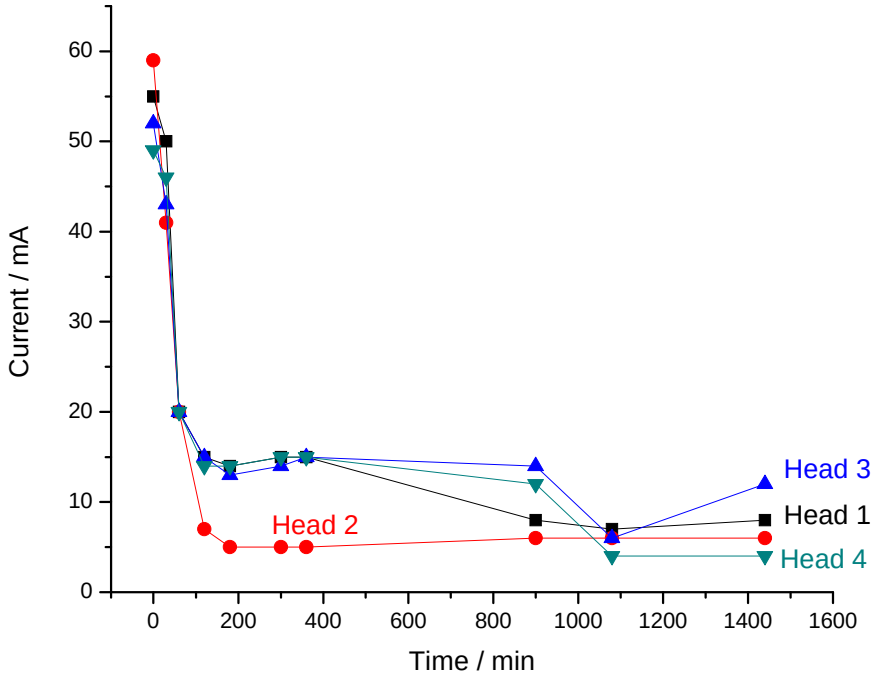

Figure 68. Current profiles for the four separation heads for the separation of the isoforms of a diagnostic monoclonal antibody.

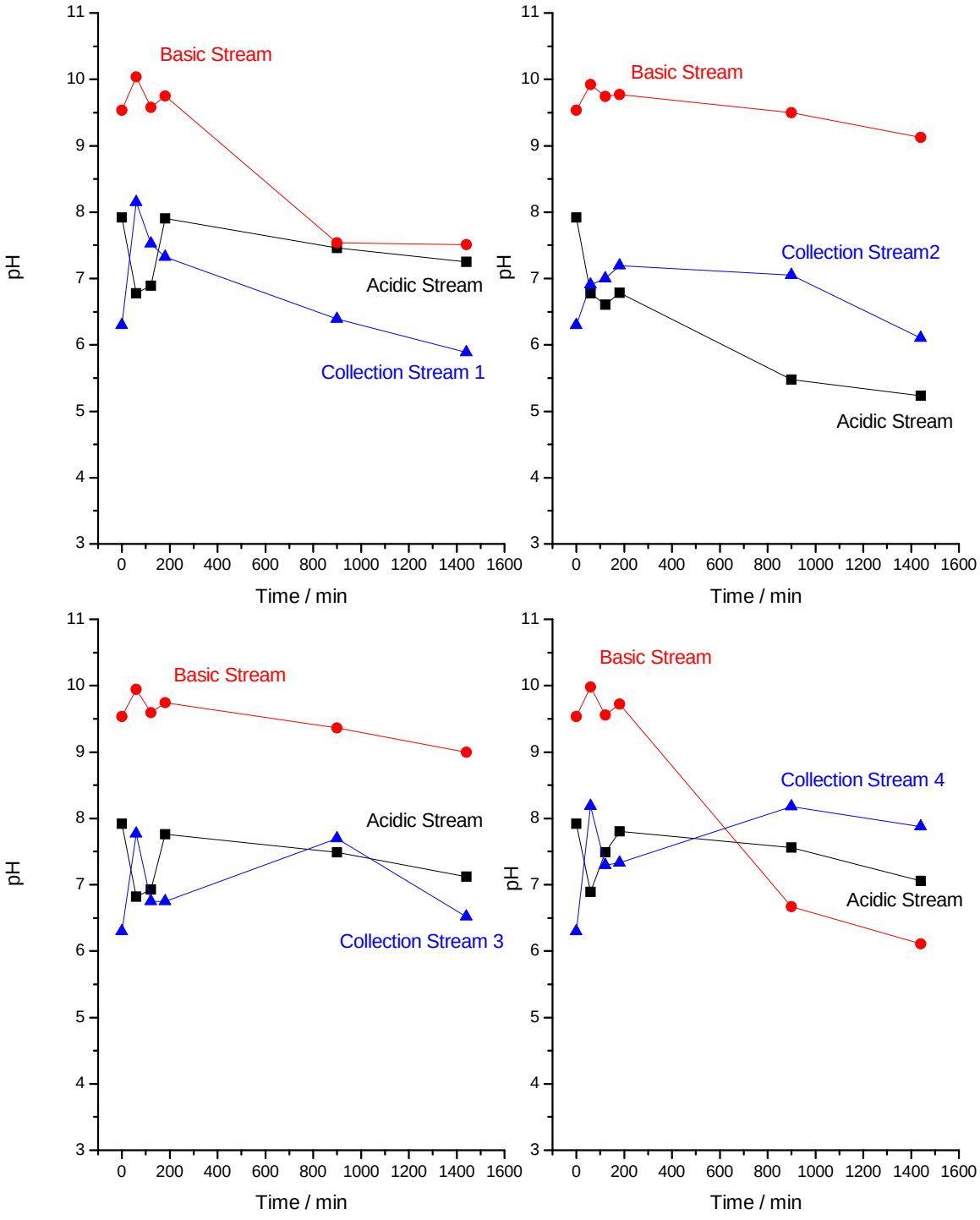

Figure 69. pH profile for each separation head for the separation of the isoforms of a diagnostic monoclonal antibody.

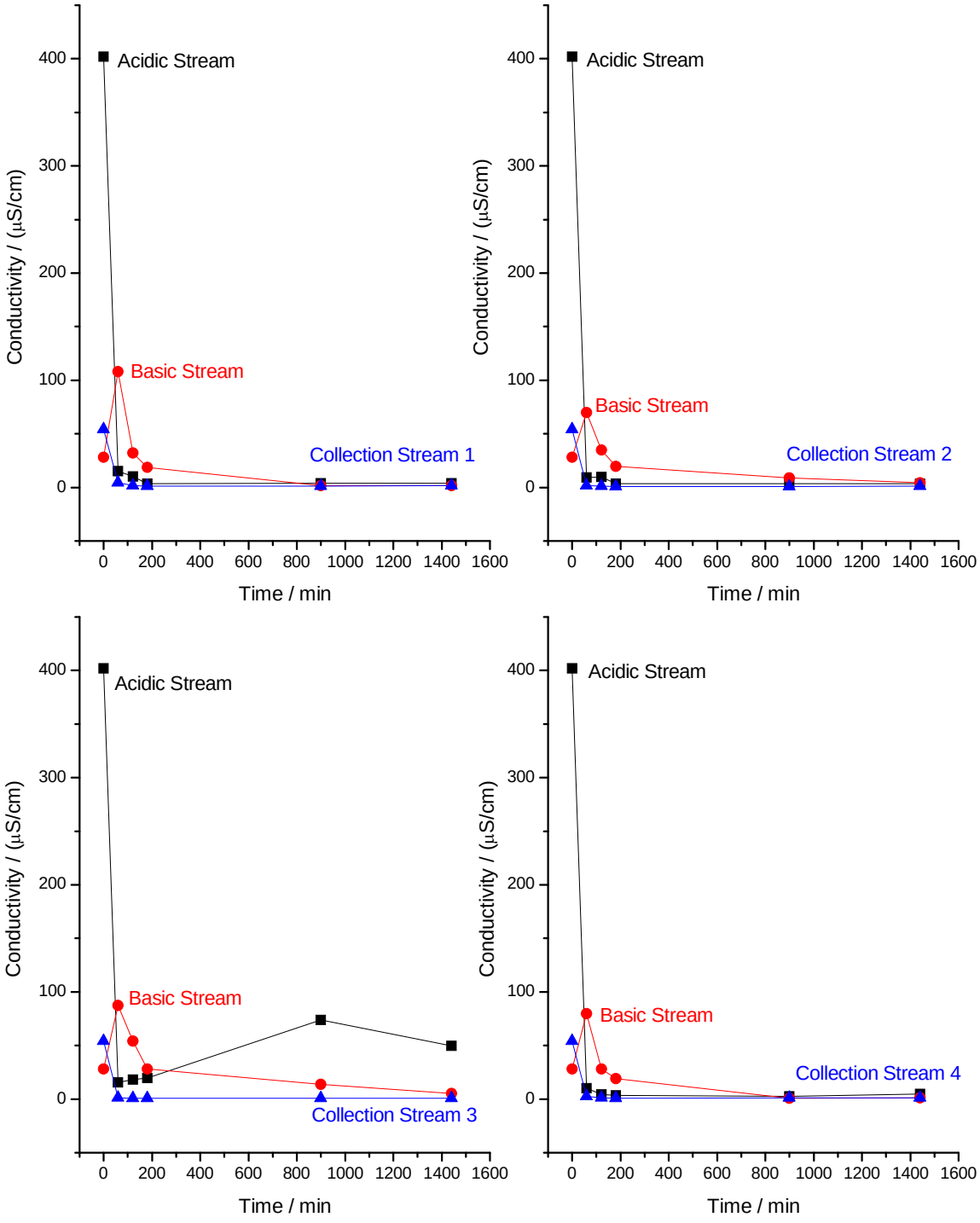

Figure 70. Conductivity profiles for the four separation heads for the separation of the isoforms of a diagnostic monoclonal antibody.

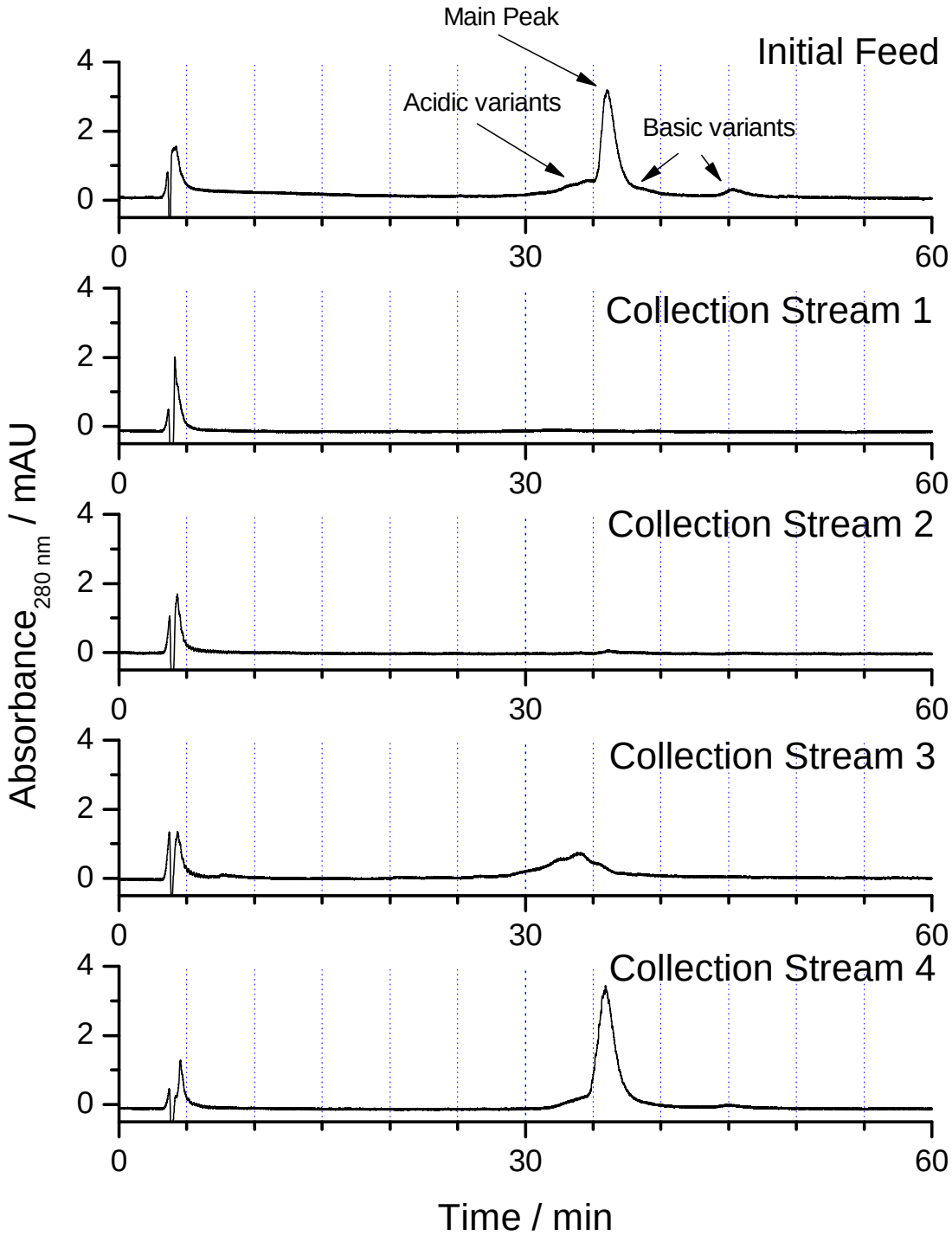

Figure 71. Chromatograms for the samples taken at 1440 min from the collection streams of each separation head.

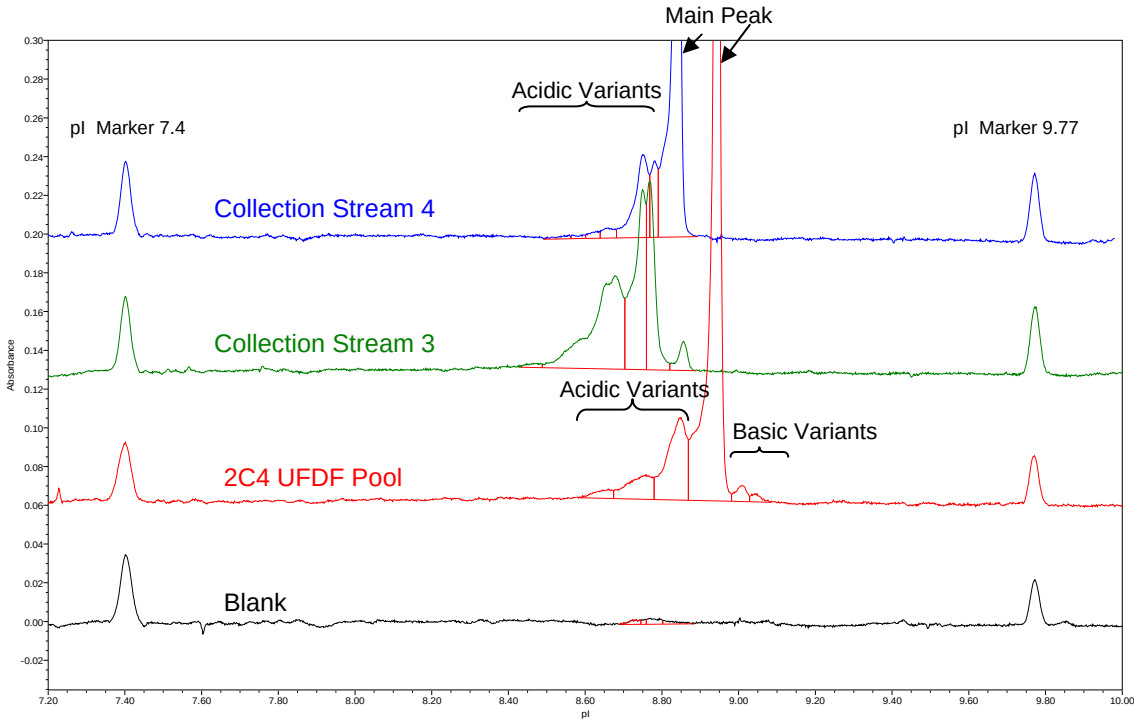

Figure 72. cIEF electropherograms for the samples taken at 1440 min from the collection streams of separation heads 3 and 4.

5.4 Operation the T-RECS as a single parallel MCE for separation of small molecule ampholytes

5.4.1 Background and objective

As in Section 5.3.1, UV-absorbing small molecule ampholytes were used to confirm the proper functioning of T-RECS when operated as a single, parallel-arranged MCE with four collection streams and two shared flow-through streams. A successful demonstration would show harvest of a single UV-absorbing small molecule ampholyte in each of the four collection chambers (with each collection chamber trapping a different species) and the depletion of all of the small molecule ampholytes in the acidic and basic flow-through streams.

5.4.2 Instrument setup, materials, and method

Figure 73 illustrates the IET arrangement for the experiment. Solutions were prepared in the same manner as Section 5.3.1. The anodic and cathodic membranes for all separation heads buffered at pH 2 and pH 10.5, respectively. Head 1 utilized pH 3.3 and pH 4.2 membranes as the acidic and basic separation membranes, respectively: this head should harvest 3-aminobenzoic acid (pI 3.9). Head 2 utilized pH 4.2 and pH 6.5 membranes and should harvest 4-(4-aminophenyl)-butyric acid (pI 4.8). Head 3 utilized pH 6.5 and 7.2 pH membranes and should harvest 3-hydroxypyridine (pI 6.7). Head 4 utilized pH 7.2 and 8.9 pH membranes and should harvest carnosine (pI 8.1). Flow-through and collection solutions were recirculated at a flow rate of about 23 mL/min. Anolyte and catholyte solutions were recirculated at a flow rate of 2 L/min. The separation was run for 480 minutes with a maximum power load setting of 40 watts per separation head. Samples were taken from the acidic flow-through, basic flow-through, and collection streams at 15, 30, 45, 60, 90, 120, 180, 240, 360, and 480 minutes. The pH and conductivity values were measured as in the previous experiments. Sample preparation and CE analysis was as described in Section 5.2.1.

5.4.3. Results and discussion

The results of the CE analysis of the samples taken are displayed in Figures 74-76. Electropherograms for the flow-through stream samples show that all markers, except for a small amount of 3-aminobenzoic acid (pI 3.9) in the acidic flow-through stream, are depleted after 480 minutes. A small amount of 3-aminobenzoic acid may be left in

the stream because either *(i)* the relatively high conductivity of the acidic flow-through stream makes the field strength across the chamber small and the ensuing transport very slow or *(ii)* a small amount of 3-aminobenzoic acid has precipitated onto the membrane surface and is slowly dissolved as the transfer progresses. Since 90% of the pI 3.9 marker is removed from the acidic flow-through stream during the first 240 minutes and 8% of it is removed during the remaining 240 minutes, harvesting the target without complete depletion of the feed stream may be an attractive option for certain separations. The electropherograms for the 480 minute samples taken from the collection streams, indicate successful harvest of the targeted marker in pure form in each of the four collection chambers.

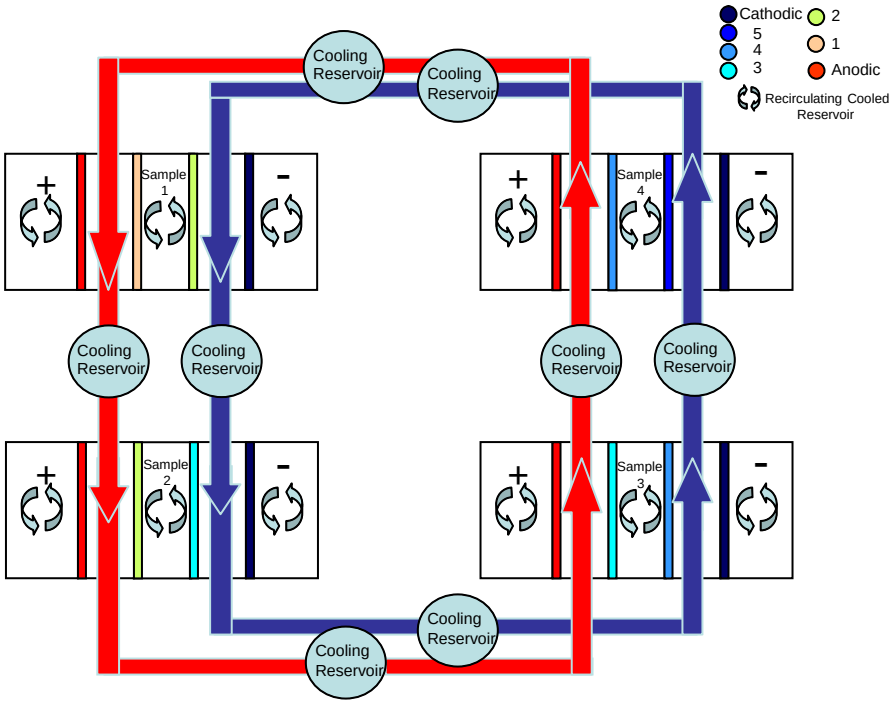

Figure 73. Schematic of operation in parallel mode.

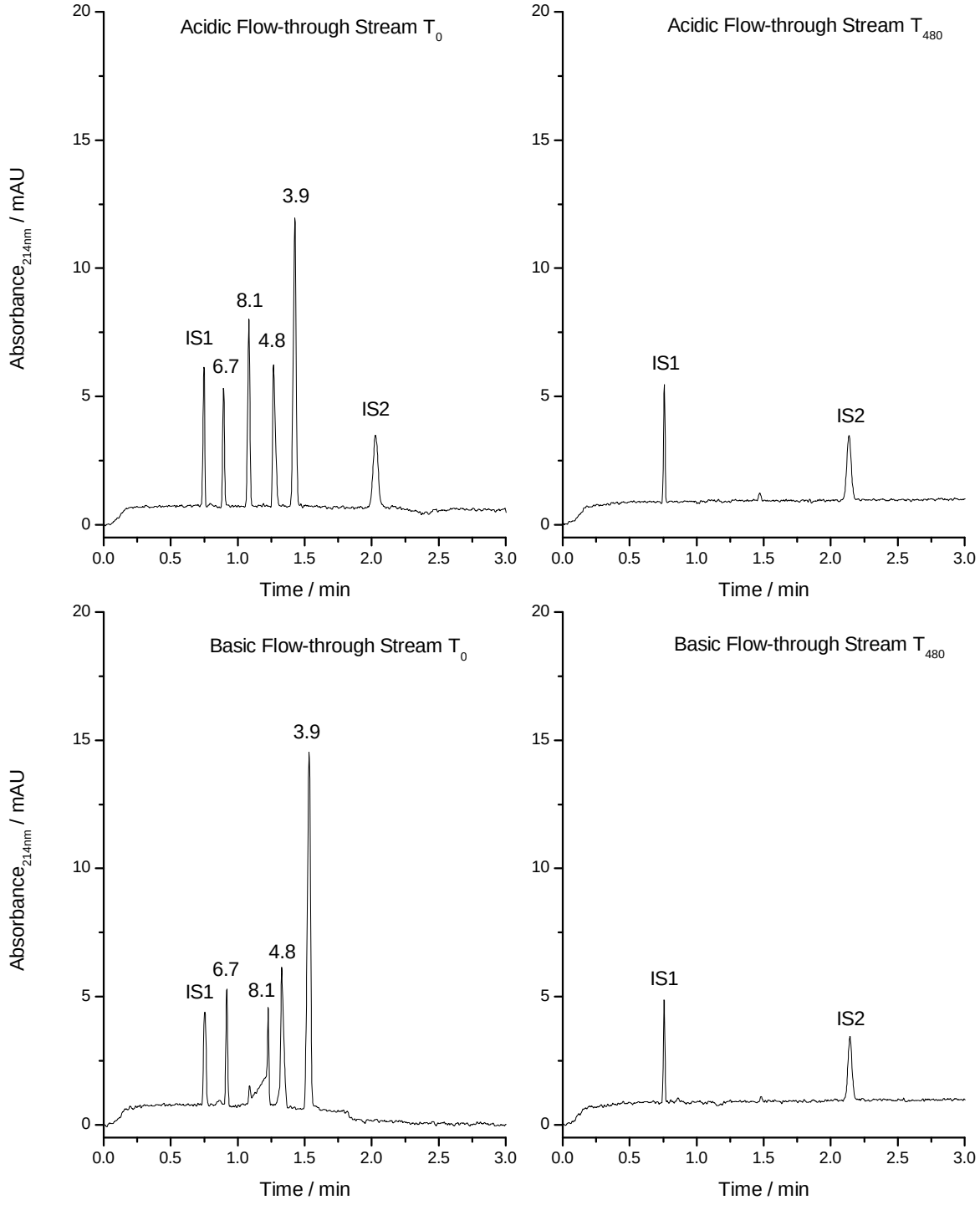

Figure 74. Electropherograms for the samples taken from the flow-through streams during operation of the T-RECS as a single parallel MCE for the separation of small molecule ampholytes.

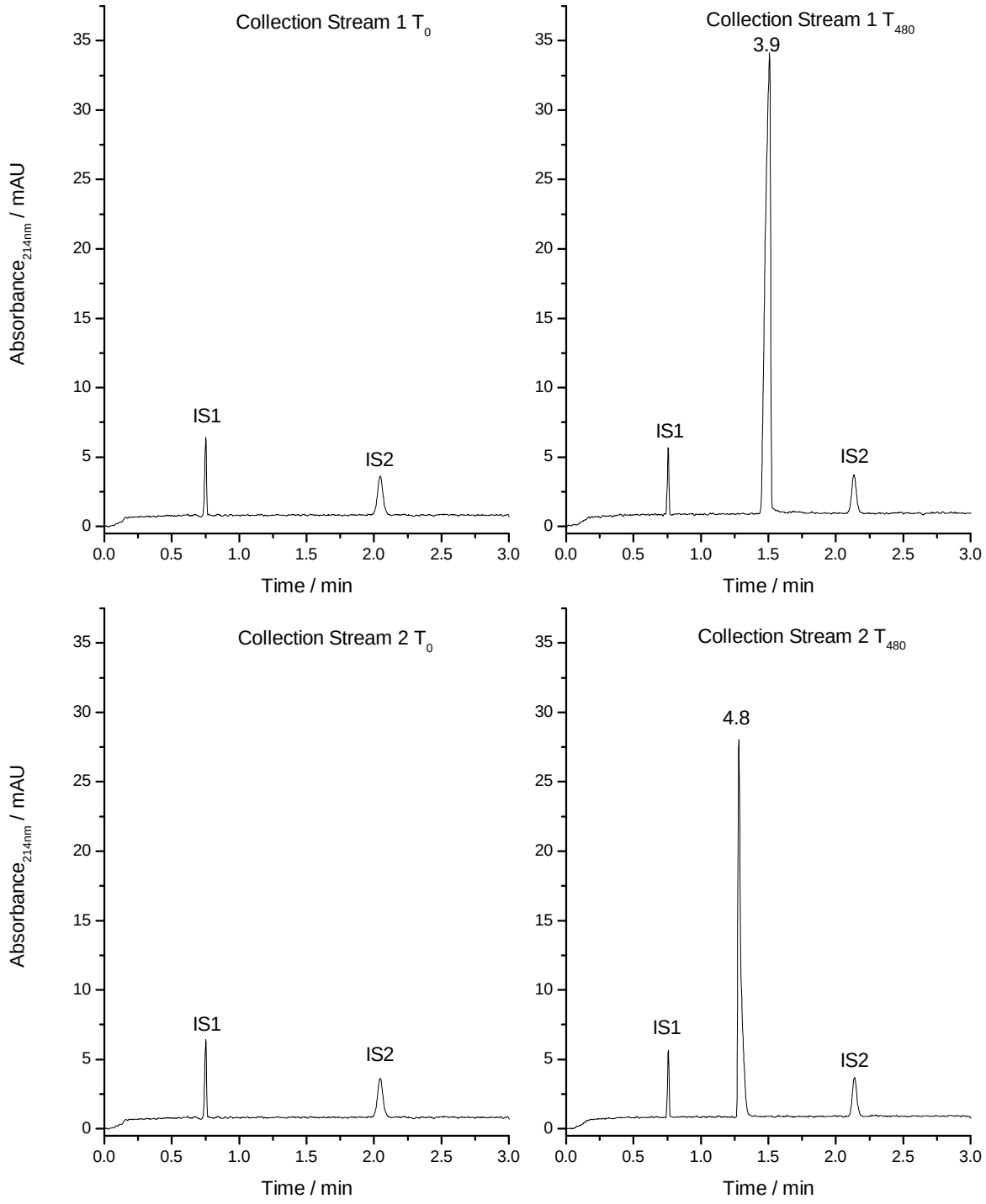

Figure 75. Electropherograms for the samples taken from collection chambers 1 and 2 during operation of the T-RECS as a single parallel MCE for the separation of small molecule ampholytes.

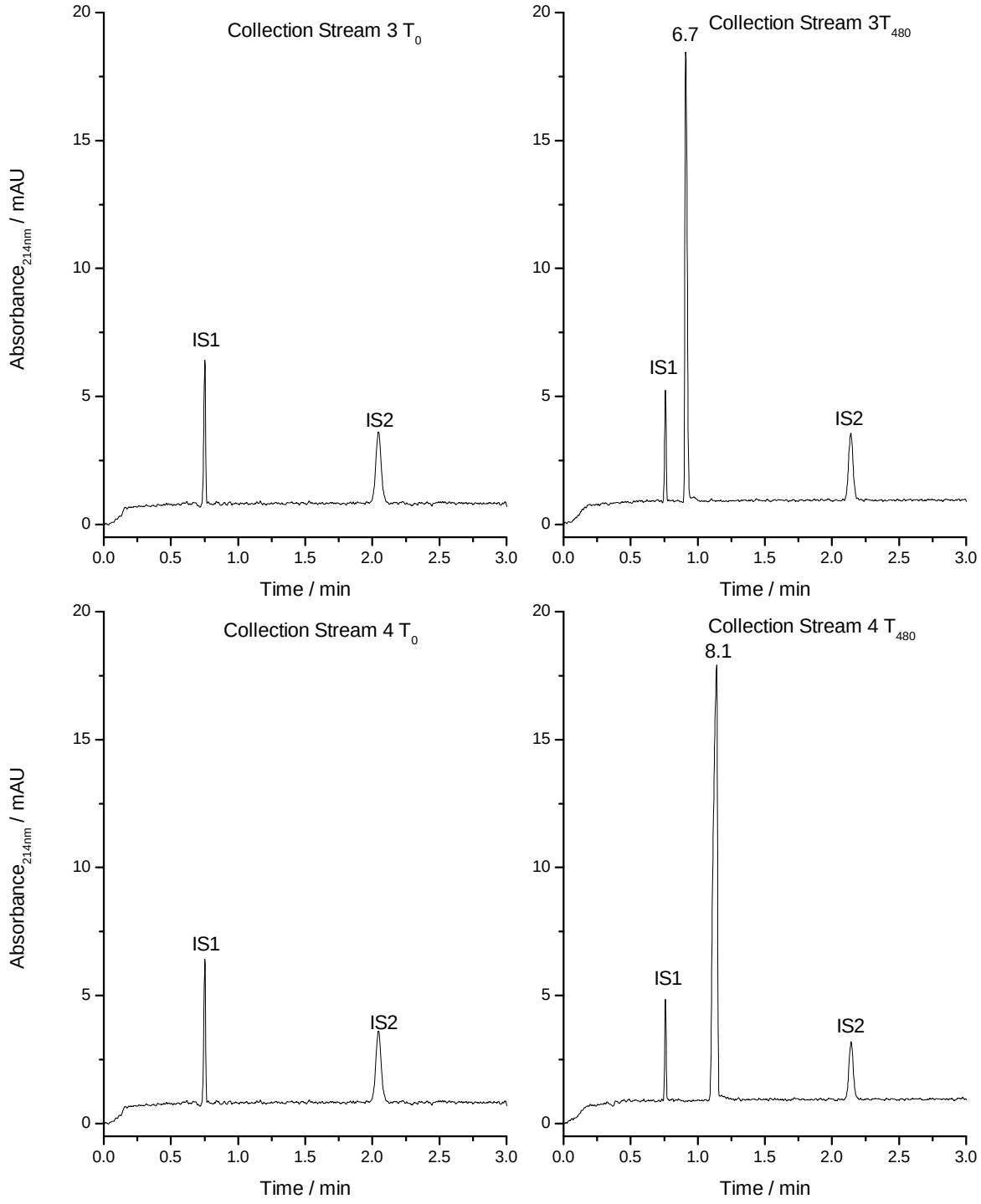

Figure 76. Electropherograms for the samples taken from collection chambers 3 and 4 during operation of the T-RECS as a single parallel MCE for the separation of small molecule ampholytes.

The pH and conductivity values, plotted in Figures 77 and 78, approach steady state final values by the end of the separation and are in good agreement with the results of the CE analysis.

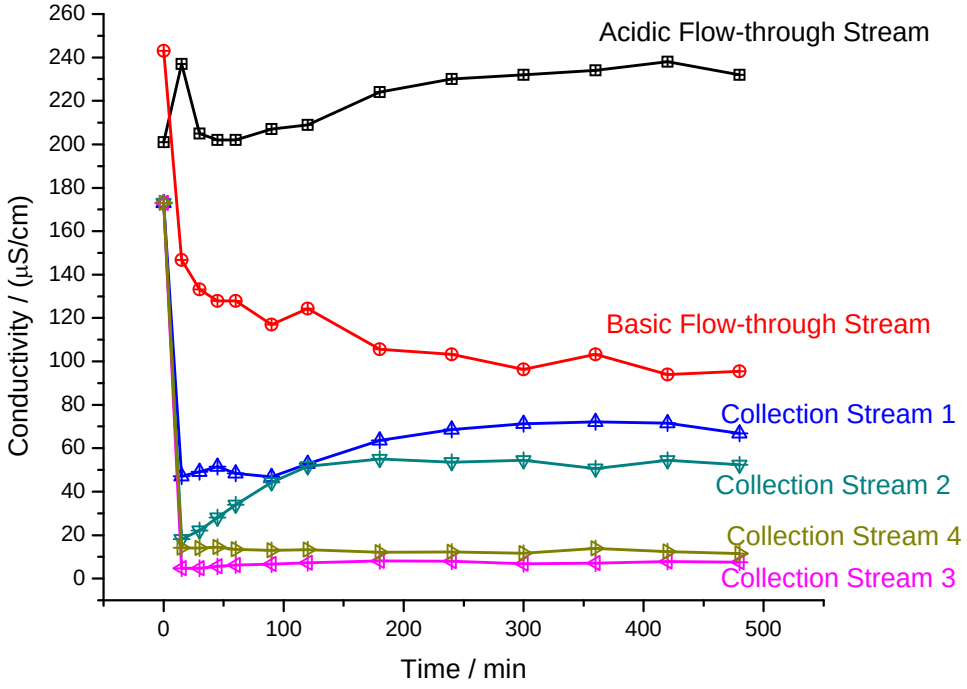

Figure 77. Conductivity profiles for the collection, acidic flow-through and basic flow-through streams during operation of the T-RECS as a single parallel MCE for the separation of small molecule ampholytes.

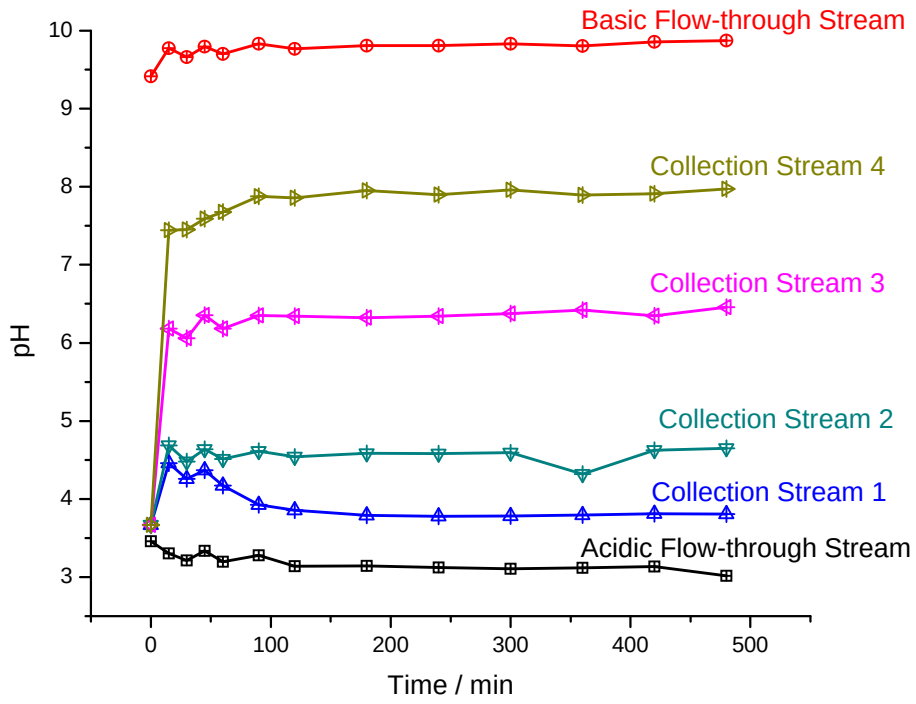

Figure 78. pH profiles for the collection, acidic flow-through and basic flow-through streams during operation of the T-RECS as a single parallel MCE for the separation of small molecule ampholytes.

The concentration values for each ampholyte in the flow-through streams are plotted in Figures 79 and 80 as a function of the harvesting time. Typically, electrophoretic depletion of each ampholyte from both the acidic and basic feed streams follows an exponential decay curve as depletion approaches completion. However, the concentrations of the most acidic marker in the acidic flow-through stream and the most basic marker in the basic flow-through stream do not follow the simple exponential decay pattern. For the pI 8.1 marker in the basic flow-through stream, a maximum is observed at 45 minutes. For the pI 3.9 marker in the acidic flow-through stream, a maximum is observed at 15 minutes. Both of these maxima are caused by the multiple electrophoretic paths that the markers can take in a parallel MCE device, as observed by

Lim [43]. Briefly, an ampholyte moving out of the acidic flow-through stream can move transiently through any of the streams bracketed by membranes having a pH lower than the pI of the ampholyte. Also, an ampholyte moving out of the basic flow-through stream can move transiently through any of the streams bracketed by membranes having a pH higher than the pI of the ampholyte. As such, ampholytes may take multiple possible paths until they migrate into a chamber where the pH values of the membranes bracket the pI of the ampholyte. In this separation, the pI 8.1 marker in the acidic flow-through migrates out as a cation, traveling through the acidic separation membranes in each of the four separation heads. For heads 1-3 the pI 8.1 marker will continue across the basic separation membrane and migrate into the basic flow-through stream. Concurrently, the pI 8.1 marker in the basic flow-through stream migrates out as an anion only through one of the basic separation membranes, in this case separation head 4. Therefore, there are 3 heads "dumping" the pI 8.1 marker into the basic flow-through stream but only one head removes it. If the rate of the "dumping" exceeds the rate of removal, a buildup of the pI 8.1 marker occurs. This "dumping" continues until the entire amount of the pI 8.1 marker has been depleted from the acidic flow-through stream and the pattern in the concentration vs. time graph returns to that of an exponential decay. A similar scenario occurs for the pI 3.9 marker in the acidic flow-through stream, except that "dumping" occurs while the pI 3.9 marker moves as an anion and removal occurs while the pI 3.9 marker moves as a cation. Surely, similar transfers occur for the pI 4.8 and pI 6.7 markers but are not seen as transport in and out of the flow-through streams can occur through two heads for each direction.

The concentration values for each ampholyte in the collection chambers are plotted as a function of the harvesting time in Figures 81-84. The ampholyte concentrations were estimated from the time-corrected relative peak areas (normalized to the imidazole internal standard, IS1), obtained by CE analysis. Each collection stream shows enrichment of the harvested marker to a concentration of about 5 mM: in collection stream one marker pI 3.9 is accumulated, in collection stream two one finds marker pI 4.8, in collection stream three marker pI 6.7, and in collection stream four marker pI 8.1. Additionally, transient concentrations of pI 4.8, 6.7, and 8.1 markers are observed in collection stream 1, pI 3.9 in collection stream 2, and pI 6.7 in collection stream 4. These transients are another reflection of the system's multiple electrophoretic pathways. Based on a separation completion time of 8 hours, the total target production rate for T-RECS, operated as a single, parallel-arranged MCE, is about 40 mg/hour.

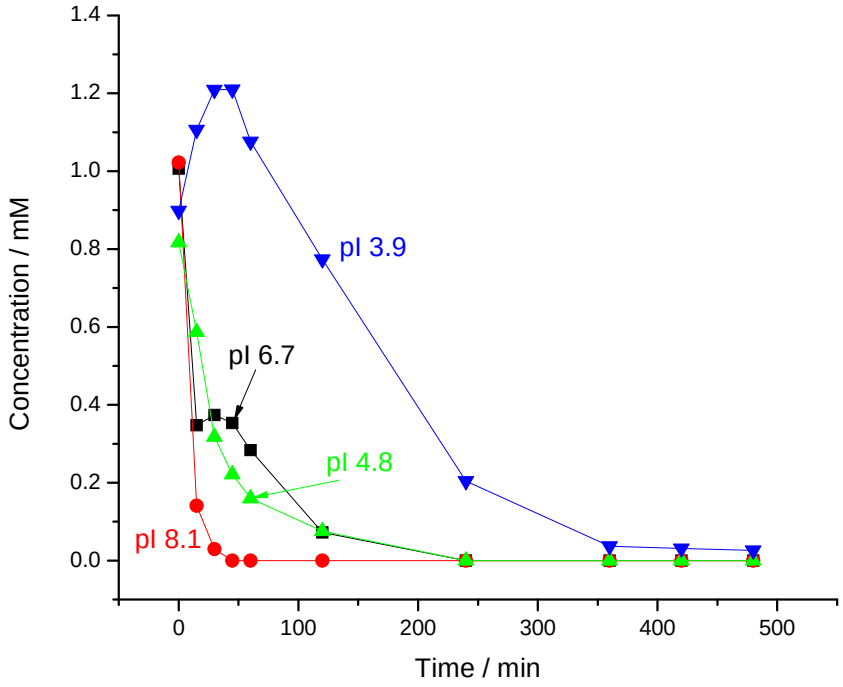

Figure 79. Concentration profiles for 3-aminobenzoic acid (pI 3.9), 4-(4-aminophenyl)-butyric acid (pI 4.8), 3-hydroxypyridine (pI 6.7) and carnosine (pI 8.1) in the acidic flow-through stream during operation of the T-RECS as a single parallel MCE for the separation of small molecule ampholytes.

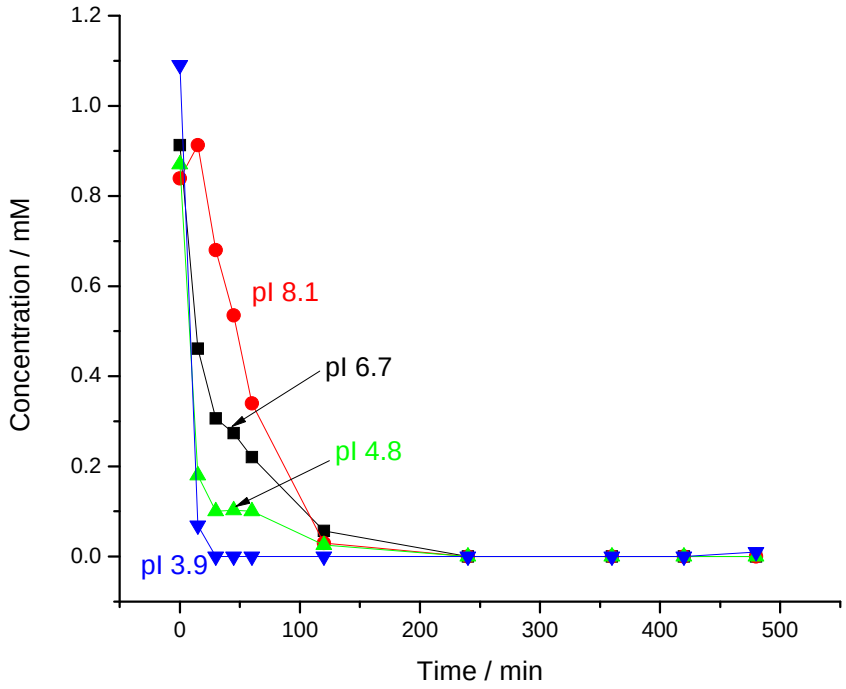

Figure 80. Concentration profiles for 3-aminobenzoic acid (pI 3.9), 4-(4-aminophenyl)-butyric acid (pI 4.8), 3-hydroxypyridine (pI 6.7) and carnosine (pI 8.1) in the basic flow-through stream during operation of the T-RECS as a single parallel MCE for the separation of small molecule ampholytes.

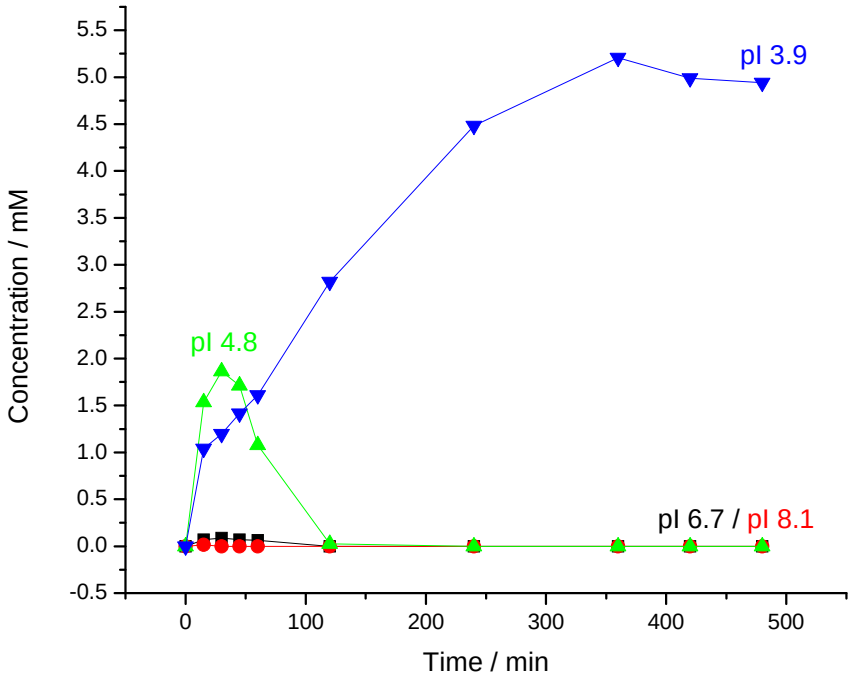

Figure 81. Concentration profiles for 3-aminobenzoic acid (pI 3.9), 4-(4-aminophenyl)-butyric acid (pI 4.8), 3-hydroxypyridine (pI 6.7) and carnosine (pI 8.1) in the first collection stream during operation of the T-RECS as a single parallel MCE for the separation of small molecule ampholytes.

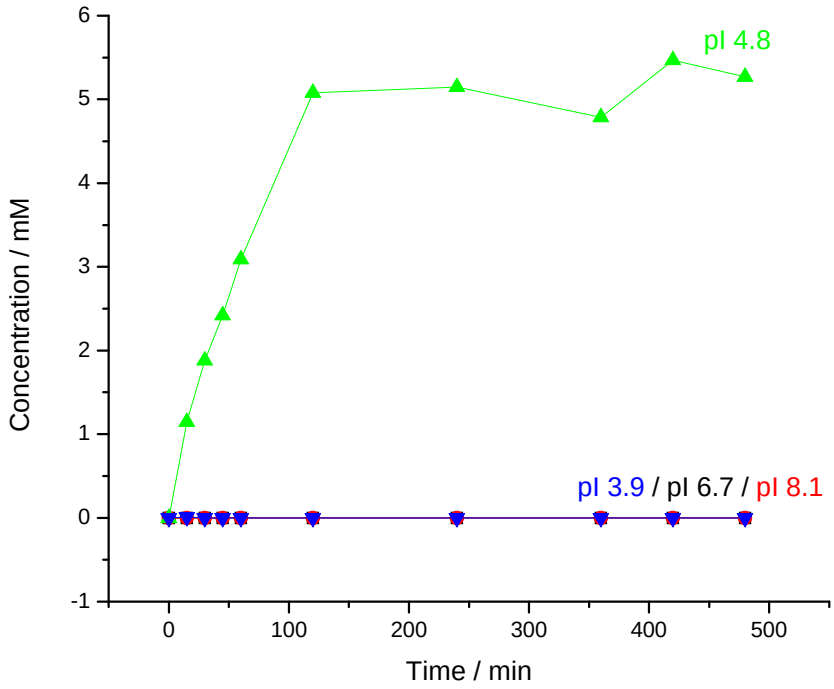

Figure 82. Concentration profiles for 3-aminobenzoic acid (pI 3.9), 4-(4-aminophenyl)-butyric acid (pI 4.8), 3-hydroxypyridine (pI 6.7) and carnosine (pI 8.1) in the second collection stream during operation of the T-RECS as a single parallel MCE for the separation of small molecule ampholytes.

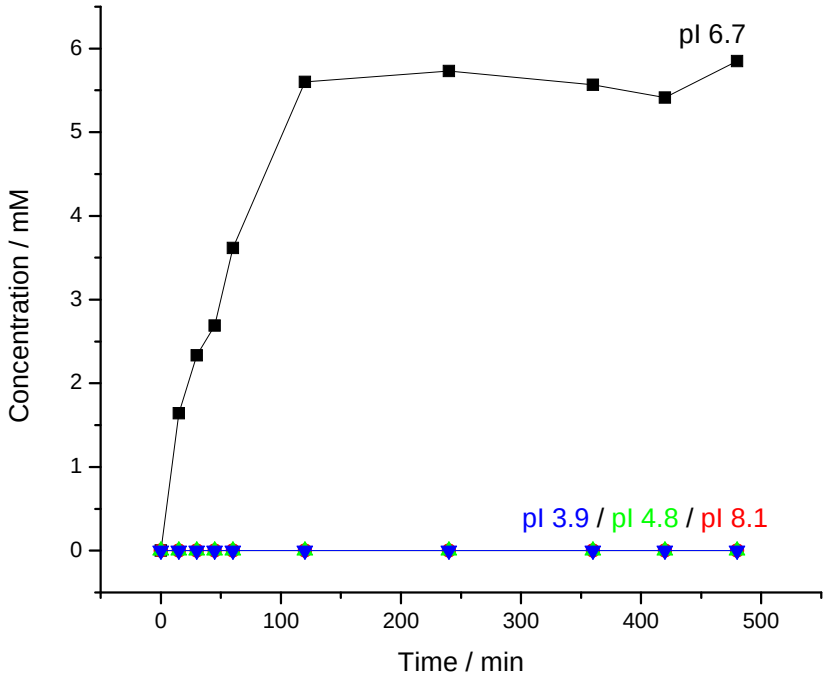

Figure 83. Concentration profiles for 3-aminobenzoic acid (pI 3.9), 4-(4-aminophenyl)-butyric acid (pI 4.8), 3-hydroxypyridine (pI 6.7) and carnosine (pI 8.1) in the third collection stream during operation of the T-RECS as a single parallel MCE for the separation of small molecule ampholytes.

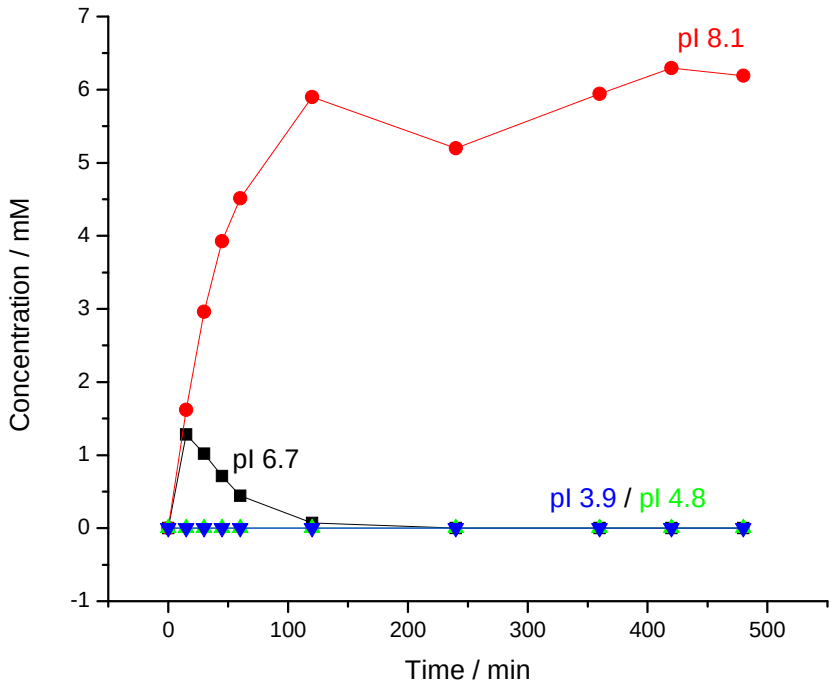

Figure 84. Concentration profiles for 3-aminobenzoic acid (pI 3.9), 4-(4-aminophenyl)-butyric acid (pI 4.8), 3-hydroxypyridine (pI 6.7) and carnosine (pI 8.1) in the fourth collection stream during operation of the T-RECS as a single parallel MCE for the separation of small molecule ampholytes.

5.5 Operation as a cascade of binary separations

5.5.1 Separation of small molecule ampholytes

5.5.1.1 Background and objective

Because of the slow transport of low pI ampholytes from the acidic flow-through stream observed in Section 5.3, a new IET arrangement was devised. This arrangement, shown in Figure 85, utilizes a three-chamber separation head as the feed point for two branches of two-chamber separation heads. The branches contain cascades of binary separations where component isolation is achieved in successively more stringent binary

separations; i.e., all ampholytes (N) pass into collection stream 1, N-x_1 (where x_1 is the number of ampholytes trapped in collection stream 1) markers are allowed to pass into collection stream 2, N-x_1-x_2 markers are allowed to pass into collection stream 3, and N-x_1-x_2-x_3 are allowed to pass into collection stream 4. Based on the separation needs, the stringency of the binary separations can be adjusted to produce collection streams which contain multiple or single products. The key advantage of this arrangement is that it allows for the use of a low conductivity feed stream. The low conductivity feed stream will result in a high field strength across the feed chamber and increase the removal rate of ampholytes from that feed stream. Additionally, extreme pI ampholytes are transported from the feed stream to their final destination in the first step. The new arrangement maintains the desirable properties of a parallel-arranged MCE. As in section 5.3.1 and 5.4, UV-absorbing small molecule ampholytes were used to confirm the proper functioning of T-RECS when the four separation heads were operated as a cascade of binary separations. Because only 4 separation heads were fabricated for the original T-RECS design, only one branch was used in the demonstration experiment.

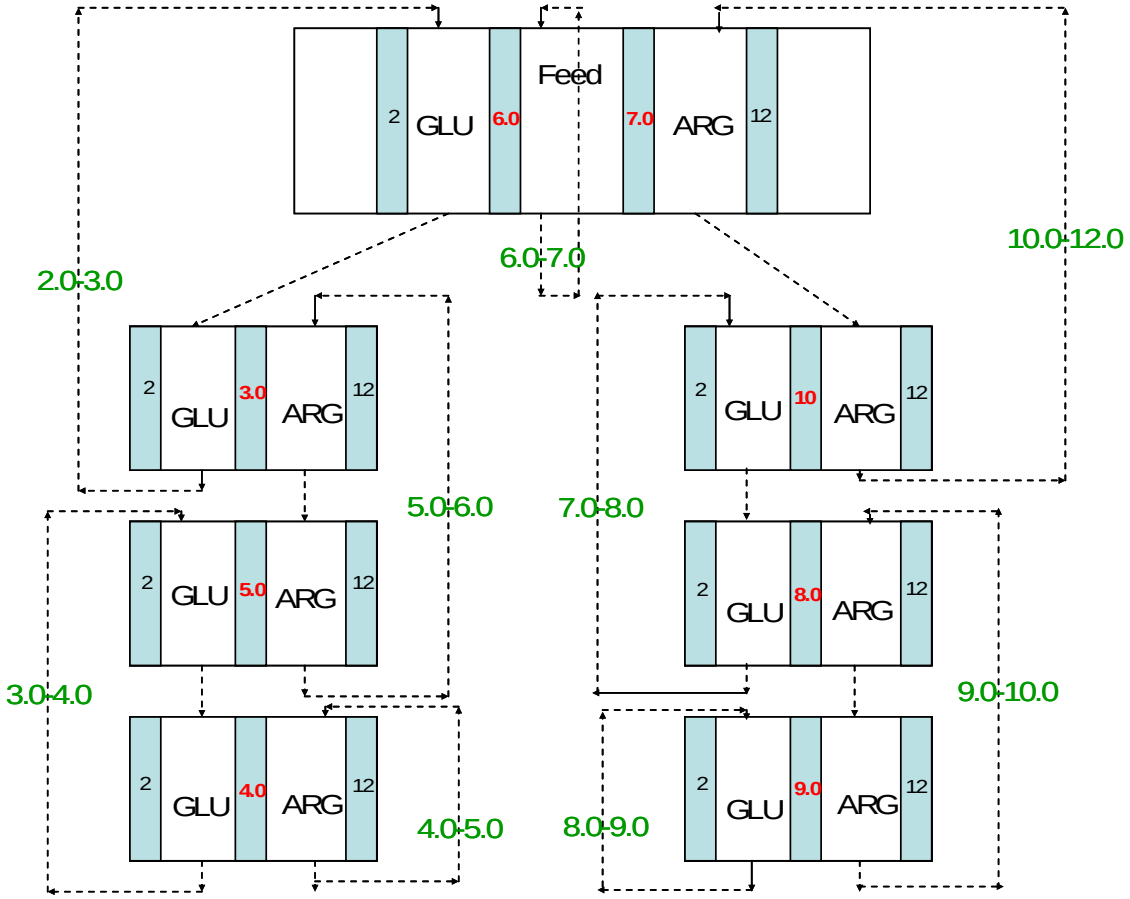

Figure 85. IET arrangement for harvesting small molecule ampholytes in the T-RECS operated as a cascade of serial binary separations. The pI range that will be trapped in each chamber is displayed in green along the respective recirculated streams.

5.5.1.2 Materials, method, and instrument setup

Figure 86 illustrates the IET arrangement for the experiment. The feed solution contained 10 mM histidine, 0.25 mM 3-aminobenzoic acid (pI 3.9), 0.25 mM 4-(4-aminophenyl)-butyric acid (pI 4.8), 0.25 mM 4-hydroxy-3-(morpholino-methyl)-benzoic acid (pI 5.8), and 0.25 mM 3-hydroxypyridine (pI 6.7). The basic flow-through stream of separation head 1 was a 20 mM lysine solution. Collection streams 1 and 3 were 5 mM

aspartic acid solutions. Collection streams 2 and 4 were 10 mM histidine solutions. The catholyte was a 13 mM NaOH solution, the anolyte was a 10 mM methanesulfonic acid solution. The anodic and cathodic membranes for all separation heads were pH 2 and pH 10.5 membranes, respectively. Head 1 utilized pH 7.2 and pH 8.5 membranes as the acidic and basic separation membranes, respectively. Head 2 utilized a pH 4.5 separation membrane. Head 3 utilized a pH 6.5 separation membrane. Head 4 utilized a pH 5.5 separation membrane. The collection solutions were recirculated at a flow rate of about 23 mL/min. The anolyte and catholyte solutions were recirculated at a flow rate of 2 L/min. The separation was run for 180 minutes with a maximum power load setting of 40 watts per separation head. Samples were taken from the feed stream, the basic flow-through stream of separation head 1, and the collection streams at 10, 20, 30, 45, 60, 90, 120, and 180 minutes. The pH and conductivity values were measured as in the previous experiments. All CE runs were completed with a 50 μm internal diameter fused silica capillary (L_t = 30.6 cm; L_d = 20.3 cm), operated at 25 kV, using two different boric acid/lithium borate buffers as the background electrolyte. For collection stream 1, a pH 9.2 BGE was used. For all other streams, a pH 8.8 BGE was used. The polarity was negative to positive. A polyvinylpyrrolidone semi-permanent coating was used to suppress the electroosmotic flow.

5.5.1.3 Results and discussion

The results of the CE analysis of the samples taken are displayed in Figures 87-89. The shape of the 3-aminobenzoic acid (pI 3.9) peak in the electropherograms for collection

stream 1 is distorted, because it co-migrates with the aspartic acid biaser. Electropherograms for the feed stream show that all markers have been removed by 90 minutes. The electropherograms for the 180 minute samples taken from the collection streams, Figures 87-89, indicate successful harvest of the targeted marker in each of the four collection streams.

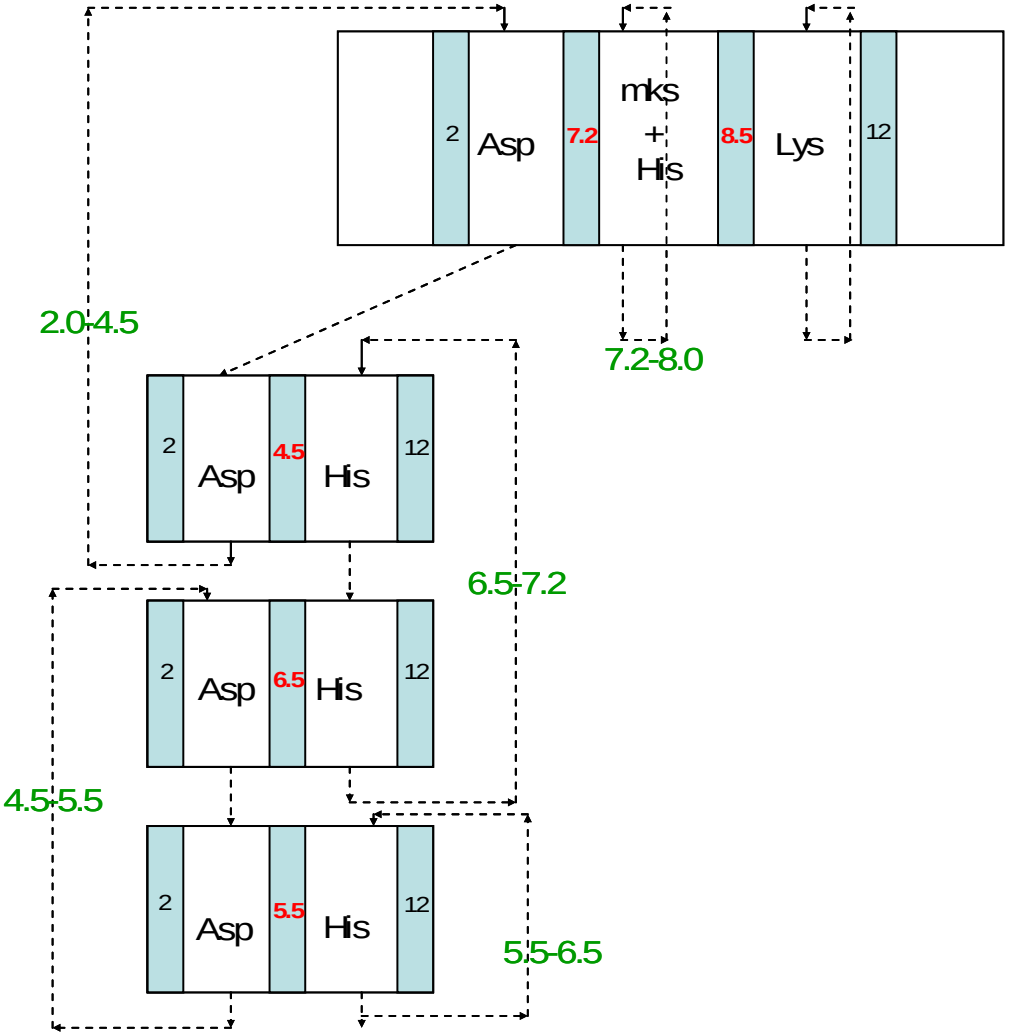

Figure 86. IET arrangement for harvesting small molecule ampholytes in the T-RECS operated as a single branch cascade of binary separations. The pI range of the components trapped in each stream is displayed in green along the respective streams.

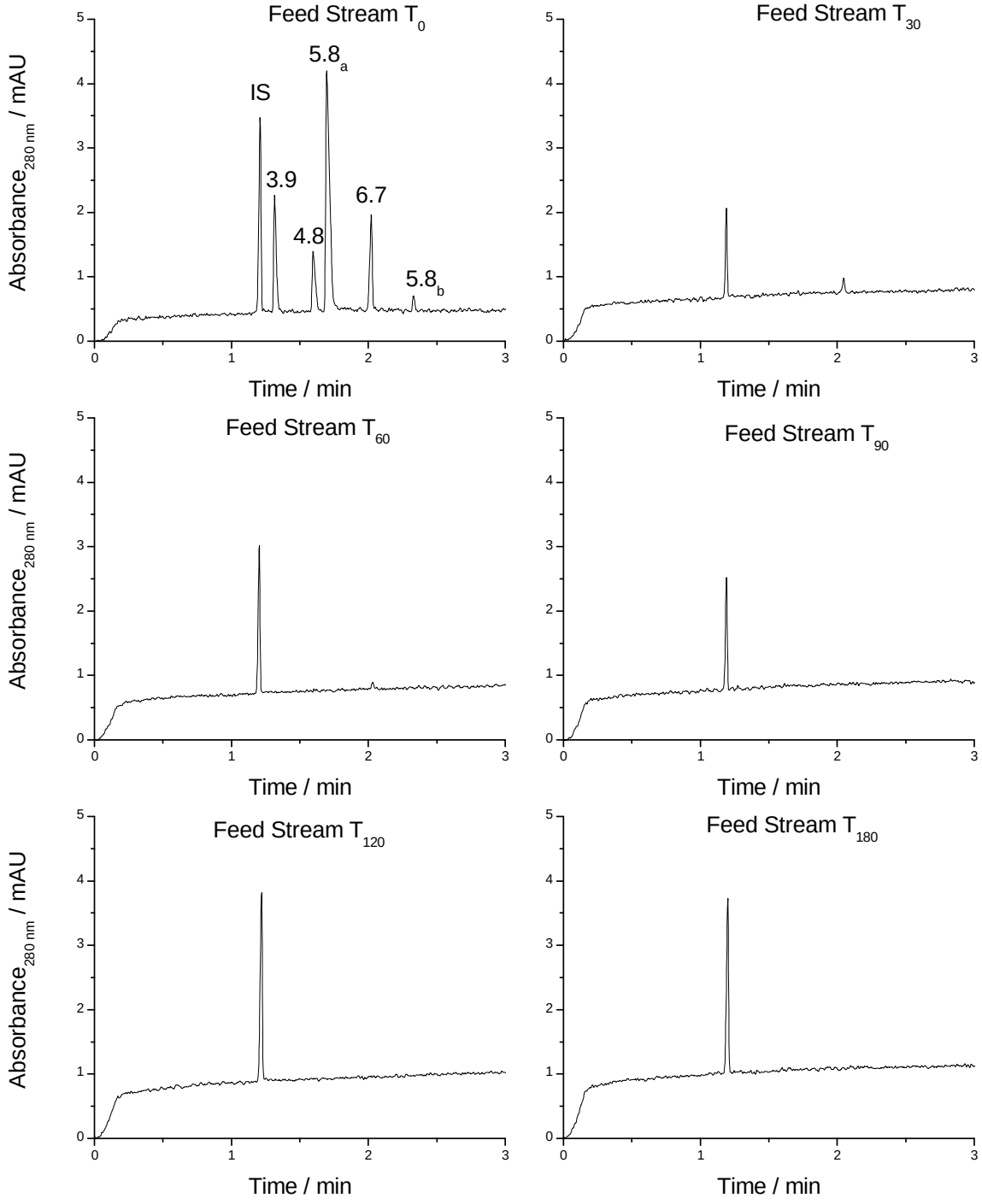

Figure 87. Electropherograms for the samples taken from the feed stream during operation of the T-RECS as a cascade of binary separations.

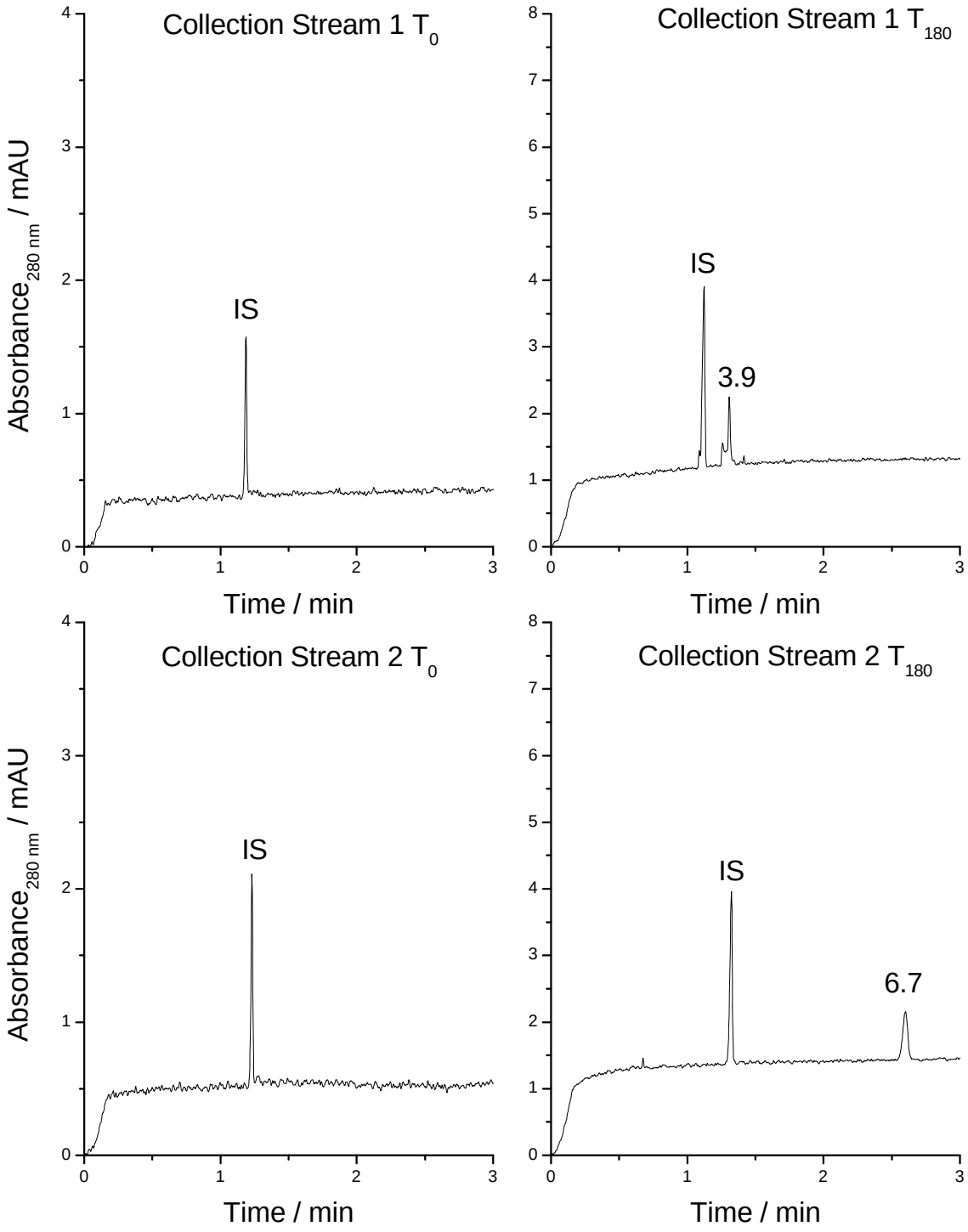

Figure 88. Electropherograms for the samples taken from collection streams 1 and 2 during operation of the T-RECS as a cascade of binary separations.

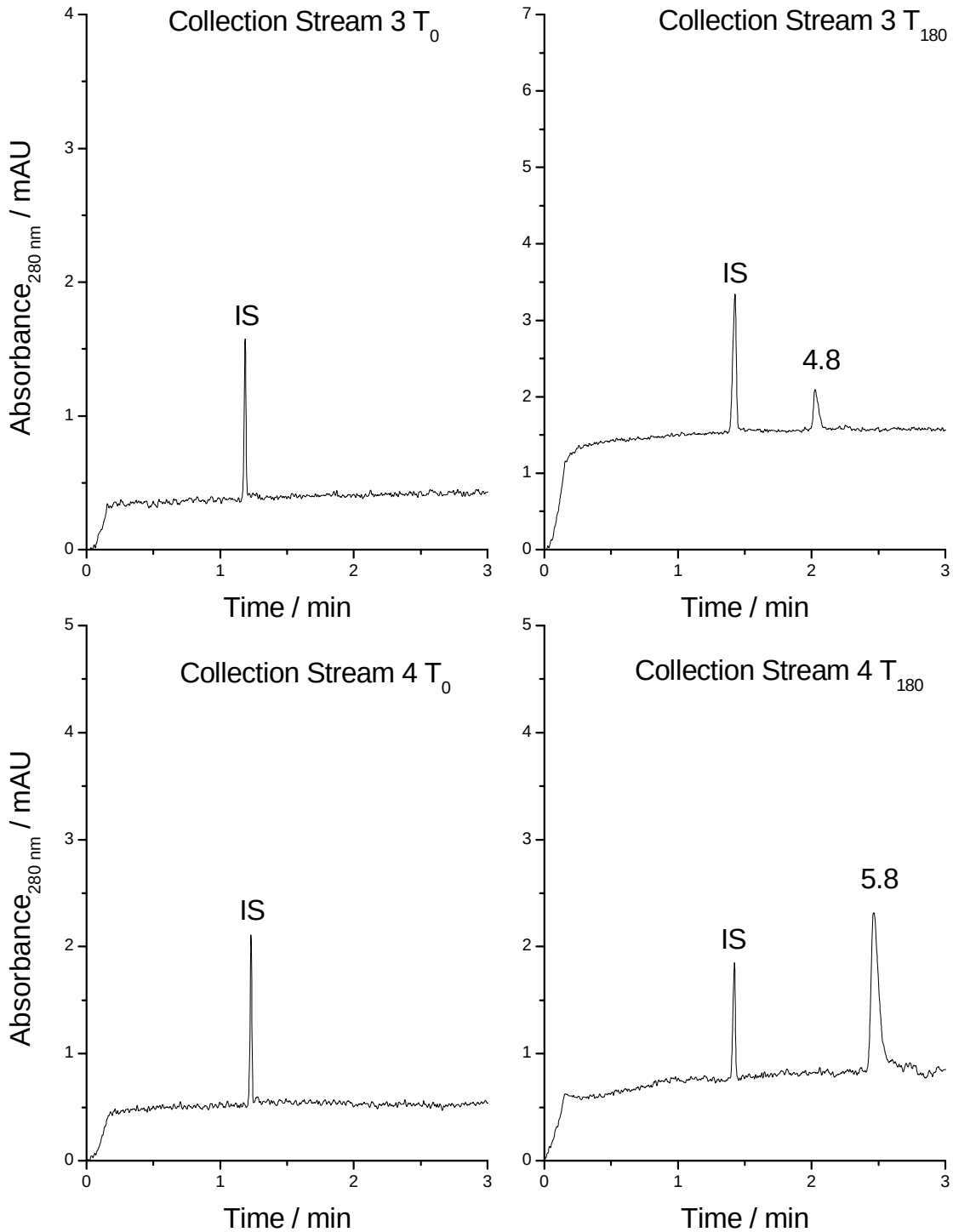

Figure 89. Electropherograms for the samples taken from collection streams 3 and 4 during operation of the T-RECS as a cascade of binary separations.

The pH and conductivity values are plotted in Figures 90 and 91. The only significant changes in the pH or conductivity profiles are a decrease in the conductivity of the feed stream over the first 10 minutes (caused by the removal of the markers from the feed stream), and a gradual loss of conductivity from the basic flow-through stream in separation head 1 (caused by a slow loss of lysine to the catholyte, similar to what was observed in Section 5.2).

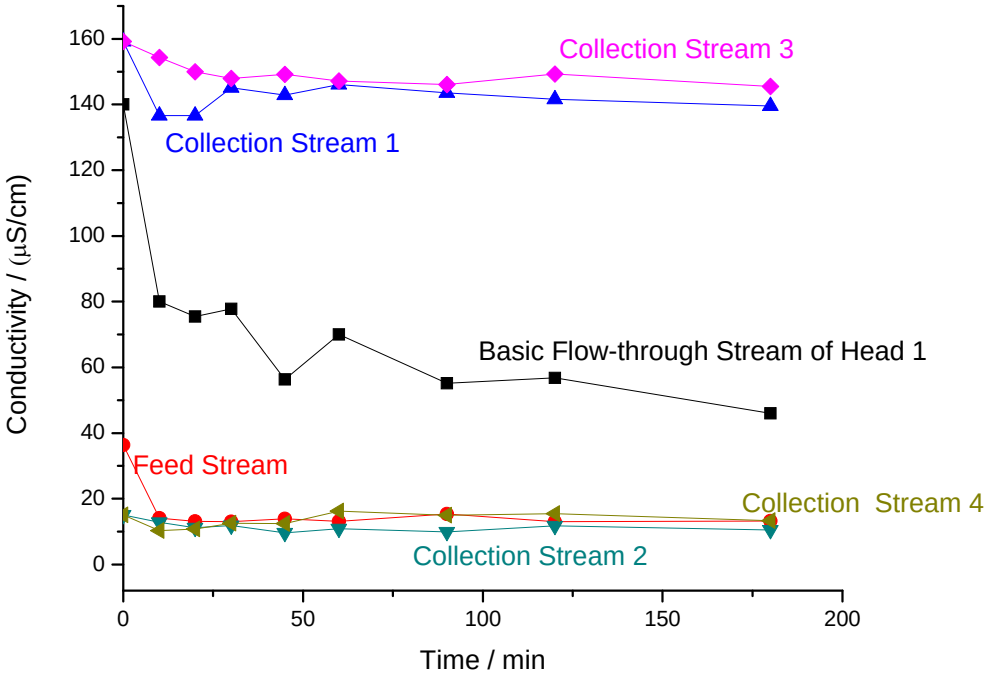

Figure 90. Conductivity profiles for the collection streams, feed stream and basic flow-through stream of separation head 1 during the operation of the T-RECS as a cascade of binary separations.

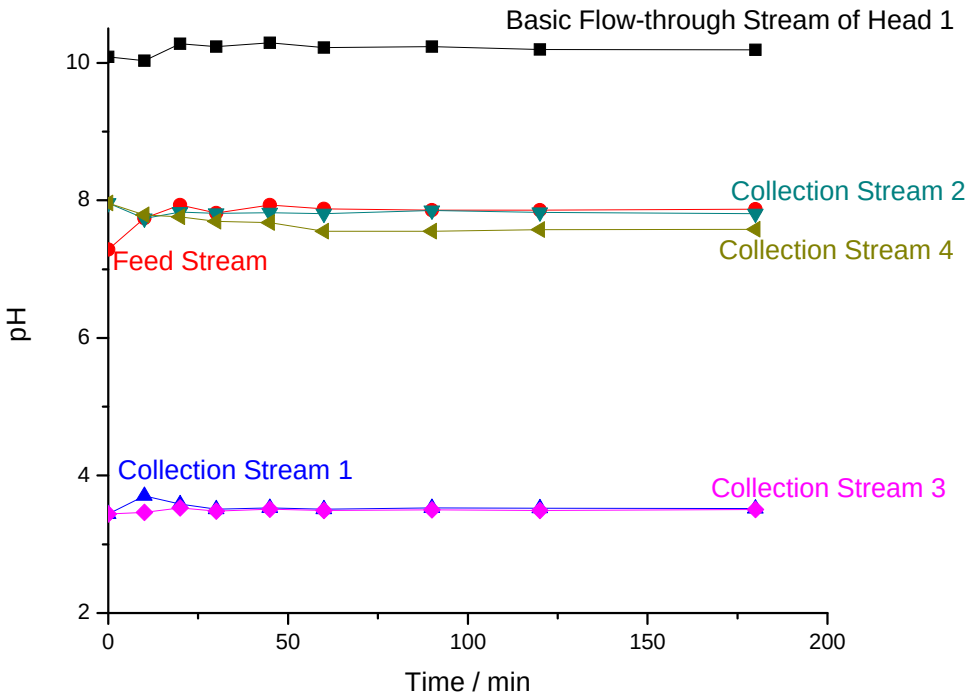

Figure 91. pH profiles for the collection stream, feed stream and basic flow-through stream of separation head 1 during the operation of the T-RECS as a cascade of binary separations.

The concentration of each ampholyte in the feed and collection streams is plotted as a function of the harvesting time in Figures 92-96. The pI 3.9, 4.8, and 5.8 markers were removed from the feed stream in less than 20 min; complete removal of the pI 6.7 marker required approximately 90 min. The slow transfer rate for the pI 6.7 marker is likely caused by its small electrophoretic mobility at a pH near its isoelectric point or the large potential loss across the near pH 7 membranes that have low conductivities. However, the depletion of even the slowest marker from the feed is finished significantly faster than in Section 5.3, indicating that having a low conductivity feed is an effective

strategy for increasing the depletion rates from the feed solution. Each collection stream shows enrichment of the harvested marker to a concentration of about 0.2 mM: collection stream 1 contains the pI 3.9 marker, collection stream 2 the pI 6.7 marker, collection stream 3 the pI 4.8 marker, and collection stream 4 the pI 5.8 marker. Additionally, markers pI 4.8, 5.8, and 6.7 are observed transiently in collection stream 1, markers pI 4.8 and 5.8 in collection stream 2, and marker pI 5.8 in collection stream 3. Unlike in Section 5.3, these transients are not caused by multiple electrophoretic migration paths, but are due to the cascade process where all four markers pass first into collection stream 1, then three markers are allowed to pass from collection stream 1 into collection stream 2, two markers are allowed to pass from collection stream 2 into collection stream 3, and only one marker is allowed to pass into collection stream 4.

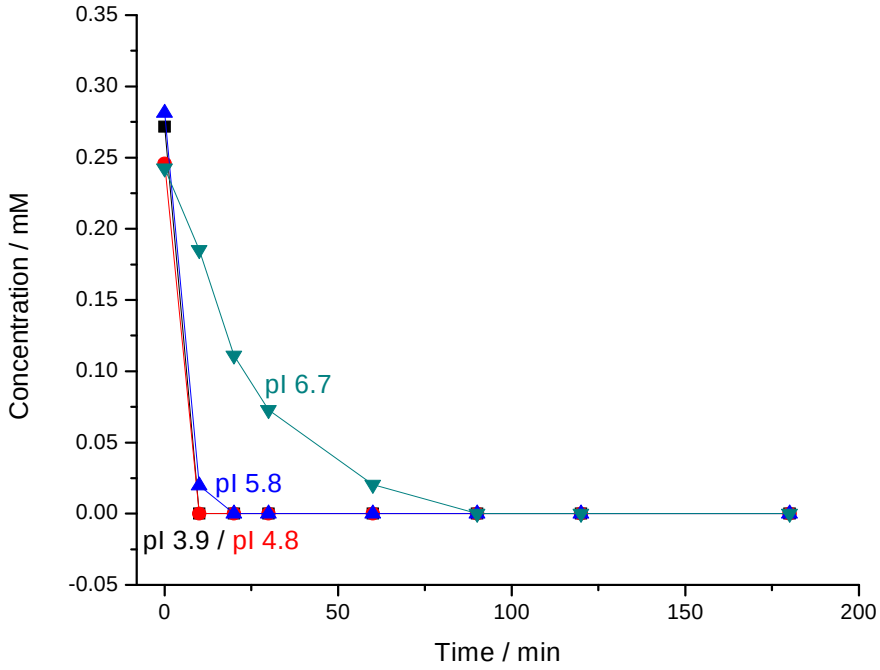

Figure 92. Concentration of 3-aminobenzoic acid (pI 3.9), 4-(4-aminophenyl)-butyric acid (pI 4.8), 4-hydroxy-3-(morpholino-methyl)-benzoic acid (pI 5.8), and 3-hydroxypyridine (pI 6.7) in the feed stream as a function of separation time during the operation of the T-RECS as a cascade of binary separations.

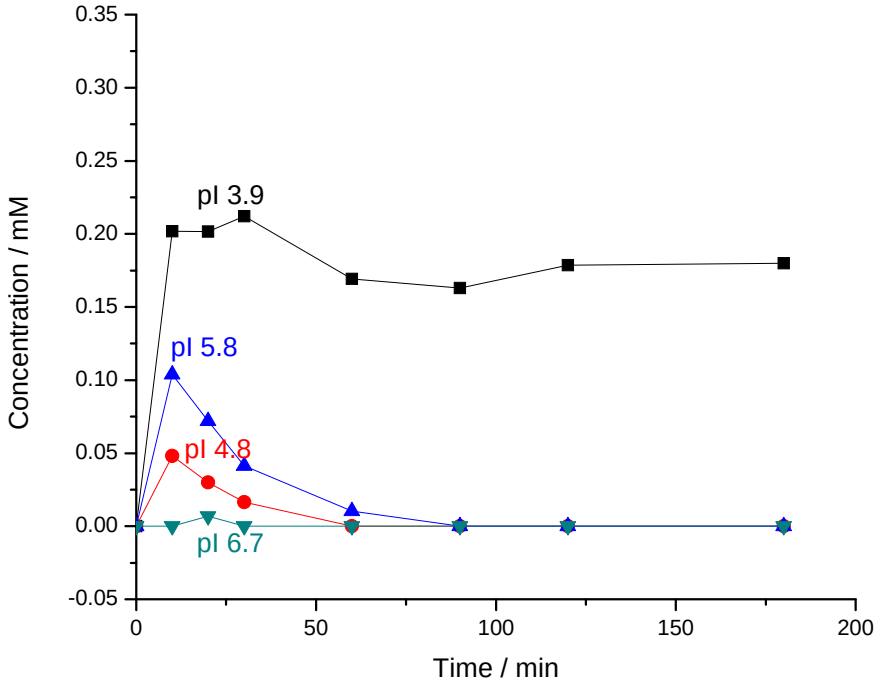

Figure 93. Concentration of 3-aminobenzoic acid (pI 3.9), 4-(4-aminophenyl)-butyric acid (pI 4.8), 4-hydroxy-3-(morpholino-methyl)-benzoic acid (pI 5.8), and 3-hydroxypyridine (pI 6.7) in collection stream 1 as a function of separation time during the operation of the T-RECS as a cascade of binary separations.

.

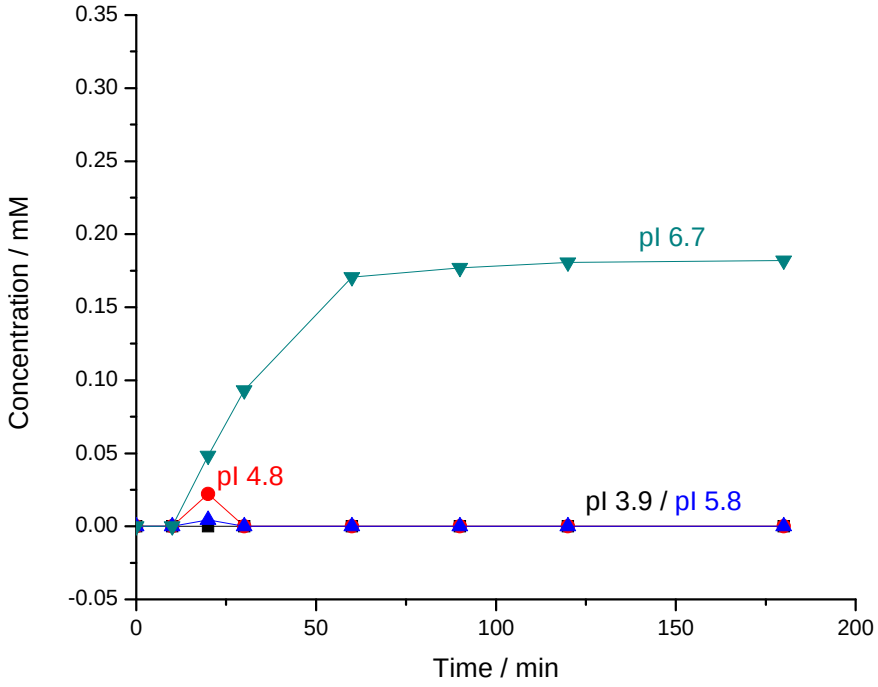

Figure 94. Concentration of 3-aminobenzoic acid (pI 3.9), 4-(4-aminophenyl)-butyric acid (pI 4.8), 4-hydroxy-3-(morpholino-methyl)-benzoic acid (pI 5.8), and 3-hydroxypyridine (pI 6.7) in collection stream 2 as a function of separation time during the operation of the T-RECS as a cascade of binary separations.

.

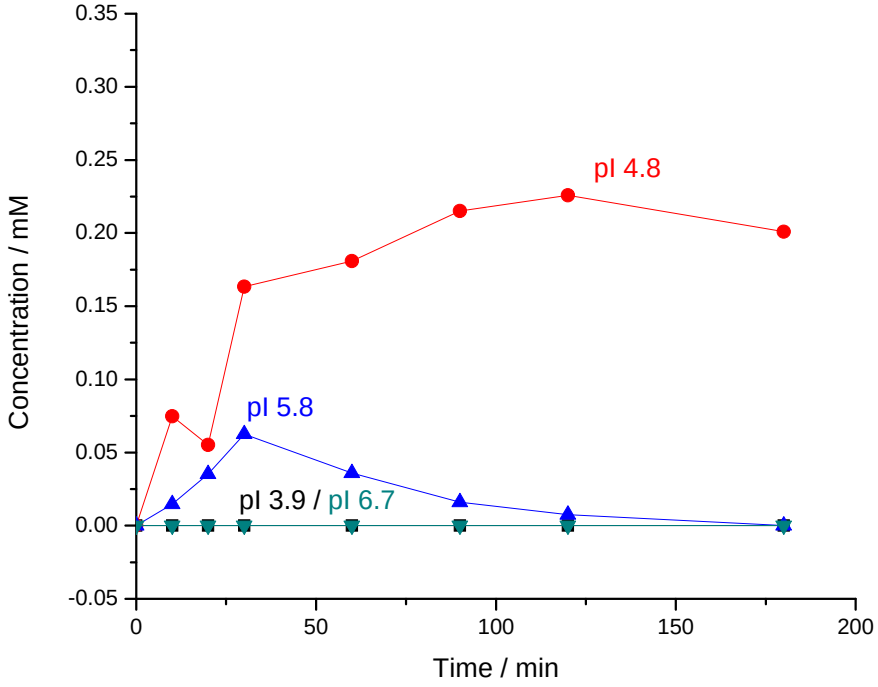

Figure 95. Concentration of 3-aminobenzoic acid (pI 3.9), 4-(4-aminophenyl)-butyric acid (pI 4.8), 4-hydroxy-3-(morpholino-methyl)-benzoic acid (pI 5.8), and 3-hydroxypyridine (pI 6.7) in collection stream 3 as a function of separation time during the operation of the T-RECS as a cascade of binary separations.

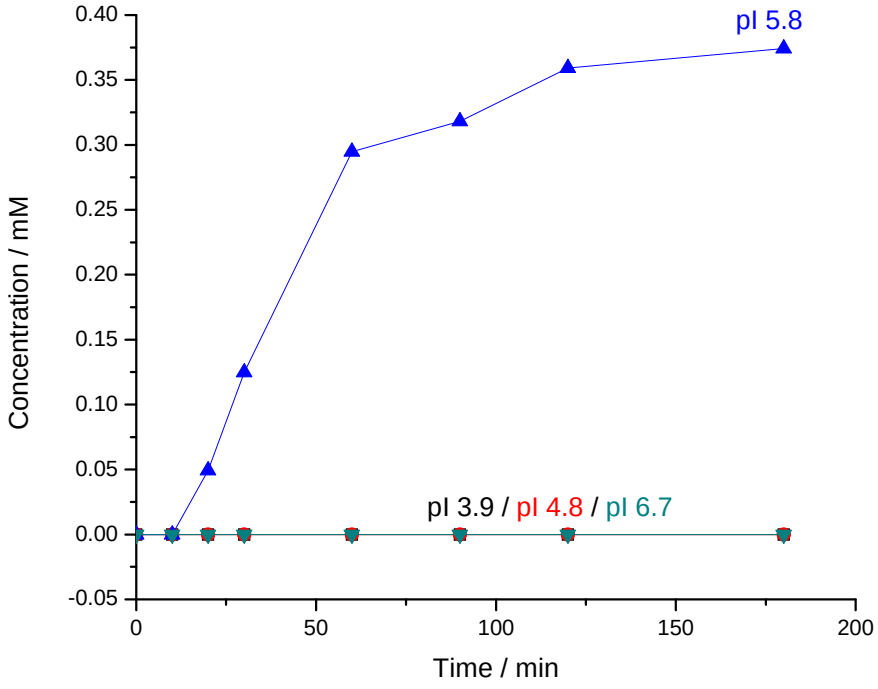

Figure 96. Concentration of 3-aminobenzoic acid (pI 3.9), 4-(4-aminophenyl)-butyric acid (pI 4.8), 4-hydroxy-3-(morpholino-methyl)-benzoic acid (pI 5.8), and 3-hydroxypyridine (pI 6.7) in collection stream 4 as a function of separation time during the operation of the T-RECS as a cascade of binary separations.

.

5.5.2 Separation of a fluorescent pI marker from a crude reaction mixture

5.5.2.1 Background and objective

Isoelectric point standards, or pI markers, are an essential tool in IEF based separations. pI markers are used to monitor the formation, stability, and linearity of pH gradients, for determination of the isoelectric point of unknown compounds, and determination of the pH inside buffering membranes used in IET [21-23, 66,67]. Purification of pI markers is important as contaminants may distort the pH gradient. Preparative IET is an attractive technique for pI marker purification as the pI value of the target is its most important property and IET separation is based on the pI value. The key advantage of utilizing the

T-RECS operated in cascade mode for purification of pI markers is that each step relies on positive transport of the target through a respective buffering membrane, ensuring high purity and continuous production of the target. Additionally, pure product can be produced from a crude reaction mixture in a single-step. Fluorescent pI markers are particularly important because of their application in cIEF-LIF separations [68-71]. A newly synthesized naphthalene chromophore-based pI marker was used to demonstrate the application of the T-RECS cascade for the processing of a complex sample.

5.5.2.2 Materials, method, and instrument setup

5.5.2.2.1 Synthesis of a naphthalene chromophore-based pI marker

The three-step reaction scheme is presented in Figure 97. Briefly, to a glass vial held in an ice bath, 80 mg of the monopotassium salt of 7-amino-1,3-napthalenedisulfonic acid (ANDS) and 1 ml chlorosulfonic acid were added. The reaction mixture was maintained at 75 °C with constant stirring. After 2 hours, ice water was slowly added to the reaction vessel to precipitate the chlorinated ANDS. The suspension was then centrifuged at 3000 RPM for about 20 minutes and the supernatant was decanted. The pellet was dissolved in 5 mL of acetonitrile and 3 equivalents of 1-methylpiperazine were added. After 30 minutes, 1.5 mL of glacial acetic acid and 10 equivalents of acrylic acid were added. The reaction mixture was stored at room temperature overnight.

5.5.2.2.2 IET purification and analysis of the target pI marker

The IET arrangement and membranes for the experiment were the same as in Section 5.5.1. The feed solution contained 10 mM histidine, the crude reaction mixture was added to it at a 1:25 ratio. The basic flow-through stream of separation head 1 was a 20 mM lysine solution. Collection streams 1 and 3 were 5 mM aspartic acid solutions. Collection stream 2 was a 10 mM histidine solution. Collection stream 4 was deionized water. The catholyte was a 13 mM NaOH solution, the anolyte was a 10 mM methanesulfonic acid solution. The separation lasted for 1120 minutes, with a maximum power load setting of 40 watts per separation head. Samples were taken from the feed stream, the basic flow-through stream of separation head 1, and the collection streams at 30, 60, 120, 240, 360, 480, 620, 920, and 1120 minutes. The pH and conductivity values were measured as in the previous experiments. All CE runs were completed with a 50 μm internal diameter fused silica capillary (L_t = 30.6 cm; L_d = 20.3 cm), operated at 25 kV, using a pH 4.7 acetic acid / lithium acetate buffer as the background electrolyte. The polarity was positive to negative. The 1120 minute sample taken from collection stream 4 was also analyzed by electrospray ionization mass spectrometry (ESI-MS).

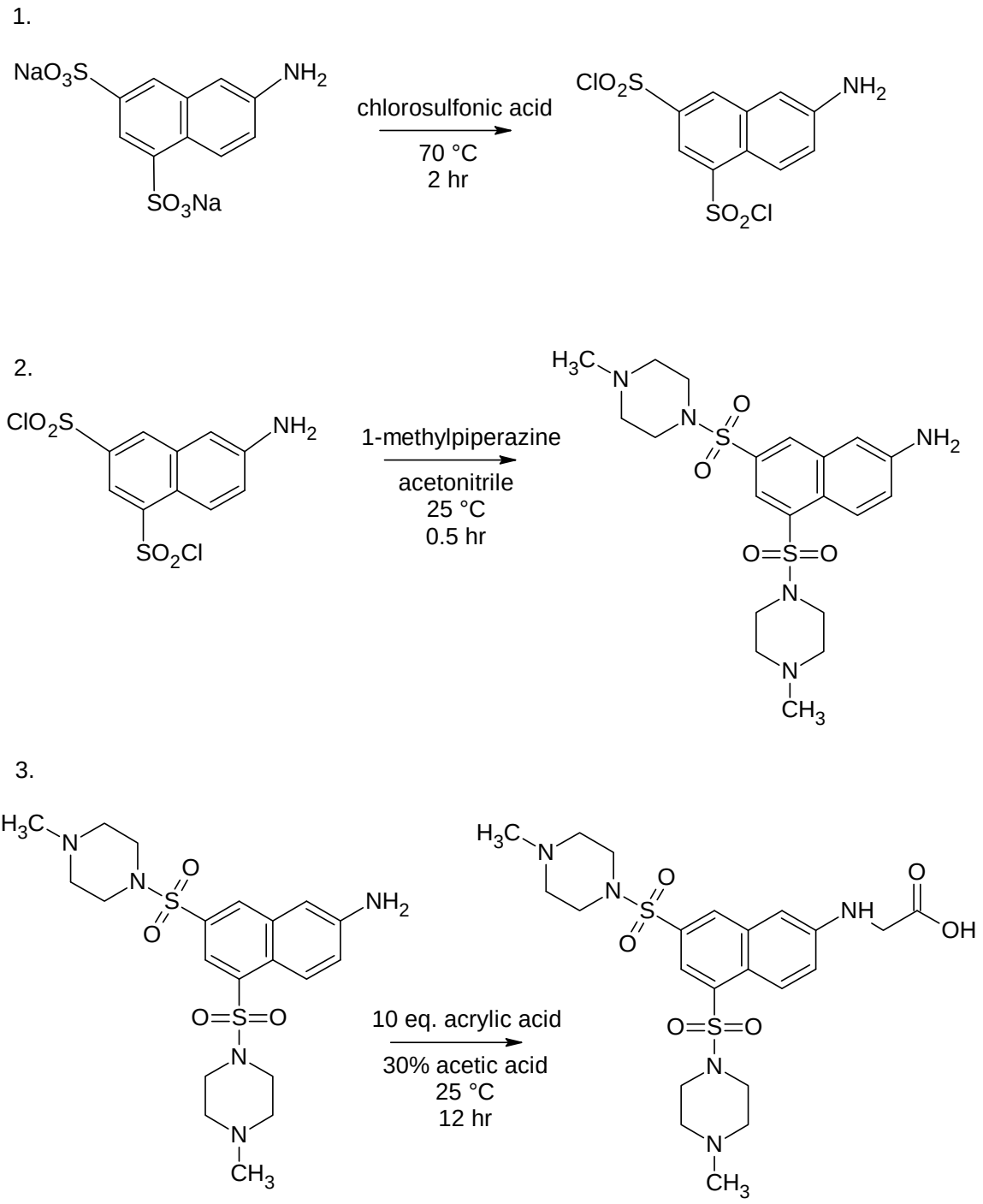

Figure 97. Reaction scheme for synthesis of a fluorescent pI marker.

5.5.2.3 Results and discussion

The results of the CE analysis of the samples taken are displayed in Figure 97. Comparison of the electropherograms for the initial feed and final collection streams indicates successful harvest of the pure target ampholyte in collection stream 4. ESI-MS, Figure 98, confirms that the intended target was harvested. The pH and conductivity values are plotted in Figures 99 and 100. The feed stream experiences a significant drop in conductivity and rise in the pH over the first 240 minutes of the separation. This is due to the removal of excess acetic acid and acrylic acid. Interestingly, an increase in conductivity and decrease in pH is observed for collection stream 1 over the same time. This is due to collection stream 1 flowing through the acidic chamber of separation head 1 where excess acid from the feed stream passes through as it migrates toward the anode. As in previous experiments, a slow loss of lysine from the basic flow-through stream was observed indicating that the cathodic membrane pH may be slightly lower than the pI of lysine. Finally, the entire collection 4 stream was lyophilized and 51 mg of the target pI marker was harvested indicating a production rate of about 2.5 mg/hour. This relatively low production rate is caused by two reasons: (i) complete electrophoretic removal of the excess acid takes approximately 6 hours and, (ii) transport into collection streams 2 and 4 is slowed by the low conductivity of these streams compared to the acidic, pH-biased streams. Though these two issues should be addressed in order to optimize this separation, the experiment successfully demonstrates the application of the T-RECS cascade to process a complex sample.

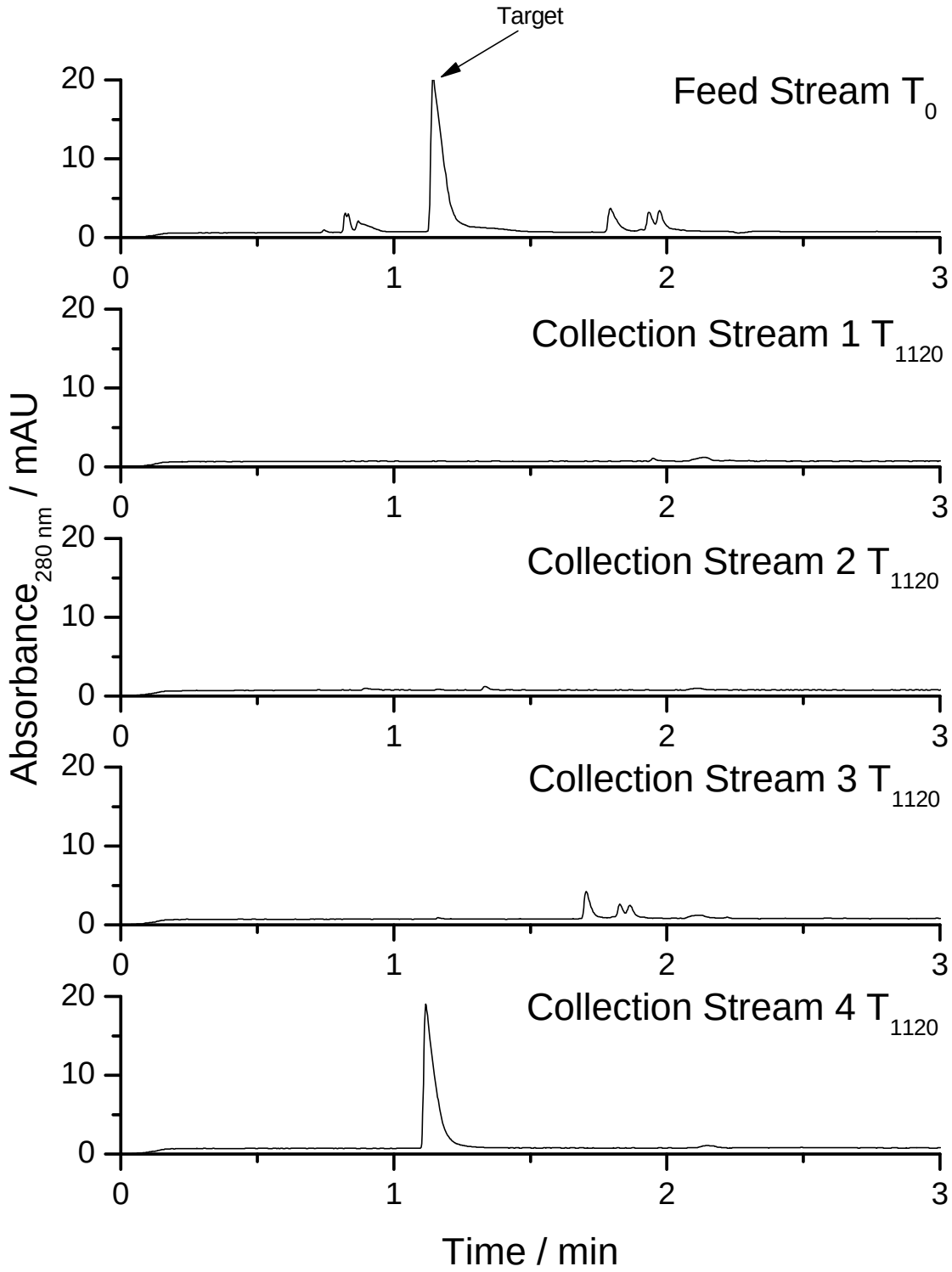

Figure 98. Electropherograms for samples taken from the initial feed stream and at 1120 minute from the collection streams during separation of a fluorescent pI marker from a crude reaction mixture.

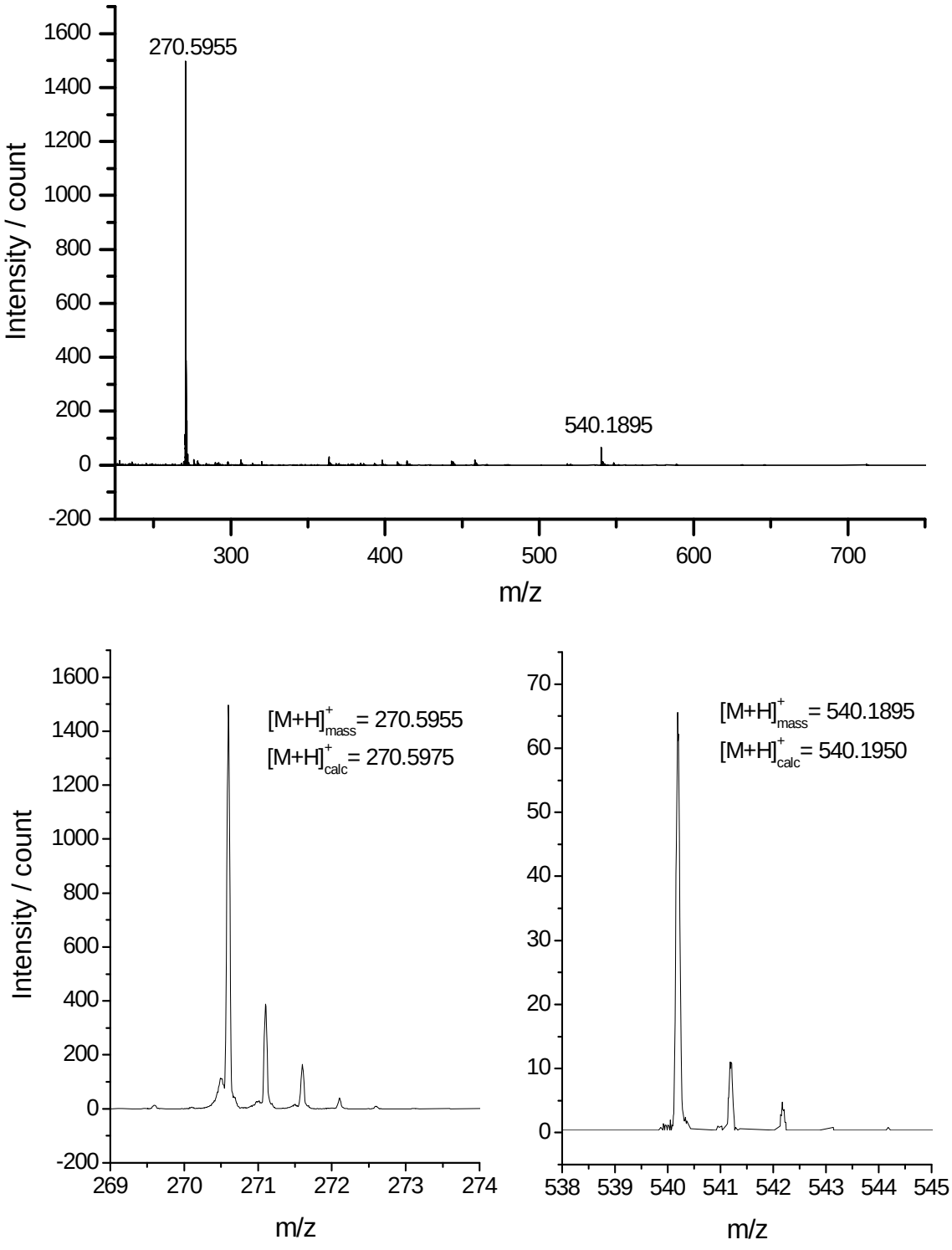

Figure 99. ESI-MS analysis of the sample taken from collection 4 stream at 1120 minutes.

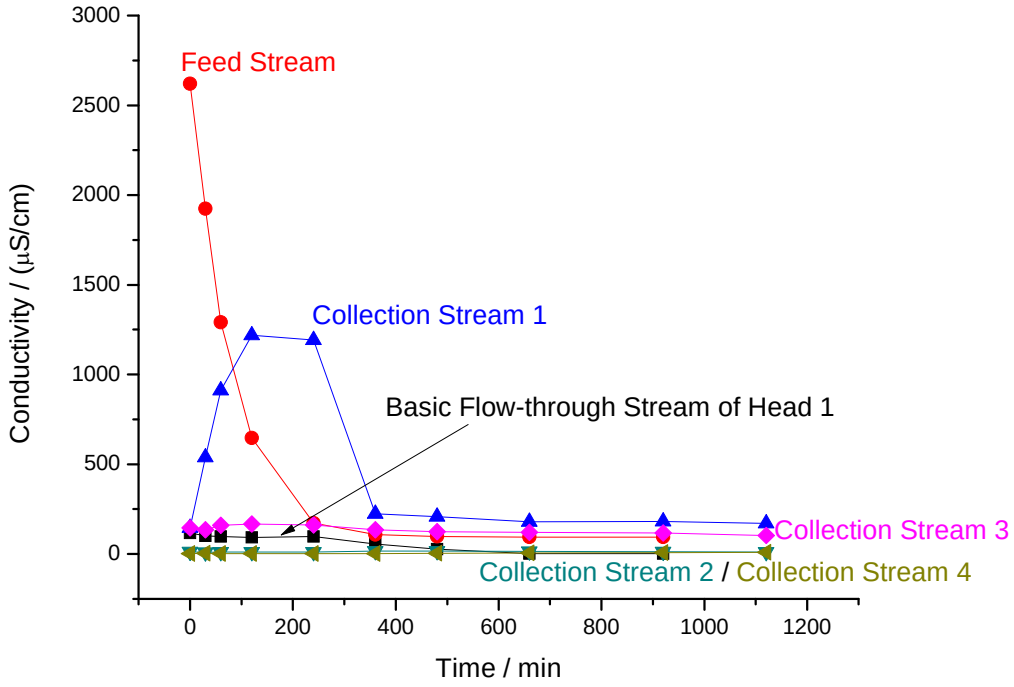

Figure 100. Conductivity in the collection streams, feed stream and basic flow-through stream of separation head 1 during separation of a fluorescent pI marker from a crude reaction mixture.

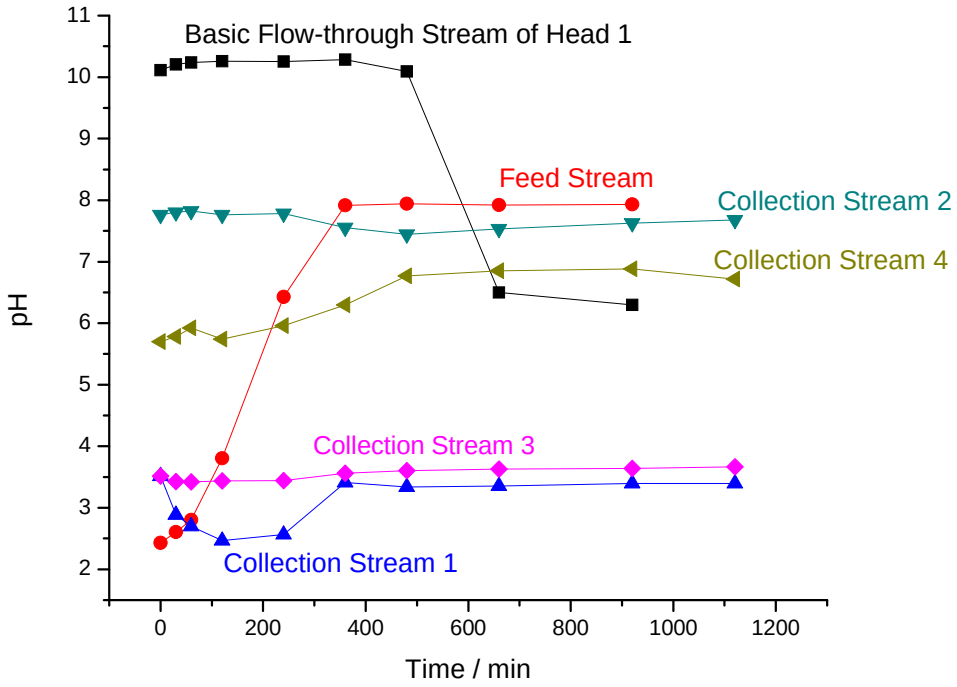

Figure 101. pH in the collection streams, feed stream and basic flow-through stream of separation head 1 during separation of a fluorescent pI marker from a crude reaction mixture.

6. CONCLUSIONS

6.1 Materials and methods for determinations of pH inside buffering membranes

Since rational IET separation design requires knowledge of the pH values of the available membranes, developing methods to determine these values are of particular importance. Current methods either rely on values calculated from the nominal composition of the membrane (which may not be representative of the pH under experimental conditions), or use values determined from experiments where the membrane to be characterized is configured as the separation membrane in a binary IET separation of a mixture of ampholytes. The latter method yields the true operational pH value of the membrane but is limited by the availability and quality (species distribution) of the ampholyte mixture. In this work, two significant advances for the determination of the operational pH value of the membranes have been developed.

The first advancement is based on a newly synthesized fluorescent carrier ampholyte mixture. The mixture was synthesized by linking 8-hydroxypyrene-1,3,6-trisulfonate to pentaethylenehexamine. The mixture was shown to contain numerous ampholytes in the $6 < pI < 9.75$ range and had suitable excitation and emission spectra for cIEF-LIF with currently available laser sources. The key advantage of the new mixture was that due to its favorable optical properties, the amount of fluorescent CA that had to be added to the non-fluorescent CA mixture to form the pH gradient could be decreased, reducing the danger of gradient distortion. Even with UV-absorbance detection, the amount of

pyrene-based carrier ampholytes used could be cut half compared to the amount required for the phenoxypropyl group-tagged CAs. This reduced load lessens the likelihood of alterations of the pH gradient set up by the UV-transparent commercial CAs. Finally, this mixture was shown to be useful for determining the pH of membranes that buffer in the alkaline range.

The second advancement is a new method that eliminates the need for the synthesis or blending of UV-absorbing carrier ampholytes and significantly simplifies the process of determining the pH inside buffering membranes. In this method, commercial UV-transparent carrier ampholytes are used as the ampholyte mixture to be separated and the monotony of pH gradients is exploited to determine the pH of the membranes. Since well defined commercial blends of $3 < pI < 10$ carrier ampholytes are readily available, this method has been applied for the determination of the pH of membranes that buffer in the acidic and basic range.

6.2 New instrumentation for preparative-scale IET separations

The performance of the current preparative-scale IET devices is limited by the serial arrangement of their separation compartments, the difficulties encountered in the selection of the appropriate buffering membranes, and the detrimental effects of Joule heating on separation selectivity. In this work, a new instrument known as the T-RECS or ***t***rapping by ***r***ecursive ***e***lectrophoresis in a ***c***ompartmentalized ***s***ystem, has been developed to help eliminate these limitations. The system features (i) parallel

arrangement of the electrodes and collection compartments, (ii) a directionally-controlled convection system that delivers the analytes, (iii) short anode-to-cathode distances, (iv) short intermembrane distances, and (v) an external cooling system to achieve these ends.

The T-RECS system was initially tested as a single separation head system. In this arrangement, the effects of Joule heating were probed, the successful desalting of strong electrolytes was shown, and the separation of small ampholytic molecules was confirmed. After construction of three additional separation heads, the system was operated as one having four isolated separation heads for the separation of small molecule ampholytes and the isoforms of a diagnostic monoclonal antibody. In the separation of small molecule ampholytes, the T-RECS was able to separate and trap four small molecules: the total processing rate and the target production rate were about 160 mg/hour and 40 mg/hour, respectively. For the separation of the isoforms of a diagnostic monoclonal antibody, the T-RECS was able to separate the acidic, main and basic variants and process 750 mg of sample in only 24 hours, representing a significant performance improvement in the preparative-scale IET separation of monoclonal antibodies. The T-RECS was then operated as a single MCE for the separation of small molecule ampholytes. As when operated in the isolated separation head mode, the T-RECS could successfully separate and trap 4 small molecule ampholytes. Operated in this fashion, the total target production rate was about 40 mg/hour. Finally, the T-RECS was operated as a cascade of binary separations. In this mode, the system was used for

the separation of small molecule ampholytes and of a fluorescent pI marker from a crude reaction mixture. For the separation of small molecule ampholytes in the binary cascade, the system was able to separate and trap four small molecules. For the isolation of a fluorescent pI marker from a crude reaction mixture, collection of a pure target ampholyte was confirmed by ESI-MS and 51 mg of the target pI marker was harvested indicating a production rate of about 2.5 mg/hour.

REFERENCES

[1] Svensson, H. *Acta Chem. Scand.* 1961, *15*, 325-341.

[2] Svensson, H. *Acta Chem. Scand.* 1962, *16*, 456-466.

[3] Bjellqvist, B., Ek, K., Righetti, P.G., Gianazza, E., et al. *J. Biochem. Biophys. Methods*. 1982, *6*, 317-339.

[4] Kolin, A., *J. Chem. Phys.* 1954, *22*, 1628-1629.

[5] Mosher, R.A., Thormann, W., Graham, A., Bier, M. *Electrophoresis* 1985, *6*, 545-551.

[6] Martin, A. J. P., Hampson, F., *J. Chromatogr.* 1979, *159*, 101-110.

[7] Luner, S.J., Kolin, A. *Proc. Natl. Acad. Sci*. 1970, *66*, 898-903.

[8] Righetti, P.G., *Isoelectric Focusing: Theory, Methodology and Applications,* Elsevier Biomedical Press, Amsterdam 1983, pp. 77.

[9] Rilbe, H., in: Catsimpoolas, N., (Ed.), *Isoelectric Focusing*, Academic Press, New York 1976, pp. 14-51.

[10] Vesterberg, O., *Acta. Chem. Scand.* 1969, *23*, 2653-2666.

[11] Vingradov, S. N., Lowenkron, S., Andonian, H. R., Bagashaw, J., Felegenhauer, K., Pak, S. J., *Biochem. Biophys. Res. Commun.* 1973, *54*, 501-506.

[12] Righetti, P. G., Pagani, M., Gianazza, E., *J. Chromatogr.*1975, *109*, 341-356.

[13] Charlionet, R., Martin, J. P., Sesboue, R., Madec, P. J., Lefebvre, F., *J. Chromatogr.* 1979, *176*, 89-101.

[14] Just, W. W., *Anal. Biochem*. 1980, *102*, 134-144.

[15] Righetti, P. G., Hjerten, S., *J. Biochem. Biophys. Methods* 1981, *5*, 259-272.

[16] Mosher, R. A., Thormann, W., Bier, M., *J. Chromatogr,* 1986, *351*, 31-38.

[17] Pettersson, E. *Acta Chem. Scand. 1969, 23,* 2631-2635.

[18] Nguyen, N.Y., Chrambach, A. *Anal. Biochem*. 1976, 74, 145-153.

[19] Righetti, P. G., *Immobilized pH Gradients: Theory and Methodology*, Elsevier Biomedical Press, Amsterdam 1990.

[20] Hruška, V., Jaroš, M., Gaš, B. *Electrophoresis*, 2006, *27*, 984-991.

[21] Lalwani, S., Shave, E., Fleisher, H. C., Nzeadibe, K., Busby, M. B., Vigh, G. *Electrophoresis* 2004, *25*, 2128-2138.

[22] Lalwani, S., Shave, E., Vigh, G., *Electrophoresis* 2004, *25*, 3323-3330.

[23] Fleisher, H. C., Vigh, G., *Electrophoresis* 2005, *26*, 2511-1519.

[24] Cretich, M., Pirri, G., Carrea, G., Chiari, M., *Electrophoresis* 2003, *24(4)*, 577-581.

[25] Fleisher-Craver, H.C., Poly(vinyl alcohol)-Based Buffering Membranes for Isoelectric Trapping Separations. Dissertation, Texas A&M University. 2007.

[26] Faupel, M., Barzaghi, B., Gelfi, C., Righetti, P.G., *J. Biochem. Biophys. Methods* 1987, *15*, 147-161.

[27] Faupel, M., Righetti, P.G., US Patent 4 971 670, 1990.

[28] Righetti, P. G., Barzaghi, B., Faupel, M. *J. Biochem. Biophys. Methods* 1987, *15,* 163-176.

[29] Barzaghi, B., Righetti, P.G., Faupel, M. *J. Biochem. Biophys. Methods* 1987, *15,* 177-188.

[30] Righetti, P.G., Barzaghi, B., Luzzana, M., Manfredi, G., et al. *J. Biochem. Biophys. Methods,* 1987, *15,* 189-198.

[31] Righetti, P.G., Barzaghi, B., Faupel, M. *Trends. Biotechnol.* 1988*, 6,* 121-125.

[32] Righetti, P.G., Wenisch, E., Faupel, M. *J. Chromatogr.* 1989*, 475,* 293-309.

[33] Righetti, P.G., Wenisch, E., Jungbauer, A., Katinger, H. et al. *J. Chromatogr*. 1990, *500*, 681-696.

[34] Zuo, X., Speicher, D. W., *Anal. Biochem.* 2000, *284*, 266-278.

[35] Lim, P., North, R., Vigh, G. *Electrophoresis* 2007, *28*, 1851-1859.

[36] *ZOOM® IEF Fractionator Instruction Manual*, Invitrogen Corp. Carlsbad, CA, 2004.

[37] *IsoelectriQ^2 Instruction Manual*, Proteome Systems Ltd. Woburn, MA, 2003.

[38] Shang, T.Q., Ginter, J.M., Johnston, M.V., Larsen, B.S., et al. *Electrophoresis* 2003, *24*, 2359-2368.

[39] Shave, E., Vigh, G., *Electrophoresis* 2004, *25*, 381-387.

[40] Ogle, D., Sheehan, M., Rumbel, B., Gibson, T., et al. *J. Chromatogr. A* 2003, *989*, 65-72.

[41] Zilberstein, G.V., Bakin, E.M., Bukshpan, S. *Electrophoresis* 2003, *24*, 3735-3744.

[42] Zilberstein, G.V., Bakin, E.M., Bukshpan, S., Korol, L.E. *Electrophoresis* 2004, *25*, 3643-3651.

[43] Lim, P.J. *Novel Devices for Analytical-Scale Isoelectric Trapping Separations*. Dissertation, Texas A&M University, 2006.

[44] Shave, E., Vigh, G. *Electrophoresis* 2007, *28*, 2291-2299.

[45] Hjertèn, S., Zhu, M.D. *J. Chromatogr.* 1985, *346*, 265-270.

[46] Hjertèn, S., Lio, J., Yao, K. *J. Chromatogr*. 1987, *387*, 127-138.

[47] Wu, J., Pawliszyn, J., *J. Chromatogr. B* 1995, *669*, 39-43.

[48] Koval, D., Kašička, V., Jiracek, J., Collinsova, M., et al. *Electrophoresis* 2002, *23*, 215-222.

[49] Včeláková, K., Zusková, I., Kenndler, E., Gaš, B. *Electrophoresis* 2004, *25*, 309-317.

[50] *Doctor pH Manual*, Amersham Pharmacia Biotech, San Francisco, CA, 1993.

[51] Giaffreda, E., Tonani, C., Righetti, P.G. *J. Chromatogr. A* 1993, *630*, 313-327.

[52] Tonani, C., Faupel, M., Righetti, P. G., *Electrophoresis* 1991, *12*, 631–636.

[53] North, R., Hwang, A., Lalwani, S., Shave, E., et al. *J. Chromatogr. A* 2006, *1130*, 232-237.

[54] Righetti, P. G., Bossi, A., Wenisch, E., Orsini, G., *J. Chromatogr. B* 1997, *699*, 105–115.

[55] Herbert, B., Righetti, P. G., *Electrophoresis* 2000, *21*, 3639– 3648.

[56] Zuo, X., Speicher, D. W., *Proteomics.* 2002, *2* 58-68.

[57] Righetti, P. G., Castagna, A., Herbert, B., Reymond, F., et al. *Proteomics* 2003, *3*, 1397–1407.

[58] Righetti, P. G., Castagna, A., Antonioli, P., Boschetti, E., *Electrophoresis* 2005, *26*, 297–319.

[59] Righetti, P. G., *J. Chromatogr. A* 2005, *1079*, 24–40.

[60] Righetti, P. G., Castagna, A., Herbert, B., Candiano, G., *Biosci. Rep.* 2005, *25*, 3–17.

[61] Righetti, P. G., *Electrophoresis* 2006, *27*, 923–938.

[62] Righetti, P. G., *Electrophoresis* 2007, *28*, 545–555.

[63] Wu, X.Z., Pawliszyn, J. *Electrophoresis* 2004, *25*, 3820-3824.

[64] Liu, Z., Pawliszyn, J. *Anal. Biochem*. 2005, *336*, 94-101.

[65] Shave, E., Vigh, G. *Electrophoresis* 2007, *28*, 587-594.

[66] Wu, J., Tiemin, H. Electrophoresis 2006, *27*, 3584-3590.

[67] Mazanec, K., Slais, K., Chmelik, J. *J. Mass Spec.* 2006, *41*, 1570-1577.

[68] Shimura, K., Kasai, K., *Electrophoresis* 1995, *16*, 1479-1484.

[69] Slais, K., Horka, M., Novackova, J., Friedl, Z. *Electrophoresis* 2002, *23*, 1682-1688.

[70] Shimura, K., Kamiya, K., Matsumoto, H., Kasai, K. *Anal. Chem*. 2002, *74*, 1046-1053.

[71] Verbeck, G.F., Beale, S.C. *J. Microcolumn Sep*. 1999, *11*, 708-715.

VITA

Robert Yates North received his Bachelor of Science degree in chemistry with a minor in biology from Hillsdale College (MI) in December 2003. After a few months of travel, he entered the graduate chemistry program at Texas A&M University in June 2004 as a member of the Separations Science Group, under the direction of Professor Gyula Vigh, and received his Doctor of Philosophy in chemistry in May 2009. His research interests include development of new instrumentation for preparative-scale electrophoretic separations, methods for determining the operational pH inside buffering membranes, and applications of chemistry in medicine.

Robert may be reached at the following address: Department of Chemistry, Texas A&M University, College Station, TX, 77840, or by email: north.ry@gmail.com.